UNDERSTANDING ENDOMEMBRANE TRAFFICKING IN PLANT CELLS USING CHEMICAL GENETICS APPROACH
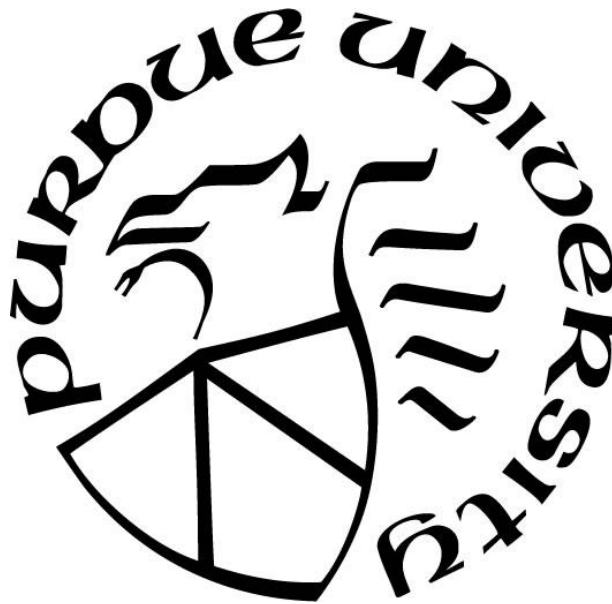
by

Diwen Wang

A Thesis

Submitted to the Faculty of Purdue University

In Partial Fulfillment of the Requirements for the degree of

Master of Science

Department of Botany and Plant Pathology

West Lafayette, Indiana

August 2020

THE PURDUE UNIVERSITY GRADUATE SCHOOL
STATEMENT OF COMMITTEE APPROVAL

Dr. Chunhua Zhang, Chair

Department of Botany and Plant Pathology

Dr. Leonor Boavida

Department of Botany and Plant Pathology

Dr. Cankui Zhang

Department of Agronomy

Approved by:

Dr. Christopher J. Staiger

Dedicated to myself and my parents

ACKNOWLEDGMENTS

My deepest gratitude goes to my advisor, Dr. Chunhua Zhang, and my committee members Dr. Leonor Boavida and Dr. Cankui Zhang. Thanks for their constant patience and guidance to my personal and scientifical growth. I truly appreciate the opportunities that my advisor Dr. Chunhua Zhang offered me to be a graduate student at Purdue University, which not only gave me an unforgettable life experience but also expanded my research interests. Many thanks go to Dr. Leonor Boavida and Dr. Cankui Zhang, because of their helpful suggestions, I was able to overcome many difficulties.

I thank all the lab members in Zhang lab at Lilly Hall of Life Science. Because of their encouragement and support, I was able to go further in plant biology step by step. As an experienced post-doc, Lei Huang taught me how to clone a gene and construct expression vectors. As a graduate student, Xiaouhi Li shared many tips for chemical screening and biochemical assays. I would like to thank Nana Liu and Hui Su as well, since they always trust me and encourage me for a bigger dream. Thanks to all the lab members, I went through a quite enjoyable time for past two years.

Personally, many thanks to my parents and all my family members. They are always the strongest backup to support me. I will keep going for a bigger dream with your love and encouragement.

TABLE OF CONTENTS

LIST OF TABLES

LIST OF FIGURES

ABSTRACT

Like other eukaryotic cells, plant cells contain an endomembrane system composed of compartmentalized organelles with specialized functions. Vesicle trafficking mediates the transport of materials between different organelles and the communication of cells and extracellular environment. The vesicle trafficking process is highly dynamic and plays essential roles in maintaining cellular homeostasis and environmental adaptation. Because of the essential roles of vesicle trafficking in plant growth and development, genes involved in vesicle trafficking often have redundant functions when they exist as a large family or cause embryonic lethality when they exist as a signal gene or small gene family. Chemical genetics uses small molecule inhibitors to affect protein function without interfering with plant's genome. Bioactive small molecules can generate a temporary perturbation of a biological system in a reversible and dose-dependent fashion, which allows the observation of dynamic cellular processes and discovery of new components in trafficking machineries. We recently discovered two small molecules named Endosidin2 (ES2) and Endosidin20 (ES20) that disrupt vesicle trafficking in plants. ES2 inhibits exocytosis by targeting the EXO70A1 subunit of the exocyst complex in plant cells. ES20 targets cellulose synthase (CESA) at the catalytic site and inhibits the delivery of Cellulose Synthase Complex (CSC) to the plasma membrane. This research thesis aims to characterize the specificity of ES2 on EXO70 homologs and identify new genes that mediate CSC trafficking. Drug Affinity Responsive Target Stability (DARTS) assay was used to test the specificity of ES2 in targeting different EXO70s in Arabidopsis. Chemical genetic screen for

11

mutants with increased sensitivity was conducted to identify novel genes related to CSC trafficking. This project provides new insights in the specificity of ES2 in targeting different EXO70s in plants and the regulatory mechanisms of CSC trafficking that control plant cellulose synthesis.

Key words: endomembrane trafficking, chemical genetics, Endosidin2, Endosidin20

CHAPTER 1.   LITERATURE REVIEW

1.1   Plant Cell Organelles and Endomembrane Trafficking System

In plant cells, the endomembrane system is responsible for protein synthesis, modification, trafficking, and storage, which requires functional integration of the Endoplasmic Reticulum (ER), Golgi apparatus, trans Golgi network (TGN), the plasma membrane and vacuoles (Alberts et al., 2002). Vesicular transport and membrane trafficking assist the exchange of components between different plant organelles (Bonifacino & Glick, 2004).

1.1.1   The Endoplasmic Reticulum

The Endoplasmic Reticulum (ER) is the largest and dynamic membrane network in cells. ER has multiple functions and is the location for Ca^{2+} storage and the biosynthesis of lipids and proteins (Phillips & Voeltz, 2016). The ER serves as the major site of protein synthesis, folding, and transport, and it is the gateway for protein trafficking (Robinson, Brandizzi, Hawes, & Nakano, 2015). Newly synthesized proteins are folded and assembled co-translationally or post-translationally at the ER. ER-localized signal recognition particles (SRPs) interact with the signal peptide of secretory proteins, leading the co-translated proteins with the ribosome and RNA to the ER membrane (Saraogi & Shan, 2011). On the ER membrane, the Sec translocation complex assists in the translocation of polypeptides into the ER lumen (Mandon, Trueman, & Gilmore, 2013). After being delivered to the ER lumen, proteins destined for secretion undergo proper folding and modifications, such as N-linked glycosylation (Cherepanova, Shrimal, & Gilmore, 2016) and disulfide bond formation (Oka & Bulleid, 2013). These modifications affect protein transport in secretory pathways.

ER has the quality control system to safeguard the folding and assembly of proteins and dispose of defective proteins (Adams, Oster, & Hebert, 2019). If proteins are recognized as being folded incompletely or incorrectly, they would be retained within the ER. The accumulation of defective proteins in the ER leads to ER stress (Senft & Ronai, 2015). In response to the ER stress, eukaryotic cells have three pathways to execute unfolded protein response (UPR), which are mediated by inositol-requiring enzyme 1 (IRE1), protein kinase RNA-like ER kinase (PERK), and activating transcription factor 6 (ATF6) (Hetz & Papa, 2018). Upon ER stress, the mRNA of transcription factors bZIP are spliced by ER transmembrane sensor IRE1, which is conserved in eukaryotic cells (Chen & Brandizzi, 2013). The spliced mRNA produces a transcription regulatory protein that regulates UPR target genes (Chen & Brandizzi, 2013). In mammalian cells, misfolded proteins activate a transmembrane kinase PERK (Chakrabarti, Chen, & Varner, 2011). It inhibits the translation initiation factor elF2α by phosphorylation, thereby reducing the general protein translation throughout the cell (Lebeau et al., 2018). Another sensor of ER stress in mammalian cells is autophagy-related protein ATF6 (Chakrabarti, Chen, & Varner, 2011). ER stress triggers the transport of ATF6 to the Golgi apparatus where it is cleaved off. ATF6 can further migrate to the nucleus and activate the transcription of genes involved in UPR (Hillary & FitzGerald, 2018).

In plant cells, the ER plays an important role in autophagy, which is a highly upregulated degradation pathway sensitive to biotic and abiotic stresses (Liu, Xiong, & Bassham, 2009;Liu et al., 2012). In Arabidopsis, ER stress upregulates autophagy and elicits UPR for degradation of misfolded proteins. bZIP28 is one arm of the UPR signaling pathway (Tajima, Iwata, Iwano, Takayama, & Koizumi, 2008). It is an ER-resident transcription factor and interacts with BiP chaperone within the ER lumen under normal conditions (Srivastava, Deng, Shah, Rao, &

Howell, 2013). In response to heat, ER stress triggers the proteolytic processing and nuclear

relocation of bZIP28, which mediated the heat tolerance responses (Liu, Srivastava, Che, &

Howell, 2007;Gao, Brandizzi, Benning, & Larkin, 2008). Another arm of UPR in Arabidopsis

involves IRE1B, which splices the mRNA of bZIP60 in response to heat or ER stress agents

(Chen & Brandizzi, 2012;Deng et al., 2011). The ribonuclease activity of IRE1B is a requisite

for the induction of autophagy by ER stress (Bao et al., 2018).

The transport from ER to the Golgi apparatus relies on COPII coated vesicles. COPII

vesicles are generated from the ER and transported to the *cis*-face of the Golgi apparatus

(Barlowe et al., 1994). The formation of COPII coated vesicles is mediated by Sar1 GTPase, a

secretion-associated Ras-related protein (Sar) (Bi, Corpina, & Goldberg, 2002a, 2002b). COPII

component Sec23/24 are recruited by activated Sar1 to form the inner layer of COPII, and the

Sec23/24-Sar1 complex interacts with Sec13/31 to form the outer cage (Bi, Corpina, &

Goldberg, 2002a;Matsuoka, Schekman, Orci, & Heuser, 2001).

1.1.2   **The Golgi Apparatus**

The Golgi apparatus is a membrane-bounded structure with five to seven flattened

cisternae stacks. Based on the spatial organization of glycosylation enzymes, stacks of the Golgi

apparatus are divided into *cis*-, medial-, and *trans*- cisternae (Dunphy & Rothman, 1985;Moore,

Swords, Lynch, & Staehelin, 1991). Polarized *cis* cisternae receives proteins and lipids from the

ER and processes them to *trans* cisternae (Mellman & Warren, 2000). In endomembrane

trafficking system, the Golgi apparatus is a central sorting station of secretory pathways.

The morphology of Golgi apparatus differs in plant, mammalian, and yeast cells (Ito,

Uemura, & Nakano, 2014). In plant cells, there are numerous individual Golgi units that are

scattered throughout the cytoplasm. Each unit keeps the *cis-trans* polarity, moving on active

filaments by myosin motors (Dupree & Sherrier, 1998;Hawes, Schoberer, Hummel, &

Osterrieder, 2010). In mammalian cells, twisted Golgi stacks are interconnected to form a

network called the Golgi ribbon, which is adjacent to the nucleus and associated to centrosomes

(Wei & Seemann, 2010). The Golgi ribbon is disintegrated by depolymerizing microtubules and

centralized on it by dynein motors (Polishchuk, Polishchuk, & Mironov, 1999;Allan, Thompson,

& McNiven, 2002). In yeast cells, the Golgi membranes are dispersed throughout the cytoplasm

in forms of individual cisternae instead of stacked structures (Preuss, Mulholland, Franzusoff,

Segev, & Botstein, 1992;Rambourg, Clermont, & Kepes, 1993). The simple organization of the

Golgi apparatus in yeast cells greatly contributed to studies of endomembrane trafficking

(Matsuura-Tokita, Takeuchi, Ichihara, Mikuriya, & Nakano, 2006).

From live cell imaging studies, plant Golgi moves along actin in cytoplasm and the

motility pattern exhibits alternative motions between pause and go (Nebenfuhr et al., 1999)

During mitosis, Golgi keeps stationary and stacks redistribute and aggregate in the equatorial

region, forming the Golgi belt, which contributes to the cell plate formation (Nebenfuhr,

Frohlick, & Staehelin, 2000). The Golgi apparatus is highly dynamic in protein sorting and

transport. As traversing the Golgi stack, cargo macromolecules undergo post-translational

modifications such as phosphorylation, sulfation, and proteolysis, to trim or rebuilt the

oligosaccharides of glycoproteins. These modifications define the correct cell addresses of cargo

molecules in following secretion process (Strasser, 2016). For example, cell wall components are

shuttled as cargoes to the plasma membrane for cell wall formation through Golgi-derived

vesicles (Driouich et al., 2012).

The membrane trafficking from Golgi to ER requires coated COPI vesicles (Serafini et

al., 1991;Waters, Serafini, & Rothman, 1991;). COPI, budding from the cis-Golgi cisternae,

mediates the retrieval of ER proteins that escapes to the Golgi complex (Letourneur et al., 1994) ADP-ribosylation factor 1 (ARF1) is mandatory for the binding of β-COP, a component of coatomer, to the Golgi membranes and regulates the formation of COPI vesicles (Donaldson, Cassel, Kahn, & Klausner, 1992). In Arabidopsis, COPI vesicles can be divided into two types: COPIa and COPIIb (Donohoe, Kang, & Staehelin, 2007). COPIa occupies the space between cis-Golgi and the ER, whereas COPIb buds from *media-* and *trans-*Golgi cisternae. Their different distribution patterns suggest that COPIa vesicles participate in the transport between the ER and the Golgi, and COPIb vesicles are involved in intra-Golgi transport (Donohoe, Kang, & Staehelin, 2007;Donohoe et al., 2013).

1.1.3 Trans Golgi Network (TGN)

After traveling through the Golgi stacks, synthesized secretory proteins are sorted in the Trans Golgi network (TGN). TGN forms membrane-closed secretory vesicles through which the proteins are delivered to the plasma membrane (Rojo & Denecke, 2008).The secretion of proteins from the ER to the plasma membrane (PM) through the Golgi apparatus is called exocytosis (Rojo & Denecke, 2008). In the opposite direction, cells uptake extracellular compounds and recycle plasma membrane proteins through endocytosis (Fan, Li, Pan, Ding, & Lin, 2015). In the endocytic pathway, the endocytosed proteins are delivered to early endosomes (EE) within endocytic vesicles that are derived from the plasma membrane, and then they are transported to the vacuole through late endosomes (LE)/multivesicular bodies (MVB) for degradation (Fan, Li, Pan, Ding, & Lin, 2015). In plants, the functions of TGN and early endosome are overlapped, therefore two endosomal compartments involved in protein recycling and degradation are TGN and pre-vacuolar compartments that are LE/MVBs (Reyes, Buono, & Otegui, 2011).

The vesicle delivery between the TGN, the plasma membrane, and endosomes are coated with clathrin coatomer (Robinson, 2015). Same with mammalian cells, the clathrin coats of plant cells are composed of clathrin heavy chain (CHC) and clathrin light chain (CLC) (Robinson, 2015). Clathrin-mediated membrane trafficking functions in multiple cell activities, such as cell plate maturation (Segui-Simarro, Austin, White, & Staehelin, 2004) and auxin transporters localization (Dhonukshe et al., 2007), which is critical for plant growth and development (Backues, Korasick, Heese, & Bednarek, 2010). Dynamin is a GTPase in clathrin mediating trafficking, regulating the departure of new formed vesicles and the targeting of vesicles to recipient compartments. There are various dynamin-related proteins (DRP) in eukaryotes (Pucadyil & Schmid, 2008). Plant cells have six DRP families (DRP1-DRP4, DRP5A and DRP5B) (Fujimoto & Tsutsumi, 2014). DRP1 and DRP2 are involved in clathrin-mediated endocytosis (CME) (Bednarek & Backues, 2010). Pleckstrin homology (PH) domain can bind phosphatidylinositol lipids, which recruits proteins to different membranes (Feng, He, Li, Xiao, & Hu, 2019). Similar to animal dynamin-1, DRP2A binds to Phosphatidylinositol 4,5-bisphosphate [PI(4,5)P$_2$] that is enriched at the plasma membrane via its PH domain (Li & Marshall, 2015). Except PH domain, other similar domains such as Src homology 3 (SH3) in Arabidopsis serve as the binding motif to dynamin, regulating the CME (Lam, Sage, Bianchi, & Blumwald, 2001). At the TGN, an Arf GAP enzyme, Van3, interacts with DRP1A, which regulates vascular formation through modulation of vesicle budding (Sawa et al., 2005).

Protein ubiquitination regulates protein quality and abundance at membranes and determines their trafficking and location through initiation of endosomal sorting (Hicke & Dunn, 2003). Ubiquitination adds a ubiquitin attachment to target proteins at the C-terminal glycine for posttranslational modification (Hicke & Dunn, 2003). In Arabidopsis, the TGN is crucial for the

degradative endosomal sorting of many ubiquitinated plasma membrane proteins, such as IRON

REGULATED TRANSPORTER 1 (IRT1) (Barberon et al., 2011), BORON TRANSPORTER 1

(BOR1) (Kasai, Takano, Miwa, Toyoda, & Fujiwara, 2011), and BRASSINOSTEROID

INSENSITIVE 1 (BRI1) (Geldner, Hyman, Wang, Schumacher, & Chory, 2007)

1.1.4 **Vacuoles**

Plant vacuoles occupy the largest cell volume and play essential roles in plant

development. Because of various morphology and versatile functions, vacuoles participate in

diverse cell activities to maintain cellular metabolism and response to diverse environmental

growth conditions (Shimada, Takagi, Ichino, Shirakawa, & Hara-Nishimura, 2018). Vacuoles

function in multiple processes such as the control of cell volume and turgor (Chrispeels,

Crawford, & Schroeder, 1999), the maintenance of cytoplasmic homeostasis (Maeshima, 2001),

the storage of metabolic products (Etxeberria, Pozueta-Romero, & Gonzalez, 2012), the

digestion of proteins (Suzuki & Emr, 2018) and detoxification (White, 2018).

Plant cells allow different types of vacuoles to present in the same cell, which is different

from other vacuolar system (Becker, 2007). The biogenesis of plant vacuoles is under debate

(Cui, Zhao, Hu, & Jiang, 2020). Plant vacuoles formation is believed to start from intracellular

biosynthesis pathways, including conventional ER-TGN secretory, endocytosis, autophagy, and

cytoplasm transmission (Tan et al., 2019). On the vacuolar pathway, the TGN-derived vesicles

form the pre-vacuolar compartment (PVC), which leads to the final vacuole biogenesis (Kwon et

al., 2018). At the exit of the Golgi complex, vacuolar soluble proteins are separated from other

secretory proteins to vacuoles because of vacuolar sorting signals (Kang et al., 2012). In

endocytosis, there is a distinct route for vacuolation, from the internalization of the plasma

membrane to PVC and the vacuoles (Zouhar & Sauer, 2014). Biotic or abiotic stresses such as

carbon starvation induces autophagy machinery, where the ER is the direct membrane source for vacuole biogenesis (Honig, Avin-Wittenberg, Ufaz, & Galili, 2012;Viotti et al., 2013). 3-D high-voltage electron microscopy reveals that early autophagosomes segregate portions of cytoplasm to form the autophagic vacuoles (Marty, 1999).

The morphology of vacuoles varies according to cell types and growth conditions (Hanamata, Kurusu, & Kuchitsu, 2014). In epidermal pavement cells of Arabidopsis cotyledon, the shape and size of vacuolar invaginations changes with the progression of pavement cell development (Saito et al., 2002). Guard cells contain a large number of vacuoles, where the biogenesis of vacuoles associates with the stomatal movement (Tanaka et al., 2007). Small vacuoles fuse to form large vacuoles during stomatal opening, and large vacuoles split into smaller vacuoles when stomata are closing (Gao et al., 2005).

According to their distinct functions, vacuoles are generally divided into two groups: protein storage vacuoles (PSV) and lytic vacuoles (LV) (Paris, Stanley, Jones, & Rogers, 1996). The PSVs present in most seeds and have a neutral environment for storing substrates (Jolliffe, Craddock, & Frigerio, 2005). LVs function as lysosomes in animal cells, which have lower pH and active proteases for digesting various macromolecules (de Marcos & Denecke, 2016). Tonoplast intrinsic proteins (TIPs) are enriched in the membrane of vacuoles, facilitating water exchanging between cytoplasm and vacuole (Muntz, 2007). TIP isoforms can act as the membrane markers for different vacuoles (Jauh, Phillips, & Rogers, 1999). From confocal immunofluorescence experiments, PSVs are marked by α-TIP and γ-TIP presents LV (Jauh, Phillips, & Rogers, 1999). Under the conditions of wounding or developmental switches, there is a unique plant vacuole that contains vegetative storage proteins, and δ-TIP is the marker protein to label these storage vacuoles (Jauh, Fischer, Grimes, Ryan, & Rogers, 1998). During seed

germination, PSVs can be transformed into LV, and this process is crucial for amino acids

recycling from autophagosomes and subsequent cell differentiation (Zheng & Staehelin, 2011).

In plant cells, vacuoles have a tight association with actin cytoskeleton. Together with

myosin proteins, actin bundles promote the arrangement and movement of transvacuolar strands

(Hoffmann & Nebenfuhr, 2004). When the organization of actin is disrupted by chemicals, the

fusion of vacuoles is inhibited as well (Li, Ren, Gao, Wei, & Wang, 2013). As an activator of

small GTPase Rho family of plants (ROP), SPIKE1 protein associates with WAVE complex and

actin-related protein ARP2/3 to regulate actin polymerization (Basu, Le J, Zakharova, Mallery,

& Szymanski, 2008). The role of ROP signaling in cytoskeleton organization leads to more

potential insights about the function of small GTPases in vacuole biogenesis and vacuolar

trafficking (Ebine et al., 2014).

1.1.5   **The Plasma Membrane**

The plasma membrane encloses the intracellular components and separates them from the

extracellular environment. The major components of the plasma membrane are lipid bilayer and

membrane proteins, which regulates the exchanging of molecules and signals response to

environmental stimuli and developmental cues (Mamode et al., 2019). The integrity and

dynamics of the plasma membrane maintain the shape of cells, exchange materials for cell

survival, and protect cells from pathogens (Jacobson, Liu, & Lagerholm, 2019).

The selective permeability of the plasma membrane controls the transport of substances

across the membrane (Alberts et al., 2002). Concentration gradient propels the diffusion of some

small molecules, such as oxygen, where small molecules move freely from high concentration to

low without energy involved (Moller et al., 2019). The nutrient up-take and metabolite exchange

depend on transmembrane protein channels and transporters on the plasma membrane (Alberts et

21

al., 2002). The transport of these organic compounds relies on the energy generated via electrochemical gradients. In plant cells, H^+-ATPases, driven by hydrolyzing ATP, are the powerhouses to provide proton motive force (Palmgren, 2001).

The membrane proteins are responsible for various biological activities that are initiated by complex mechanisms, involving a system of internal membranes and protein transport (Alberts B et al, 2002). Proteomic analysis identified 238 putative membrane proteins in Arabidopsis (Alexandersson, Saalbach, Larsson, & Kjellbom, 2004). Among these proteins, a large group of proteins participate in transport such as intrinsic water channel aquaporins (PIPs) (Pawlowicz & Masajada, 2019). Half of them are receptor-like kinases (RLKs) involved in signal transduction, such as calcium-dependent protein kinases (CDPKs) (Shi et al., 2018). Several membrane proteins take part in membrane trafficking, such as syntaxins. There are many proteins with specific functions as well, including stress-induced proteins, metabolic enzymes etc. (Alexandersson, Saalbach, Larsson, & Kjellbom, 2004)

The identification of membrane protein PIN-FORMED (PIN) in Arabidopsis significantly facilitates analysis of the dynamics of plasma membrane proteins in plants (Luschnig & Vert, 2014). The PIN protein family is the auxin efflux carriers, which act as secondary transporters and manipulate the translocation of auxin through the plasma membrane (Chen et al., 1998;Galweiler et al., 1998). The spatiotemporal distribution of auxin is mediated by the asymmetrical localization of PIN proteins on the plasma membrane (Wisniewska et al., 2006). The subcellular movement of PIN proteins between the plasma membrane and endosomes provide a useful tool to understand the possible mechanisms of secretory proteins (Luschnig & Vert, 2014). With the wortmannin treatment, an inhibitor for phosphatidylinositol-3-OH, the accumulation of PIN2 in AtSNX1-containing endosomes reveals the role of SNX1 protein in

PIN2 endocytic sorting, which defines a new endosomal compartment in auxin-carrier trafficking pathways in plant cells (Jaillais, Fobis-Loisy, Miege, Rollin, & Gaude, 2006). Vacuolar protein sorting 29 (VPS29) was identified as a key factor in plant endosome homeostasis through analysis of PIN1 and PIN2 performance in *vps29* mutants in Arabidopsis (Jaillais et al., 2007).

The dynamic trafficking behaviors of other membrane proteins, such as Auxin transporter protein 1 (AUX1), and BRASSINOSTEROID INSENSITIVE 1 (BRI1) provide insights into the trafficking mechanisms in plants. AUX1 is an auxin influx carrier (Marchant et al., 1999), and BRI1 is a receptor for the steroidal plant hormone, brassinosteroid (Wang, Seto, Fujioka, Yoshida, & Chory, 2001). The small molecule Endosidin1 (ES1) was identified to inhibit the recycling of several membrane proteins in Arabidopsis (Robert et al., 2008). PIN2, BRI1, and AUX1 agglomerate in endosomal compartments forming endosidin bodies when the seedlings are exposed to ES1 but the trafficking of PIN1 and PIN7 are not affected. It suggests at least two pathways in endocytosis (Robert et al., 2008).

1.1.6 Protein Secretion and Small GTPases

In eukaryotic cells, protein secretion is a fundamental and significant physiological process. Many cell growing processes and plant developmental activities rely on protein secretion, such as homeostasis, cytokinesis, cell wall assembly and hormone release (Chung & Zeng, 2017). There are two pathways for protein secretion: conventional protein secretion (CPS) pathway and unconventional protein secretion (UPS) pathway (Wang, Chung, Lin, & Jiang, 2017). In yeast, mammalian and plant cells, CPS is conserved, by which proteins can be delivered to the plasma membrane from the ER through the Golgi complex (Viotti, 2016). The proteins secreted through CPS have a N-terminal signal peptide or transmembrane domain that direct them to the final cellular destinations. In alternative trafficking routes, numerous

macromolecules without leading sequences are delivered to reach their location through UPS (Rabouille, 2017). In most cases, mechanical stress or ER stress that impairs the functional integrity of CPS initiates the UPS, indicating that UPS has a more complicated mechanism (Giuliani, Grieve, & Rabouille, 2011). In UPS, there are three pathways for leaderless proteins (Rabouille, Malhotra, & Nickel, 2012). In the Type I pathway of UPS, the formation of lipidic pores on the plasma membrane allows the translocation of cytoplasmic cargos. For the Type III pathway, it is proposed that endosomes and autophagosomes assist secretory proteins to translocate across plasma membrane by UPS. Distinct from Type I and Type III pathways, proteins with ER high-mannose oligosaccharides reach to the plasma membrane bypassing the Golgi Type IV pathway (Rabouille, 2017).

In the regulation of membrane trafficking, small GTPase family proteins act as molecular switches (Reiner & Lundquist, 2018). Small GTPases switch between GTP-bound state (active) and GDP-bound state (inactive) to turn on/off the molecular processes (Reiner & Lundquist, 2018). The cycle of GTP-GDP exchange relies on Guanine nucleotide exchange factors (GEF) and GTPase-activating proteins (GAP). GEFs promote GTP loading, while GAPs hydrolyze GTP (Reiner & Lundquist, 2018). For example, ADP-ribosylation factor (ARF) and secretion-associated Ras-related protein (Sar) are two types of small GTPases, which play a critical role in biogenesis of transport vesicles (Yorimitsu, Sato, & Takeuchi, 2014). In plant cells, GBF1, BIGs, and GNOM-LIKE1 (GNL1) are identified as the ARF GEFs (Manolea, Claude, Chun, Rosas, & Melancon, 2008;Teh & Moore, 2007). ARF GEFs contain a conserved Sec7 catalytic domain (Jackson & Casanova, 2000). For the GDP or GTP binding of Sar, Sec12 encodes guanine-nucleotide exchange factor and catalyzes the guanine-nucleotide dissociation from Sar1

(Barlowe & Schekman, 1993). Sar GEF mediates GDP or GTP binding of Sar1, which initiates or inhibits Sar1's activation.

1.2　Exocytosis and The Exocyst Complex

Exocytosis refers to the delivery of secretory proteins from the ER to the plasma membrane through Golgi complex. In exocytosis, secretory vesicles move along the actin in cytoplasm and arrives at the plasma membrane. At the last stage of exocytosis, the exocyst complex, an octameric multiprotein complex, assists the secretory vesicles to tether with the fusion site on the plasma membrane. After tethering and docking, the membrane of vesicles and the plasma membrane fuse together and completes the exocytosis (Alberts et al., 2002).

1.2.1　The Function of Plant Exocytosis

Exocytosis in plant cells is required for many cell activities, such as cell growth (Luo et al., 2017), immune responses (Gu, Zavaliev, & Dong, 2017), and stress responses (Wang et al., 2020). It continuously supplies cell wall components, membrane materials, and signaling molecules that are necessary for cell extension and rapid response to diverse environmental conditions. For cell growth, exocytosis is highly localized in tip-growing cells, such as root hairs and pollen tubes (Wang, Xue, Willcox, & Thakur, 2008). Exocytosis machinery promotes the extension of Arabidopsis pollen tube with the regulation of F-actin dynamics and ROP1 Rho GTPase involved (Lee, Szumlanski, Nielsen, & Yang, 2008). In the plant secretory pathway, many proteins are involved in pathogen defenses. For example, when cells are infected by powdery mildew fungus *Golovinomyces cichoracearum*, TGN-localized KEEP ON GOING (KEG) protein is specifically degraded, which is postulated to be an anti-virulence strategy (Gu & Innes, 2012). In abiotic stress response, the TGN-localized Q-SNARE protein, SNARE

protein Syntaxin of Plants 61 (SYP61) is well studied for ionic and nonionic osmotic stress

responses (Zhu et al., 2002).

1.2.2 **The Composition and Function of Plant Exocyst Complex**

The exocyst complex was first identified and characterized in budding yeast

Saccharomyces cerevisiae (Novick, Field, & Schekman, 1980; TerBush & Novick, 1995;

TerBush, Maurice, Roth, & Novick, 1996). Then its subunits were found in mammal (Ting et al.,

1995) and in plant (Elias et al., 2003). This complex has eight subunits of this complex: SEC3,

SEC5, SEC6, SEC8, SEC10, SEC15, EXO70, and EXO84. From cryo-electron microscopy, the

structure of the exocyst complex in yeast indicates that eight subunits knit each other in a

hierarchical manner through long helical bundles, and four pairs of interaction between subunits

support the molecular organization of this complex (Mei et al., 2018).

The exocyst complex is evolutionarily conserved in eukaryotes, from yeasts to mammals

and plants. Plants, as all multicellular organisms, have numerous processes requiring polarized

exocytosis, which involves various types of secretion (Zhang, Liu, Emons, & Ketelaar, 2010).

Different from a single copy of gene encoding the exocyst subunit in yeast and most mammalian

cells, plants have expanded gene family related to the exocyst complex. For example, there are as

many as 23 genes in Arabidopsis related to EXO70, two genes for SEC3, SEC5, SEC10, and

SEC15, three genes for EXO84, one for SEC6 and SEC8 (Cvrckova et al., 2012). The loss of

SEC3 in maize leads to a retard in root hair elongation (Wen, Hochholdinger, Sauer, Bruce, &

Schnable, 2005). Defects in pollen germination and pollen tube growth might result from

mutations in SEC3, SEC5, SEC6, and SEC8 in Arabidopsis (Safavian et al., 2015; Li et al.,

2017).

Surprisingly, it is common for plants to have multiple copies of EXO70 genes. Sorghum has 31and rice has 47 EXO70 genes (Cvrckova et al., 2012). The dramatic expansion of the EXO70 gene family in plant cells imply that they are likely responsible for specialized functions. GUS expression on all 23 EXO70 genes in Arabidopsis and reverse transcription PCR of them show distinct expression patterns, suggesting their functional divergence and specificity (Li et al., 2010). It is hypothesized that the regulation of these 23 genes is cell type-specific and/or they play a role in developmental state-specific exocytosis (Li et al., 2010;Zarsky, Kulich, Fendrych, & Pecenkova, 2013)

1.2.3 **Cellular Components in Exocytosis**

During the final stage of exocytosis, the exocyst complex achieves the polarized localization on the plasma membrane depending on interactions with actin. Live-cell imaging and fluorescence recovery after photobleaching (FRAP) analysis in yeast cells revealed that SEC3 and EXO70 create points at the plasma membrane where they interact with the remaining subunits and assist the vesicle to tether at fusion points (Finger, Hughes, & Novick, 1998;Boyd, Hughes, Pypaert, & Novick, 2004). SEC3 and EXO70 are the first to arrive at the polarized localization, completely or partially independent of actin cables. The remaining subunits including SEC5, SEC6, SEC8, SEC10, SEC15, and EXO80 are associated with the secretory vesicles and are delivered to the plasma membrane along the actin cables (Zhang et al., 2005). In yeast and mammalian cells, The recruitment of SEC3 and EXO70 to the fusion site depends on Phosphatidylinositol 4,5 bisphosphate [$PI(4,5)P_2$], and the reduction of cellular $PI(4,5)P_2$ leads to the inhibition of the exocyst complex assembly (Liu, Zuo, Yue, & Guo, 2007). At the inner leaflet of the plasma membrane, $PI(4,5)P_2$ interacts a polybasic region at the N-terminal of SEC3 directly, and a number of residues at the C-terminal of EXO70. (He, Xi, Zhang, Zhang, & Guo,

2007;Zhang et al., 2008). In plant cells, the interaction between Arabidopsis SEC3 and PI(4,5)P$_2$

is partially conserved, but roles of EXO70s in targeting to the plasma membrane is under debate

(Bloch et al., 2016;Sekeres et al., 2017).

In addition, small GTPases contribute to this polarized process. Rab and Rho small

GTPases are two major key regulators along the exocytic pathway. In yeast cells, SEC15

interacted with the Rab GTPase SEC4, which is responsible for the regulation of the subunits

assembly (Guo, Roth, Walch-Solimena, & Novick, 1999). Activated Rho family GTPases such

as CDC42 and Rho3 interact with SEC3 and EXO70 (Zhang et al., 2008;Roumanie et al., 2005).

Compared with 6-10 members in yeast Rab family, Arabidopsis has 57 Rab GTPases that are

divided into eight clades (Rab A-H) (Woollard & Moore, 2008). Five member of Rab-E clade

exhibit interactions with PI(4,5)P$_2$, which assist the membrane identity in plant exocytosis

(Camacho, Smertenko, Perez-Gomez, Hussey, & Moore, 2009). Rho-like GTPases of plant

(ROPs) are activated by auxin to promote the organization of microtubules and actin filaments to

regulate the secretory pathway (Lin et al., 2013;Xu et al., 2014;).

1.3   Chemical Genetics and Plant Endomembrane Trafficking

The delivery of macromolecules within eukaryotic cells is necessary for cell development

and plant growth. Molecular biology techniques and confocal imaging methods such as T-DNA

insertional mutagenesis (Krysan, Young, & Sussman, 1999) and recombinant GFP markers

(Tsien, 1998) contribute to reveal the regulatory mechanisms of vesicular transport. However,

these approaches are not sufficient for further exploitation in mechanisms of endomembrane

trafficking. Chemical genetics, a novel interdisciplinary approach that combinates specific

chemical inhibitors with quantitative microscopy, provides a very powerful tool to study the

regulatory mechanisms of vesicular transport routes in plant cells (Stockwell, 2000).

1.3.1 **Chemical Genetics Strategy**

In traditional molecular genetics, knocking out or introducing mutations are wildly used approaches to alter a gene and understand its protein functions (Hartwell, 1991). Gene redundancy is the biggest problem to understand protein functions in multicellular organisms. More than one homolog belongs to the same gene family, and these homologous genes are functionally compromised to mutagenesis of one loss-of-function gene (Zhang, Luo, Kishino, & Kearsey, 2005). Alterations happening at genetic level easily cause lethality, which is another limitation for classical genetic approaches in the dissection of complicated regulatory mechanisms (Candela, Perez-Perez, & Micol, 2011).

Instead of mutations, small molecules are used as an alternative approach to perturb specific protein and dissect gene functions, which refers to chemical genetics approach (Stockwell, 2004). In chemical genetics approach, exogenous ligands bind to target proteins specifically and alter protein functions in some molecular pathways, which can be used as chemical knock-out of a specific gene. The exogenous control of protein function caused by small molecules can be added and washed away at any time points (Blackwell & Zhao, 2003). The rapid and reversible responses of cell biological system to small molecules allow temporal analysis of protein changes. The perturbation caused by small molecules leads to phenotypic responses on the cellular or the organismal level, which facilities the screening of mutants with drug-sensitive nodes (Blackwell & Zhao, 2003).

The most promising contribution of chemical genetics approach is to establish an integrated system to identify more specific and targeted small molecules (Raikhel & Pirrung, 2005). Chemical genetics approach consists of three major steps. The first step is to screen out bioactive ligands of interest from chemical libraries. High-throughput experimental screening and structure-based virtual screening are two major approaches in new ligands identification

(Bajorath, 2002). The second step is to characterize small molecules of interest. Cellular

phenotypes caused by exogenous ligands exhibit biological activity towards small molecules,

which provides a metrics to characterize the diversity of selected chemicals from libraries. The

third step is to identify targets of the small molecule. With specific chemicals, chemical

screening and ligand-protein interaction tests can assist identification of putative target proteins,

which facilitates the application of small molecules in cell biology analysis (Stockwell, 2000).

1.3.2 **Target Protein Identification and Validated Approaches**

Target identification methods are divided into two categories: phenotype-based methods

and affinity-based methods (Lomenick et al., 2009). Phenotype-based methods are affinity-free

and indirect, which relies on physiological responses caused by small molecules. In classical

genetics, according to the phenotypes caused by small molecules, isolating mutants that are

insensitive to the chemical of interest can identify target downstream regulators through genetic

sequencing (Heitman, Movva, & Hall, 1991). Genome-wide expression profiling is an alternative

affinity-free approach to probe the drug target in transcriptome changes using simple model

organisms such as yeast (Luesch et al., 2005).

Affinity-based methods through biochemical analysis show solid bindings between small

molecule and the protein, which is a direct way to detect the drug target (McCourt & Desveaux,

2010). Biochemical protein-binding assays prove the affinity relationship between small

molecules and its target proteins, such as nuclear magnetic resonance (NMR), mass spectrometry

(MS), and fluorescence correlation spectroscopy (Burdine & Kodadek, 2004;Stockwell, 2004).

For example, trapoxin is a derived cyclotetrapeptide and it inhibits histone deacetylation in

mammalian cells. A synthesized analog of trapoxin, K-trap, was used to set up an affinity matrix

and caught binding proteins. Through biochemical analysis, proteins showing binding affinity

with K-trap are related to a histone deacetylase in yeast, Rpd3 (De Rubertis et al., 1996). The target of trapoxin was finally identified to be the human histone deacetylases (HDACs). The identification of trapoxin target proteins highlighted the role of HDACs in repression of gene transcription in mammalian cells (Taunton, Hassig, & Schreiber, 1996).

Among the diverse small molecule target identification methods, quick and inexpensive methods are well developed and applicable for most labs. For instances, Drug Affinity Responsive Target Stability (DARTS) assay is based on the principle that small molecule stabilizes its target protein upon binding and protects the protein from protease digestion (Lomenick et al., 2009). DARTS assay uses native ligand without any chemical modifications or immobilization, which is advantageous in keeping binding specificity and affinity (Pai et al., 2015). Differential scanning fluorimetry (DSF) relies on the thermodynamic stability of ligand-protein interactions (Niesen, Berglund, & Vedadi, 2007). Increasing temperature drives the combination of fluorescent dye and hydrophobic core of unfolding proteins. In presence of small molecules, target proteins are stabilized upon binding and slower protein denaturation is monitored through corresponding changes of fluorescence emission (Vivoli, Novak, Littlechild, & Harmer, 2014). DSF can be conducted in quantitative PCR machine at large scale, which provides a powerful tool for high-throughput chemical library screening (Gao, Oerlemans, & Groves, 2020).

1.3.3 Chemical Genetics Screen and Gene Discovery in Plants

The key to identify novel genes involved in specific molecular pathways in chemical genetics approaches is to obtain mutations in genes that are related to specific ligands. In plant biology, the model plant Arabidopsis is an ideal material for phenotypic screening to identify novel genes (Meinke, Cherry, Dean, Rounsley, & Koornneef, 1998). Ethyl methanesulfonate

(EMS) generates point mutations in Arabidopsis seeds by nucleotide substitution (Sega, 1984).

After the mutagenesis, a large collection of the seeds is systematically screened for specific

phenotypes caused by small molecules. Plants with these phenotypes exhibit various responses at

a seedling age when they are exposed to the specific chemicals. These chemicals target specific

proteins in different molecular pathways and alter the structures of the target proteins. They can

therefore be used to probe biological activities by changing protein functions, mimicking loss-

and gain- of function alleles (Stockwell, 2000).

The goal of phenotypic screening with chemicals is to identify resistant or hypersensitive

mutants (Raikhel & Pirrung, 2005). In resistant mutants, the chemicals lost their target proteins

because of the genetic mutations and the corresponding molecular pathways are no longer

inhibited, so plants show resistance when they are exposed to the drug. Hypersensitivity is

exhibited when plants are treated with low dosage chemicals and perform more sensitivity with

the specific phenotypes, and plants will be back to normal growth once the drug is removed

(Raikhel & Pirrung, 2005). The advantage of using small molecules in forward genetics

screening is that the perturbation of molecular pathways caused by small molecules allow us to

analyze protein alterations *in vivo* temporally, and small molecules probe the gene functions

mimicking the exogenous mutations (Ong et al., 2009).

Chemical genetics in Arabidopsis identify many significant plant growth inhibitors and

discover multiple novel gene in molecular pathways. For example, fermentation-derived

yokonolides A and B probe auxin transduction pathway and inhibit the expression of auxin-

responsive genes (Hayashi, Ogino, Oono, Uchimiya, & Nozaki, 2001). The synthetic molecule

sirtinol affects the development of roots and vascular tissue in Arabidopsis. In chemical

screening of resistant and hypersensitive mutants, auxin-resistance gene AXR1 were screened

out, and sirtinol resistant 1 (SIR1) was identified as a novel negative regulator of auxin signaling (Blackwell & Zhao, 2003;Zhao, Dai, Blackwell, Schreiber, & Chory, 2003). Endosidin20 (ES20) causes short root length and swollen roots in Arabidopsis and chemical genetic analysis revealed that its target is CESA6, which defines ES20 as a novel cellulose synthesis inhibitor (Huang et al., 2020).

1.4   Cellulose and Cellulose Synthase Complex

The major component of the plan cell wall is cellulose, which is the most widely distributed and most abundant polysaccharide on earth and benefits human life in diverse aspects. Cellulose is synthesized by Cellulose Synthase Complex (CSC) at the plasma membrane (Polko & Kieber, 2019).

1.4.1   Cellulose Composition and Function

Plant cell wall determines cell shape, supports plant body structure, and protects cells from pathogens (Lampugnani, Khan, Somssich, & Persson, 2018). The primary component of the cell wall is cellulose, which is a polymer of β-1,4-D-glucose (Burton, Gidley, & Fincher, 2010). In plant cells, cellulose is largely required for the formation of cell wall in growing cells and the formation of cell plate during mitosis (Miart et al., 2014). Apart from plants, microorganisms also produce cellulose. With different structural properties, microbial cellulose is characterized with high purity and moldability (Wang, Tavakoli, & Tang, 2019). For human, cellulosic biofuels is the most cost-effective way to store the energy from sun, which benefits our life in a sustainable way (Carroll & Somerville, 2009).

1.4.2 **Cellulose Synthase and Cellulose Synthase Complex**

The synthesis of cellulose depends on CSCs, which consist of multiple units of cellulose synthase (CESA) forming a rosette hexagonally (Kimura et al., 1999). Arabidopsis genome encodes10 CESA genes. CESA1, CESA3, and CESA6 or CESA6-like (CESA2, CESA5, CESA9) genes are responsible for the primary cell wall formation (Persson et al., 2007), and CESA4, CESA7, and CESA8 are involved in the biosynthesis of the secondary cell wall (Turner & Somerville, 1997). CESAs are hypothesized to be assembled to CSC at the ER or Golgi apparatus and then transported to the plasma membrane to synthesize cellulose. The CSC contains at least 18 units of CESA, and a single CESA protein is 122kDa that contains multiple transmembrane domains and a central catalytic loop for binding substrate uridine diphosphate glucose (UDP-Glucose) (Sethaphong et al., 2013;Hill, Hammudi, & Tien, 2014).

1.4.3 **Subcellular Trafficking of Cellulose Synthase Complex**

As a large protein complex, CSC requires multiple proteins to facilitate its subcellular trafficking. There are many identified proteins involved in the CSC trafficking, such as POM-POM2/cellulose synthase interactive protein 1 (POM2/CSI1) (Gu et al., 2010) and the endoglucanase KORRIGAN1 (KOR1) (Lane et al., 2001). POM2/CSI1 binds to microtubules directly and links CSC to microtubules (Li, Lei, Somerville, & Gu, 2012). As an integral part of CSC, KOR1 is required for cellulose synthesis and the motility of CSCs (Vain et al., 2014).

The subcellular trafficking of CSCs depends on the vesicle transport machinery. Vesicles that contains small CESA compartments (SmaCCs) or microtubule-associated CESA compartments (MASCs) associate with the cortical microtubules (CMT) that defines the delivery sites on the plasma membrane (Crowell et al., 2009;Gutierrez, Lindeboom, Paredez, Emons, & Ehrhardt, 2009). In exocytic route, Golgi-localized STELLO proteins interact with CESAs and

assist the assembly of CSC (Zhang et al., 2016). Exiting from Golgi apparatus, POM2/CSI1 connects PM-localized-CESAs and SmaCCs/MASCs to microtubules (Bringmann et al., 2012). Myosin XI promotes the movement of SmaCCs/MASCs along actin filaments (Zhang, Cai, & Staiger, 2019). PROTON ATPASE TRANSLOCATION CONTROL 1 (PATROL1) protein interacts with POM2/CSI1 and the exocyst complex assisting the exocytic delivery of SmaCCs/MASCs (Zhu, Li, Pan, Xin, & Gu, 2018). The simple model of CESA trafficking is that secretory vesicles containing CESAs are delivered to the insertion sites marked by CMT, with the assistance of POM2/CSI1 and PTL1 interacting with the exocyst complex.

More proteins and trafficking mechanisms related to CSC are being discovered, such as COMPANION OF CELLULOSE SYNTHASE1 (CC1) and SHOU4. As the key to the microtubule binding, CC1 mediates the cortical microtubule array and sustains cellulose synthesis under salt stress (Kesten et al., 2019). SHOU4 is a negative regulator of CESA exocytosis since the disruption of SHOU proteins results in enhanced accumulation of CESA at the plasma membrane (Polko et al., 2018). CSC is one of the cargo proteins in the endomembrane trafficking, and its trafficking mechanisms are essential for understanding how the large protein complexes are trafficking in plant cells.

1.4.4 Cellulose Synthesis Inhibitors and Their Application in Agriculture

Cellulose biosynthesis inhibitor (CBI) refers to small molecules that target CESAs or other required proteins in cellulose synthesis. CBI is a multifunctional toolbox for cellulose study, since small molecules can be developed into herbicides for weed control and decode fundamental mechanisms of cell wall biogenesis combined with genetics (Tateno, Brabham, & DeBolt, 2016).

With the application of time-lapse confocal microscopy, the trafficking velocity and localization of CESA are documented (Paredez, Somerville, & Ehrhardt, 2006). Based on the responses of fluorescently labeled CESAs on the plasma membrane, CBIs are clustered into three primary groups (Tateno, Brabham, & DeBolt, 2016). The first group causes CESA clearance from the plasma membrane and accumulation in MASCs/SmaCCs, which includes isoxaben, thaxtomin A, quinoxyphen, etc. (Duval & Beaudoin, 2009). The second group is small molecules that cause immobility and accumulation of YFP:CESA in the plasma membrane, such as dichlobenil (DCB) (Melida, Caparros-Ruiz, Alvarez, Acebes, & Encina, 2011). Small molecules disrupt the association between CSCs and cortical microtubules is classified as the third group of CBIs. Morlin and cobtorin are chemicals found early in this group (DeBolt et al., 2007;Yoneda et al., 2010).

Isoxaben, thaxtomin A, and Morlin are small molecules that were defined to be CBI at early time. Isoxaben (IXB) has high efficiency in inhibiting growth of broad-leaf plants and it is a widely used herbicide for weed management (Jamet & Thoisy-Dur, 1988). In Arabidopsis cells, IXB was found to inhibit cell wall synthesis, and missense mutations in CESA3 and CESA6 can lead to resistance to IXB (Heim, Skomp, Tschabold, & Larrinua, 1990;Scheible, Eshed, Richmond, Delmer, & Somerville, 2001;Desprez et al., 2002). Thaxtomin A (TA) is a natural toxin secreted by *Streptomyces* eubacteria, a pathogen for potato common scab (King & Calhoun, 2009). TA treatment causes isotropic expansion of hypocotyl cells and inhibits root growth >50% (Scheible et al., 2003). In Arabidopsis, the designated *TXR1* gene exhibits high tolerance to thaxtomin A because of the reduced toxin uptake rate (Scheible et al., 2003). IXB and TA are closely linked inhibitors that can initiate programmed cell death (PCD) in Arabidopsis cells and activate the expression of a similar subset of genes (Duval, Brochu,

Simard, Beaulieu, & Beaudoin, 2005;Duval & Beaudoin, 2009). Morlin is screened out from

chemical libraries because of the swollen root phenotype, and it disrupts the array organization

of cortical microtubules to alter the CESA movement, which makes it a good probe for

understanding the relation between CESA and microtubules (DeBolt et al., 2007).

There are some recently characterized CBIs contributing to this multifunctional toolbox.

Indaziflam is identified as CBI since its treatment causes root swollenness and reduction of

cellulose in a dose-dependent manner (Brabham et al., 2014). Indaziflam treatment causes the

accumulation of CESAs on the plasma membrane at a reduced velocity. The morphology and

motility of microtubules are not affected by indaziflam treatment, but the associations between

CESAs and microtubules are interrupted (Brabham et al., 2014). Its strong CBI activity on

monocotyledons and dicotyledons makes Indaziflam to be a mode for weed management

(Sebastian, Fleming, Patterson, Sebastian, & Nissen, 2017). CESA TRAFFICKING INHIBITOR

(CESTRIN) is an inhibitor to affect proteins involved in CSC trafficking. The localization of

CSC trafficking associated proteins, POM2/CSI1 and KOR1, are interrupted by CESTRIN, and

the stability of microtubules are altered (Worden et al., 2015). The selectivity of CESTRIN is a

good tool in chemical genetics to dissect the trafficking routes of CSC. Through phenotype-

based chemical screening, C17 is identified as a novel CBI, which depletes CSC from the plasma

membrane resulting in a weak cell wall (Hu et al., 2016). Mutations in CESA1 and CESA3 are

able to rescue the C17 triggered growth inhibition, and pentatricopeptide repeat (PPR)-like

proteins (CELL WALL MAINTAINER1 [CWM1] and CWM2) can confer C17 tolerance.

Because of the roles of CWM1 and CWM2 in mitochondrial RNA editing, the tolerance against

cellulose deficiency is most likely linked to mitochondrial defects (Hu et al., 2016). The efficient

growth inhibition of C17 on dicotyledonous crops make it a good candidate for new herbicide by

generating C17-resistent plants (Hu et al., 2019). Endosidin20 targets the catalytic domain of CESA6 to inhibit cellulose synthesis, which is a powerful probe in studying the mechanism of CESA activity and a pre-emergent herbicide for weed control (Huang et al., 2020).

1.5 References

Adams, B. M., Oster, M. E., Hebert, D. N. (2019). Protein Quality Control in the Endoplasmic Reticulum. *Protein J, 38*(3), 317-329.

Alberts, B., Alexander, J., Julian, L., Martin, R., Keith, R., Peter, W. (2002). *Molecular Biology of the Cell. 4th edition*: New York: Garland Science.

Alexandersson, E., Saalbach, G., Larsson, C., Kjellbom, P. (2004). Arabidopsis plasma membrane proteomics identifies components of transport, signal transduction and membrane trafficking. *Plant Cell Physiol, 45*(11), 1543-1556.

Allan, V. J., Thompson, H. M., McNiven, M. A. (2002). Motoring around the Golgi. *Nat Cell Biol, 4*(10), E236-E242.

Backues, S. K., Korasick, D. A., Heese, A., Bednarek, S. Y. (2010). The Arabidopsis dynamin-related protein2 family is essential for gametophyte development. *Plant Cell, 22*(10), 3218-3231.

Bajorath, J. (2002). Integration of virtual and high-throughput screening. *Nat Rev Drug Discov, 1*(11), 882-894.

Bao, Y., Pu, Y., Yu, X., Gregory, B. D., Srivastava, R., Howell, S. H., et al. (2018). IRE1B degrades RNAs encoding proteins that interfere with the induction of autophagy by ER stress in Arabidopsis thaliana. *Autophagy, 14*(9), 1562-1573.

Barberon, M., Zelazny, E., Robert, S., Conejero, G., Curie, C., Friml, J., et al. (2011). Monoubiquitin-dependent endocytosis of the iron-regulated transporter 1 (IRT1) transporter controls iron uptake in plants. *Proc Natl Acad Sci U S A, 108*(32), E450-E458.

Barlowe, C., Orci, L., Yeung, T., Hosobuchi, M., Hamamoto, S., Salama, N., et al. (1994). COPII: a membrane coat formed by Sec proteins that drive vesicle budding from the endoplasmic reticulum. *Cell, 77*(6), 895-907.

Barlowe, C., Schekman, R. (1993). SEC12 encodes a guanine-nucleotide-exchange factor essential for transport vesicle budding from the ER. *Nature, 365*(6444), 347-349.

Basu, D., Le J, Zakharova, T., Mallery, E. L., Szymanski, D. B. (2008). A SPIKE1 signaling complex controls actin-dependent cell morphogenesis through the heteromeric WAVE and ARP2/3 complexes. *Proc Natl Acad Sci U S A, 105*(10), 4044-4049.

Becker, B. (2007). Function and evolution of the vacuolar compartment in green algae and land plants (Viridiplantae). *Int Rev Cytol, 264*, 1-24.

Bednarek, S. Y., Backues, S. K. (2010). Plant dynamin-related protein families DRP1 and DRP2 in plant development. *Biochem Soc Trans, 38*(3), 797-806.

Bi, X., Corpina, R. A., Goldberg, J. (2002). Structure of the Sec23/24-Sar1 pre-budding complex of the COPII vesicle coat. *Nature, 419*(6904), 271-277.

Blackwell, H. E., Zhao, Y. (2003). Chemical genetic approaches to plant biology. *Plant Physiol, 133*(2), 448-455.

Bloch, D., Pleskot, R., Pejchar, P., Potocky, M., Trpkosova, P., Cwiklik, L., et al. (2016). Exocyst SEC3 and Phosphoinositides Define Sites of Exocytosis in Pollen Tube Initiation and Growth. *Plant Physiol, 172*(2), 980-1002.

Bonifacino, J. S., Glick, B. S. (2004). The mechanisms of vesicle budding and fusion. *Cell, 116*(2), 153-166.

Boyd, C., Hughes, T., Pypaert, M., Novick, P. (2004). Vesicles carry most exocyst subunits to exocytic sites marked by the remaining two subunits, Sec3p and Exo70p. *J Cell Biol, 167*(5), 889-901.

Brabham, C., Lei, L., Gu, Y., Stork, J., Barrett, M., DeBolt, S. (2014). Indaziflam herbicidal action: a potent cellulose biosynthesis inhibitor. *Plant Physiol, 166*(3), 1177-1185.

Bringmann, M., Li, E., Sampathkumar, A., Kocabek, T., Hauser, M. T., Persson, S. (2012). POM-POM2/cellulose synthase interacting1 is essential for the functional association of cellulose synthase and microtubules in Arabidopsis. *Plant Cell, 24*(1), 163-177.

Burdine, L., Kodadek, T. (2004). Target identification in chemical genetics: the (often) missing link. *Chem Biol, 11*(5), 593-597.

Burton, R. A., Gidley, M. J., Fincher, G. B. (2010). Heterogeneity in the chemistry, structure and function of plant cell walls. *Nat Chem Biol, 6*(10), 724-732.

Camacho, L., Smertenko, A. P., Perez-Gomez, J., Hussey, P. J., Moore, I. (2009). Arabidopsis Rab-E GTPases exhibit a novel interaction with a plasma-membrane phosphatidylinositol-4-phosphate 5-kinase. *J Cell Sci, 122*(Pt 23), 4383-4392.

Candela, H., Perez-Perez, J. M., Micol, J. L. (2011). Uncovering the post-embryonic functions of gametophytic- and embryonic-lethal genes. *Trends Plant Sci, 16*(6), 336-345.

Carroll, A., Somerville, C. (2009). Cellulosic biofuels. *Annu Rev Plant Biol, 60*, 165-182.

Chakrabarti, A., Chen, A. W., Varner, J. D. (2011). A review of the mammalian unfolded protein response. *Biotechnol Bioeng, 108*(12), 2777-2793.

Chen, R., Hilson, P., Sedbrook, J., Rosen, E., Caspar, T., Masson, P. H. (1998). The arabidopsis thaliana AGRAVITROPIC 1 gene encodes a component of the polar-auxin-transport efflux carrier. *Proc Natl Acad Sci U S A, 95*(25), 15112-15117.

Chen, Y., Brandizzi, F. (2012). AtIRE1A/AtIRE1B and AGB1 independently control two essential unfolded protein response pathways in Arabidopsis. *Plant J, 69*(2), 266-277.

Chen, Y., Brandizzi, F. (2013). IRE1: ER stress sensor and cell fate executor. *Trends Cell Biol, 23*(11), 547-555.

Cherepanova, N., Shrimal, S., Gilmore, R. (2016). N-linked glycosylation and homeostasis of the endoplasmic reticulum. *Curr Opin Cell Biol, 41*, 57-65.

Chrispeels, M. J., Crawford, N. M., Schroeder, J. I. (1999). Proteins for transport of water and mineral nutrients across the membranes of plant cells. *Plant Cell, 11*(4), 661-676.

Chung, K. P., Zeng, Y. (2017). An Overview of Protein Secretion in Plant Cells. *Methods Mol Biol, 1662*, 19-32.

Crowell, E. F., Bischoff, V., Desprez, T., Rolland, A., Stierhof, Y. D., Schumacher, K., et al. (2009). Pausing of Golgi bodies on microtubules regulates secretion of cellulose synthase complexes in Arabidopsis. *Plant Cell, 21*(4), 1141-1154.

Cruz-Garcia, D., Malhotra, V., Curwin, A. J. (2018). Unconventional protein secretion triggered by nutrient starvation. *Semin Cell Dev Biol, 83*, 22-28.

Cui, Y., Zhao, Q., Hu, S., Jiang, L. (2020). Vacuole Biogenesis in Plants: How Many Vacuoles, How Many Models? *Trends Plant Sci, 25*(6), 538-548.

Cvrckova, F., Grunt, M., Bezvoda, R., Hala, M., Kulich, I., Rawat, A., et al. (2012). Evolution of the land plant exocyst complexes. *Front Plant Sci, 3*, 159.

de Marcos, L. C., Denecke, J. (2016). Lysosomal and vacuolar sorting: not so different after all!. *Biochem Soc Trans, 44*(3), 891-897.

De Rubertis, F., Kadosh, D., Henchoz, S., Pauli, D., Reuter, G., Struhl, K., et al. (1996). The histone deacetylase RPD3 counteracts genomic silencing in Drosophila and yeast. *Nature, 384*(6609), 589-591.

DeBolt, S., Gutierrez, R., Ehrhardt, D. W., Melo, C. V., Ross, L., Cutler, S. R., et al. (2007). Morlin, an inhibitor of cortical microtubule dynamics and cellulose synthase movement. *Proc Natl Acad Sci U S A, 104*(14), 5854-5859.

Deng, Y., Humbert, S., Liu, J. X., Srivastava, R., Rothstein, S. J., Howell, S. H. (2011). Heat induces the splicing by IRE1 of a mRNA encoding a transcription factor involved in the unfolded protein response in Arabidopsis. *Proc Natl Acad Sci U S A, 108*(17), 7247-7252.

Desprez, T., Vernhettes, S., Fagard, M., Refregier, G., Desnos, T., Aletti, E., et al. (2002). Resistance against herbicide isoxaben and cellulose deficiency caused by distinct mutations in same cellulose synthase isoform CESA6. *Plant Physiol, 128*(2), 482-490.

Dhonukshe, P., Aniento, F., Hwang, I., Robinson, D. G., Mravec, J., Stierhof, Y. D., et al. (2007). Clathrin-mediated constitutive endocytosis of PIN auxin efflux carriers in Arabidopsis. *Curr Biol, 17*(6), 520-527.

Donaldson, J. G., Cassel, D., Kahn, R. A., Klausner, R. D. (1992). ADP-ribosylation factor, a small GTP-binding protein, is required for binding of the coatomer protein beta-COP to Golgi membranes. *Proc Natl Acad Sci U S A, 89*(14), 6408-6412.

Donohoe, B. S., Kang, B. H., Gerl, M. J., Gergely, Z. R., McMichael, C. M., Bednarek, S. Y., et al. (2013). Cis-Golgi cisternal assembly and biosynthetic activation occur sequentially in plants and algae. *Traffic, 14*(5), 551-567.

Donohoe, B. S., Kang, B. H., Staehelin, L. A. (2007). Identification and characterization of COPIa- and COPIb-type vesicle classes associated with plant and algal Golgi. *Proc Natl Acad Sci U S A, 104*(1), 163-168.

Driouich, A., Follet-Gueye, M. L., Bernard, S., Kousar, S., Chevalier, L., Vicre-Gibouin, M., et al. (2012). Golgi-mediated synthesis and secretion of matrix polysaccharides of the primary cell wall of higher plants. *Front Plant Sci, 3*, 79.

Dunphy, W. G., Rothman, J. E. (1985). Compartmental organization of the Golgi stack. *Cell, 42*(1), 13-21.

Dupree, P., Sherrier, D. J. (1998). The plant Golgi apparatus. *Biochim Biophys Acta, 1404*(1-2), 259-270.

Duval, I., Beaudoin, N. (2009). Transcriptional profiling in response to inhibition of cellulose synthesis by thaxtomin A and isoxaben in Arabidopsis thaliana suspension cells. *Plant Cell Rep, 28*(5), 811-830.

Duval, I., Brochu, V., Simard, M., Beaulieu, C., Beaudoin, N. (2005). Thaxtomin A induces programmed cell death in Arabidopsis thaliana suspension-cultured cells. *Planta, 222*(5), 820-831.

Ebine, K., Inoue, T., Ito, J., Ito, E., Uemura, T., Goh, T., et al. (2014). Plant vacuolar trafficking occurs through distinctly regulated pathways. *Curr Biol, 24*(12), 1375-1382.

Elias, M., Drdova, E., Ziak, D., Bavlnka, B., Hala, M., Cvrckova, F., et al. (2003). The exocyst complex in plants. *Cell Biol Int, 27*(3), 199-201.

Etxeberria, E., Pozueta-Romero, J., Gonzalez, P. (2012). In and out of the plant storage vacuole. *Plant Sci, 190*, 52-61.

Fan, L., Li, R., Pan, J., Ding, Z., Lin, J. (2015). Endocytosis and its regulation in plants. *Trends Plant Sci, 20*(6), 388-397.

Feng, J., He, L., Li, Y., Xiao, F., Hu, G. (2019). Modeling of PH Domains and Phosphoinositides Interactions and Beyond. *Adv Exp Med Biol, 1111*, 19-32.

Finger, F. P., Hughes, T. E., Novick, P. (1998). Sec3p is a spatial landmark for polarized secretion in budding yeast. *Cell, 92*(4), 559-571.

Fujimoto, M., Tsutsumi, N. (2014). Dynamin-related proteins in plant post-Golgi traffic. *Front Plant Sci, 5*, 408.

Galweiler, L., Guan, C., Muller, A., Wisman, E., Mendgen, K., Yephremov, A., et al. (1998). Regulation of polar auxin transport by AtPIN1 in Arabidopsis vascular tissue. *Science, 282*(5397), 2226-2230.

Gao, H., Brandizzi, F., Benning, C., Larkin, R. M. (2008). A membrane-tethered transcription factor defines a branch of the heat stress response in Arabidopsis thaliana. *Proc Natl Acad Sci U S A, 105*(42), 16398-16403.

Gao, K., Oerlemans, R., Groves, M. R. (2020). Theory and applications of differential scanning fluorimetry in early-stage drug discovery. *Biophys Rev, 12*(1), 85-104.

Gao, X. Q., Li, C. G., Wei, P. C., Zhang, X. Y., Chen, J., Wang, X. C. (2005). The dynamic changes of tonoplasts in guard cells are important for stomatal movement in Vicia faba. *Plant Physiol, 139*(3), 1207-1216.

Geldner, N., Hyman, D. L., Wang, X., Schumacher, K., Chory, J. (2007). Endosomal signaling of plant steroid receptor kinase BRI1. *Genes Dev, 21*(13), 1598-1602.

Giuliani, F., Grieve, A., Rabouille, C. (2011). Unconventional secretion: a stress on GRASP. *Curr Opin Cell Biol, 23*(4), 498-504.

Gu, Y., Innes, R. W. (2012). The KEEP ON GOING protein of Arabidopsis regulates intracellular protein trafficking and is degraded during fungal infection. *Plant Cell, 24*(11), 4717-4730.

Gu, Y., Kaplinsky, N., Bringmann, M., Cobb, A., Carroll, A., Sampathkumar, A., et al. (2010). Identification of a cellulose synthase-associated protein required for cellulose biosynthesis. *Proc Natl Acad Sci U S A, 107*(29), 12866-12871.

Gu, Y., Zavaliev, R., Dong, X. (2017). Membrane Trafficking in Plant Immunity. *Mol Plant, 10*(8), 1026-1034.

Guo, W., Roth, D., Walch-Solimena, C., Novick, P. (1999). The exocyst is an effector for Sec4p, targeting secretory vesicles to sites of exocytosis. *EMBO J, 18*(4), 1071-1080.

Gutierrez, R., Lindeboom, J. J., Paredez, A. R., Emons, A. M., Ehrhardt, D. W. (2009). Arabidopsis cortical microtubules position cellulose synthase delivery to the plasma membrane and interact with cellulose synthase trafficking compartments. *Nat Cell Biol, 11*(7), 797-806.

Hanamata, S., Kurusu, T., Kuchitsu, K. (2014). Roles of autophagy in male reproductive development in plants. *Front Plant Sci, 5*, 457.

Hartwell, L. H. (1991). Twenty-five years of cell cycle genetics. *Genetics, 129*(4), 975-980.

Hawes, C., Schoberer, J., Hummel, E., Osterrieder, A. (2010). Biogenesis of the plant Golgi apparatus. *Biochem Soc Trans, 38*(3), 761-767.

Hayashi, K., Ogino, K., Oono, Y., Uchimiya, H., Nozaki, H. (2001). Yokonolide A, a new inhibitor of auxin signal transduction, from Streptomyces diastatochromogenes B59. *J Antibiot (Tokyo), 54*(7), 573-581.

He, B., Xi, F., Zhang, X., Zhang, J., Guo, W. (2007). Exo70 interacts with phospholipids and mediates the targeting of the exocyst to the plasma membrane. *EMBO J, 26*(18), 4053-4065.

Heim, D. R., Skomp, J. R., Tschabold, E. E., Larrinua, I. M. (1990). Isoxaben Inhibits the Synthesis of Acid Insoluble Cell Wall Materials In Arabidopsis thaliana. *Plant Physiol, 93*(2), 695-700.

Heitman, J., Movva, N. R., Hall, M. N. (1991). Targets for cell cycle arrest by the immunosuppressant rapamycin in yeast. *Science, 253*(5022), 905-909.

Hetz, C., Papa, F. R. (2018). The Unfolded Protein Response and Cell Fate Control. *Mol Cell, 69*(2), 169-181.

Hicke, L., Dunn, R. (2003). Regulation of membrane protein transport by ubiquitin and ubiquitin-binding proteins. *Annu Rev Cell Dev Biol, 19*, 141-172.

Hill, J. J., Hammudi, M. B., Tien, M. (2014). The Arabidopsis cellulose synthase complex: a proposed hexamer of CESA trimers in an equimolar stoichiometry. *Plant Cell, 26*(12), 4834-4842.

Hillary, R. F., FitzGerald, U. (2018). A lifetime of stress: ATF6 in development and homeostasis. *J Biomed Sci, 25*(1), 48.

Hoffmann, A., Nebenfuhr, A. (2004). Dynamic rearrangements of transvacuolar strands in BY-2 cells imply a role of myosin in remodeling the plant actin cytoskeleton. *Protoplasma, 224*(3-4), 201-210.

Honig, A., Avin-Wittenberg, T., Ufaz, S., Galili, G. (2012). A new type of compartment, defined by plant-specific Atg8-interacting proteins, is induced upon exposure of Arabidopsis plants to carbon starvation. *Plant Cell, 24*(1), 288-303.

Hu, Z., Vanderhaeghen, R., Cools, T., Wang, Y., De Clercq, I., Leroux, O., et al. (2016). Mitochondrial Defects Confer Tolerance against Cellulose Deficiency. *Plant Cell, 28*(9), 2276-2290.

Hu, Z., Zhang, T., Rombaut, D., Decaestecker, W., Xing, A., D'Haeyer, S., et al. (2019). Genome Editing-Based Engineering of CESA3 Dual Cellulose-Inhibitor-Resistant Plants. *Plant Physiol, 180*(2), 827-836.

Huang, L., Li, X., Zhang, W., Ung, N., Liu, N., Yin, X., et al. (2020). Endosidin20 Targets the Cellulose Synthase Catalytic Domain to Inhibit Cellulose Biosynthesis. *Plant Cell*.

Ito, Y., Uemura, T., Nakano, A. (2014). Formation and maintenance of the Golgi apparatus in plant cells. *Int Rev Cell Mol Biol, 310*, 221-287.

Jackson, C. L., Casanova, J. E. (2000). Turning on ARF: the Sec7 family of guanine-nucleotide-exchange factors. *Trends Cell Biol, 10*(2), 60-67.

Jacobson, K., Liu, P., Lagerholm, B. C. (2019). The Lateral Organization and Mobility of Plasma Membrane Components. *Cell, 177*(4), 806-819.

Jaillais, Y., Fobis-Loisy, I., Miege, C., Rollin, C., Gaude, T. (2006). AtSNX1 defines an endosome for auxin-carrier trafficking in Arabidopsis. *Nature, 443*(7107), 106-109.

Jaillais, Y., Santambrogio, M., Rozier, F., Fobis-Loisy, I., Miege, C., Gaude, T. (2007). The retromer protein VPS29 links cell polarity and organ initiation in plants. *Cell, 130*(6), 1057-1070.

Jamet, P., Thoisy-Dur, J. C. (1988). Pesticide mobility in soils: assessment of the movement of isoxaben by soil thin-layer chromatography. *Bull Environ Contam Toxicol, 41*(1), 135-142.

Jauh, G. Y., Fischer, A. M., Grimes, H. D., Ryan, C. J., Rogers, J. C. (1998). delta-Tonoplast intrinsic protein defines unique plant vacuole functions. *Proc Natl Acad Sci U S A, 95*(22), 12995-12999.

Jauh, G. Y., Phillips, T. E., Rogers, J. C. (1999). Tonoplast intrinsic protein isoforms as markers for vacuolar functions. *Plant Cell, 11*(10), 1867-1882.

Jolliffe, N. A., Craddock, C. P., Frigerio, L. (2005). Pathways for protein transport to seed storage vacuoles. *Biochem Soc Trans, 33*(Pt 5), 1016-1018.

Kang, H., Kim, S. Y., Song, K., Sohn, E. J., Lee, Y., Lee, D. W., et al. (2012). Trafficking of vacuolar proteins: the crucial role of Arabidopsis vacuolar protein sorting 29 in recycling vacuolar sorting receptor. *Plant Cell, 24*(12), 5058-5073.

Kasai, K., Takano, J., Miwa, K., Toyoda, A., Fujiwara, T. (2011). High boron-induced ubiquitination regulates vacuolar sorting of the BOR1 borate transporter in Arabidopsis thaliana. *J Biol Chem, 286*(8), 6175-6183.

Kesten, C., Wallmann, A., Schneider, R., McFarlane, H. E., Diehl, A., Khan, G. A., et al. (2019). The companion of cellulose synthase 1 confers salt tolerance through a Tau-like mechanism in plants. *Nat Commun, 10*(1), 857.

Kimura, S., Laosinchai, W., Itoh, T., Cui, X., Linder, C. R., Brown, R. J. (1999). Immunogold labeling of rosette terminal cellulose-synthesizing complexes in the vascular plant vigna angularis. *Plant Cell, 11*(11), 2075-2086.

King, R. R., Calhoun, L. A. (2009). The thaxtomin phytotoxins: sources, synthesis, biosynthesis, biotransformation and biological activity. *Phytochemistry, 70*(7), 833-841.

Krysan, P. J., Young, J. C., Sussman, M. R. (1999). T-DNA as an insertional mutagen in Arabidopsis. *Plant Cell, 11*(12), 2283-2290.

Kwon, Y., Shen, J., Lee, M. H., Geem, K. R., Jiang, L., Hwang, I. (2018). AtCAP2 is crucial for lytic vacuole biogenesis during germination by positively regulating vacuolar protein trafficking. *Proc Natl Acad Sci U S A, 115*(7), E1675-E1683.

Lam, B. C., Sage, T. L., Bianchi, F., Blumwald, E. (2001). Role of SH3 domain-containing proteins in clathrin-mediated vesicle trafficking in Arabidopsis. *Plant Cell, 13*(11), 2499-2512.

Lampugnani, E. R., Khan, G. A., Somssich, M., Persson, S. (2018). Building a plant cell wall at a glance. *J Cell Sci, 131*(2).

Lane, D. R., Wiedemeier, A., Peng, L., Hofte, H., Vernhettes, S., Desprez, T., et al. (2001). Temperature-sensitive alleles of RSW2 link the KORRIGAN endo-1,4-beta-glucanase to cellulose synthesis and cytokinesis in Arabidopsis. *Plant Physiol, 126*(1), 278-288.

Lebeau, J., Saunders, J. M., Moraes, V., Madhavan, A., Madrazo, N., Anthony, M. C., et al. (2018). The PERK Arm of the Unfolded Protein Response Regulates Mitochondrial Morphology during Acute Endoplasmic Reticulum Stress. *Cell Rep, 22*(11), 2827-2836.

Lee, Y. J., Szumlanski, A., Nielsen, E., Yang, Z. (2008). Rho-GTPase-dependent filamentous actin dynamics coordinate vesicle targeting and exocytosis during tip growth. *J Cell Biol, 181*(7), 1155-1168.

Letourneur, F., Gaynor, E. C., Hennecke, S., Demolliere, C., Duden, R., Emr, S. D., et al. (1994). Coatomer is essential for retrieval of dilysine-tagged proteins to the endoplasmic reticulum. *Cell, 79*(7), 1199-1207.

Li, H., Marshall, A. J. (2015). Phosphatidylinositol (3,4) bisphosphate-specific phosphatases and effector proteins: A distinct branch of PI3K signaling. *Cell Signal, 27*(9), 1789-1798.

Li, L. J., Ren, F., Gao, X. Q., Wei, P. C., Wang, X. C. (2013). The reorganization of actin filaments is required for vacuolar fusion of guard cells during stomatal opening in Arabidopsis. *Plant Cell Environ, 36*(2), 484-497.

Li, S., Lei, L., Somerville, C. R., Gu, Y. (2012). Cellulose synthase interactive protein 1 (CSI1) links microtubules and cellulose synthase complexes. *Proc Natl Acad Sci U S A, 109*(1), 185-190.

Li, S., van Os, G. M., Ren, S., Yu, D., Ketelaar, T., Emons, A. M., et al. (2010). Expression and functional analyses of EXO70 genes in Arabidopsis implicate their roles in regulating cell type-specific exocytosis. *Plant Physiol, 154*(4), 1819-1830.

Li, Y., Tan, X., Wang, M., Li, B., Zhao, Y., Wu, C., et al. (2017). Exocyst subunit SEC3A marks the germination site and is essential for pollen germination in Arabidopsis thaliana. *Sci Rep, 7*, 40279.

Lin, D., Cao, L., Zhou, Z., Zhu, L., Ehrhardt, D., Yang, Z., et al. (2013). Rho GTPase signaling activates microtubule severing to promote microtubule ordering in Arabidopsis. *Curr Biol, 23*(4), 290-297.

Liu, J. X., Srivastava, R., Che, P., Howell, S. H. (2007). An endoplasmic reticulum stress response in Arabidopsis is mediated by proteolytic processing and nuclear relocation of a membrane-associated transcription factor, bZIP28. *Plant Cell, 19*(12), 4111-4119.

Liu, J., Zuo, X., Yue, P., Guo, W. (2007). Phosphatidylinositol 4,5-bisphosphate mediates the targeting of the exocyst to the plasma membrane for exocytosis in mammalian cells. *Mol Biol Cell, 18*(11), 4483-4492.

Liu, Y., Burgos, J. S., Deng, Y., Srivastava, R., Howell, S. H., Bassham, D. C. (2012). Degradation of the endoplasmic reticulum by autophagy during endoplasmic reticulum stress in Arabidopsis. *Plant Cell, 24*(11), 4635-4651.

Liu, Y., Xiong, Y., Bassham, D. C. (2009). Autophagy is required for tolerance of drought and salt stress in plants. *Autophagy, 5*(7), 954-963.

Lomenick, B., Hao, R., Jonai, N., Chin, R. M., Aghajan, M., Warburton, S., et al. (2009). Target identification using drug affinity responsive target stability (DARTS). *Proc Natl Acad Sci U S A, 106*(51), 21984-21989.

Luesch, H., Wu, T. Y., Ren, P., Gray, N. S., Schultz, P. G., Supek, F. (2005). A genome-wide overexpression screen in yeast for small-molecule target identification. *Chem Biol, 12*(1), 55-63.

Luo, N., Yan, A., Liu, G., Guo, J., Rong, D., Kanaoka, M. M., et al. (2017). Exocytosis-coordinated mechanisms for tip growth underlie pollen tube growth guidance. *Nat Commun, 8*(1), 1687.

Luschnig, C., Vert, G. (2014). The dynamics of plant plasma membrane proteins: PINs and beyond. *Development, 141*(15), 2924-2938.

Maeshima, M. (2001). TONOPLAST TRANSPORTERS: Organization and Function. *Annu Rev Plant Physiol Plant Mol Biol, 52*, 469-497.

Mamode, C. A., Gouguet, P., Gronnier, J., Laurent, N., Germain, V., Grison, M., et al. (2019). Plant lipids: Key players of plasma membrane organization and function. *Prog Lipid Res, 73*, 1-27.

Mandon, E. C., Trueman, S. F., Gilmore, R. (2013). Protein translocation across the rough endoplasmic reticulum. *Cold Spring Harb Perspect Biol, 5*(2).

Manolea, F., Claude, A., Chun, J., Rosas, J., Melancon, P. (2008). Distinct functions for Arf guanine nucleotide exchange factors at the Golgi complex: GBF1 and BIGs are required for assembly and maintenance of the Golgi stack and trans-Golgi network, respectively. *Mol Biol Cell, 19*(2), 523-535.

Marchant, A., Kargul, J., May, S. T., Muller, P., Delbarre, A., Perrot-Rechenmann, C., et al. (1999). AUX1 regulates root gravitropism in Arabidopsis by facilitating auxin uptake within root apical tissues. *EMBO J, 18*(8), 2066-2073.

Marty, F. (1999). Plant vacuoles. *Plant Cell, 11*(4), 587-600.

Matsuoka, K., Schekman, R., Orci, L., Heuser, J. E. (2001). Surface structure of the COPII-coated vesicle. *Proc Natl Acad Sci U S A, 98*(24), 13705-13709.

Matsuura-Tokita, K., Takeuchi, M., Ichihara, A., Mikuriya, K., Nakano, A. (2006). Live imaging of yeast Golgi cisternal maturation. *Nature, 441*(7096), 1007-1010.

McCourt, P., Desveaux, D. (2010). Plant chemical genetics. *New Phytol, 185*(1), 15-26.

Mei, K., Li, Y., Wang, S., Shao, G., Wang, J., Ding, Y., et al. (2018). Cryo-EM structure of the exocyst complex. *Nat Struct Mol Biol, 25*(2), 139-146.

Meinke, D. W., Cherry, J. M., Dean, C., Rounsley, S. D., Koornneef, M. (1998). Arabidopsis thaliana: a model plant for genome analysis. *Science, 282*(5389), 662, 679-682.

Melida, H., Caparros-Ruiz, D., Alvarez, J., Acebes, J. L., Encina, A. (2011). Deepening into the proteome of maize cells habituated to the cellulose biosynthesis inhibitor dichlobenil. *Plant Signal Behav, 6*(1), 143-146.

Mellman, I., Warren, G. (2000). The road taken: past and future foundations of membrane traffic. *Cell, 100*(1), 99-112.

Miart, F., Desprez, T., Biot, E., Morin, H., Belcram, K., Hofte, H., et al. (2014). Spatio-temporal analysis of cellulose synthesis during cell plate formation in Arabidopsis. *Plant J, 77*(1), 71-84.

Moller, M. N., Cuevasanta, E., Orrico, F., Lopez, A. C., Thomson, L., Denicola, A. (2019). Diffusion and Transport of Reactive Species Across Cell Membranes. *Adv Exp Med Biol, 1127*, 3-19.

Moore, P. J., Swords, K. M., Lynch, M. A., Staehelin, L. A. (1991). Spatial organization of the assembly pathways of glycoproteins and complex polysaccharides in the Golgi apparatus of plants. *J Cell Biol, 112*(4), 589-602.

Muntz, K. (2007). Protein dynamics and proteolysis in plant vacuoles. *J Exp Bot, 58*(10), 2391-2407.

Nebenfuhr, A., Frohlick, J. A., Staehelin, L. A. (2000). Redistribution of Golgi stacks and other organelles during mitosis and cytokinesis in plant cells. *Plant Physiol, 124*(1), 135-151.

Nebenfuhr, A., Gallagher, L. A., Dunahay, T. G., Frohlick, J. A., Mazurkiewicz, A. M., Meehl, J. B., et al. (1999). Stop-and-go movements of plant Golgi stacks are mediated by the acto-myosin system. *Plant Physiol, 121*(4), 1127-1142.

Niesen, F. H., Berglund, H., Vedadi, M. (2007). The use of differential scanning fluorimetry to detect ligand interactions that promote protein stability. *Nat Protoc, 2*(9), 2212-2221.

Novick, P., Field, C., Schekman, R. (1980). Identification of 23 complementation groups required for post-translational events in the yeast secretory pathway. *Cell, 21*(1), 205-215.

Oka, O. B., Bulleid, N. J. (2013). Forming disulfides in the endoplasmic reticulum. *Biochim Biophys Acta, 1833*(11), 2425-2429.

Ong, S. E., Schenone, M., Margolin, A. A., Li, X., Do, K., Doud, M. K., et al. (2009). Identifying the proteins to which small-molecule probes and drugs bind in cells. *Proc Natl Acad Sci U S A, 106*(12), 4617-4622.

Pai, M. Y., Lomenick, B., Hwang, H., Schiestl, R., McBride, W., Loo, J. A., et al. (2015). Drug affinity responsive target stability (DARTS) for small-molecule target identification. *Methods Mol Biol, 1263*, 287-298.

Palmgren, M. G. (2001). PLANT PLASMA MEMBRANE H+-ATPases: Powerhouses for Nutrient Uptake. *Annu Rev Plant Physiol Plant Mol Biol, 52*, 817-845.

Paredez, A. R., Somerville, C. R., Ehrhardt, D. W. (2006). Visualization of cellulose synthase demonstrates functional association with microtubules. *Science, 312*(5779), 1491-1495.

Paris, N., Stanley, C. M., Jones, R. L., Rogers, J. C. (1996). Plant cells contain two functionally distinct vacuolar compartments. *Cell, 85*(4), 563-572.

Pawlowicz, I., Masajada, K. (2019). Aquaporins as a link between water relations and photosynthetic pathway in abiotic stress tolerance in plants. *Gene, 687*, 166-172.

Persson, S., Paredez, A., Carroll, A., Palsdottir, H., Doblin, M., Poindexter, P., et al. (2007). Genetic evidence for three unique components in primary cell-wall cellulose synthase complexes in Arabidopsis. *Proc Natl Acad Sci U S A, 104*(39), 15566-15571.

Phillips, M. J., Voeltz, G. K. (2016). Structure and function of ER membrane contact sites with other organelles. *Nat Rev Mol Cell Biol, 17*(2), 69-82.

Polishchuk, R. S., Polishchuk, E. V., Mironov, A. A. (1999). Coalescence of Golgi fragments in microtubule-deprived living cells. *Eur J Cell Biol, 78*(3), 170-185.

Polko, J. K., Barnes, W. J., Voiniciuc, C., Doctor, S., Steinwand, B., Hill, J. J., et al. (2018). SHOU4 Proteins Regulate Trafficking of Cellulose Synthase Complexes to the Plasma Membrane. *Curr Biol, 28*(19), 3174-3182.

Polko, J. K., Kieber, J. J. (2019). The Regulation of Cellulose Biosynthesis in Plants. *Plant Cell, 31*(2), 282-296.

Preuss, D., Mulholland, J., Franzusoff, A., Segev, N., Botstein, D. (1992). Characterization of the Saccharomyces Golgi complex through the cell cycle by immunoelectron microscopy. *Mol Biol Cell, 3*(7), 789-803.

Pucadyil, T. J., Schmid, S. L. (2008). Real-time visualization of dynamin-catalyzed membrane fission and vesicle release. *Cell, 135*(7), 1263-1275.

Rabouille, C. (2017). Pathways of Unconventional Protein Secretion. *Trends Cell Biol, 27*(3), 230-240.

Rabouille, C., Malhotra, V., Nickel, W. (2012). Diversity in unconventional protein secretion. *J Cell Sci, 125*(Pt 22), 5251-5255.

Raikhel, N., Pirrung, M. (2005). Adding precision tools to the plant biologists' toolbox with chemical genomics. *Plant Physiol, 138*(2), 563-564.

Rambourg, A., Clermont, Y., Kepes, F. (1993). Modulation of the Golgi apparatus in Saccharomyces cerevisiae sec7 mutants as seen by three-dimensional electron microscopy. *Anat Rec, 237*(4), 441-452.

Reiner, D. J., Lundquist, E. A. (2018). Small GTPases. *WormBook, 2018*, 1-65.

Reyes, F. C., Buono, R., Otegui, M. S. (2011). Plant endosomal trafficking pathways. *Curr Opin Plant Biol, 14*(6), 666-673.

Robert, S., Chary, S. N., Drakakaki, G., Li, S., Yang, Z., Raikhel, N. V., et al. (2008). Endosidin1 defines a compartment involved in endocytosis of the brassinosteroid receptor BRI1 and the auxin transporters PIN2 and AUX1. *Proc Natl Acad Sci U S A, 105*(24), 8464-8469.

Robinson, D. G., Brandizzi, F., Hawes, C., Nakano, A. (2015). Vesicles versus Tubes: Is Endoplasmic Reticulum-Golgi Transport in Plants Fundamentally Different from Other Eukaryotes? *Plant Physiol, 168*(2), 393-406.

Robinson, M. S. (2015). Forty Years of Clathrin-coated Vesicles. *Traffic, 16*(12), 1210-1238.

Rojo, E., Denecke, J. (2008). What is moving in the secretory pathway of plants? *Plant Physiol, 147*(4), 1493-1503.

Roumanie, O., Wu, H., Molk, J. N., Rossi, G., Bloom, K., Brennwald, P. (2005). Rho GTPase regulation of exocytosis in yeast is independent of GTP hydrolysis and polarization of the exocyst complex. *J Cell Biol, 170*(4), 583-594.

Safavian, D., Zayed, Y., Indriolo, E., Chapman, L., Ahmed, A., Goring, D. R. (2015). RNA Silencing of Exocyst Genes in the Stigma Impairs the Acceptance of Compatible Pollen in Arabidopsis. *Plant Physiol, 169*(4), 2526-2538.

Saito, C., Ueda, T., Abe, H., Wada, Y., Kuroiwa, T., Hisada, A., et al. (2002). A complex and mobile structure forms a distinct subregion within the continuous vacuolar membrane in young cotyledons of Arabidopsis. *Plant J, 29*(3), 245-255.

Saraogi, I., Shan, S. O. (2011). Molecular mechanism of co-translational protein targeting by the signal recognition particle. *Traffic, 12*(5), 535-542.

Sawa, S., Koizumi, K., Naramoto, S., Demura, T., Ueda, T., Nakano, A., et al. (2005). DRP1A is responsible for vascular continuity synergistically working with VAN3 in Arabidopsis. *Plant Physiol, 138*(2), 819-826.

Scheible, W. R., Eshed, R., Richmond, T., Delmer, D., Somerville, C. (2001). Modifications of cellulose synthase confer resistance to isoxaben and thiazolidinone herbicides in Arabidopsis Ixr1 mutants. *Proc Natl Acad Sci U S A, 98*(18), 10079-10084.

Scheible, W. R., Fry, B., Kochevenko, A., Schindelasch, D., Zimmerli, L., Somerville, S., et al. (2003). An Arabidopsis mutant resistant to thaxtomin A, a cellulose synthesis inhibitor from Streptomyces species. *Plant Cell, 15*(8), 1781-1794.

Sebastian, D. J., Fleming, M. B., Patterson, E. L., Sebastian, J. R., Nissen, S. J. (2017). Indaziflam: a new cellulose-biosynthesis-inhibiting herbicide provides long-term control of invasive winter annual grasses. *Pest Manag Sci, 73*(10), 2149-2162.

Sega, G. A. (1984). A review of the genetic effects of ethyl methanesulfonate. *Mutat Res, 134*(2-3), 113-142.

Segui-Simarro, J. M., Austin, J. N., White, E. A., Staehelin, L. A. (2004). Electron tomographic analysis of somatic cell plate formation in meristematic cells of Arabidopsis preserved by high-pressure freezing. *Plant Cell, 16*(4), 836-856.

Sekeres, J., Pejchar, P., Santrucek, J., Vukasinovic, N., Zarsky, V., Potocky, M. (2017). Analysis of Exocyst Subunit EXO70 Family Reveals Distinct Membrane Polar Domains in Tobacco Pollen Tubes. *Plant Physiol, 173*(3), 1659-1675.

Senft, D., Ronai, Z. A. (2015). UPR, autophagy, and mitochondria crosstalk underlies the ER stress response. *Trends Biochem Sci, 40*(3), 141-148.

Serafini, T., Stenbeck, G., Brecht, A., Lottspeich, F., Orci, L., Rothman, J. E., et al. (1991). A coat subunit of Golgi-derived non-clathrin-coated vesicles with homology to the clathrin-coated vesicle coat protein beta-adaptin. *Nature, 349*(6306), 215-220.

Sethaphong, L., Haigler, C. H., Kubicki, J. D., Zimmer, J., Bonetta, D., DeBolt, S., et al. (2013). Tertiary model of a plant cellulose synthase. *Proc Natl Acad Sci U S A, 110*(18), 7512-7517.

Shi, S., Li, S., Asim, M., Mao, J., Xu, D., Ullah, Z., et al. (2018). The Arabidopsis Calcium-Dependent Protein Kinases (CDPKs) and Their Roles in Plant Growth Regulation and Abiotic Stress Responses. *Int J Mol Sci, 19*(7).

Shimada, T., Takagi, J., Ichino, T., Shirakawa, M., Hara-Nishimura, I. (2018). Plant Vacuoles. *Annu Rev Plant Biol, 69*, 123-145.

Srivastava, R., Deng, Y., Shah, S., Rao, A. G., Howell, S. H. (2013). BINDING PROTEIN is a master regulator of the endoplasmic reticulum stress sensor/transducer bZIP28 in Arabidopsis. *Plant Cell, 25*(4), 1416-1429.

Stockwell, B. R. (2000). Chemical genetics: ligand-based discovery of gene function. *Nat Rev Genet, 1*(2), 116-125.

Stockwell, B. R. (2004). Exploring biology with small organic molecules. *Nature, 432*(7019), 846-854.

Strasser, R. (2016). Plant protein glycosylation. *Glycobiology, 26*(9), 926-939.

Suzuki, S. W., Emr, S. D. (2018). Membrane protein recycling from the vacuole/lysosome membrane. *J Cell Biol, 217*(5), 1623-1632.

Tajima, H., Iwata, Y., Iwano, M., Takayama, S., Koizumi, N. (2008). Identification of an Arabidopsis transmembrane bZIP transcription factor involved in the endoplasmic reticulum stress response. *Biochem Biophys Res Commun, 374*(2), 242-247.

Tan, X., Li, K., Wang, Z., Zhu, K., Tan, X., Cao, J. (2019). A Review of Plant Vacuoles: Formation, Located Proteins, and Functions. *Plants (Basel), 8*(9).

Tanaka, Y., Kutsuna, N., Kanazawa, Y., Kondo, N., Hasezawa, S., Sano, T. (2007). Intra-vacuolar reserves of membranes during stomatal closure: the possible role of guard cell vacuoles estimated by 3-D reconstruction. *Plant Cell Physiol, 48*(8), 1159-1169.

Tateno, M., Brabham, C., DeBolt, S. (2016). Cellulose biosynthesis inhibitors - a multifunctional toolbox. *J Exp Bot, 67*(2), 533-542.

Taunton, J., Hassig, C. A., Schreiber, S. L. (1996). A mammalian histone deacetylase related to the yeast transcriptional regulator Rpd3p. *Science, 272*(5260), 408-411.

Teh, O. K., Moore, I. (2007). An ARF-GEF acting at the Golgi and in selective endocytosis in polarized plant cells. *Nature, 448*(7152), 493-496.

TerBush, D. R., Maurice, T., Roth, D., Novick, P. (1996). The Exocyst is a multiprotein complex required for exocytosis in Saccharomyces cerevisiae. *EMBO J, 15*(23), 6483-6494.

TerBush, D. R., Novick, P. (1995). Sec6, Sec8, and Sec15 are components of a multisubunit complex which localizes to small bud tips in Saccharomyces cerevisiae. *J Cell Biol, 130*(2), 299-312.

Ting, A. E., Hazuka, C. D., Hsu, S. C., Kirk, M. D., Bean, A. J., Scheller, R. H. (1995). rSec6 and rSec8, mammalian homologs of yeast proteins essential for secretion. *Proc Natl Acad Sci U S A, 92*(21), 9613-9617.

Tsien, R. Y. (1998). The green fluorescent protein. *Annu Rev Biochem, 67*, 509-544.

Turner, S. R., Somerville, C. R. (1997). Collapsed xylem phenotype of Arabidopsis identifies mutants deficient in cellulose deposition in the secondary cell wall. *Plant Cell, 9*(5), 689-701.

Vain, T., Crowell, E. F., Timpano, H., Biot, E., Desprez, T., Mansoori, N., et al. (2014). The Cellulase KORRIGAN Is Part of the Cellulose Synthase Complex. *Plant Physiol, 165*(4), 1521-1532.

Viotti, C. (2016). ER to Golgi-Dependent Protein Secretion: The Conventional Pathway. *Methods Mol Biol, 1459*, 3-29.

Viotti, C., Kruger, F., Krebs, M., Neubert, C., Fink, F., Lupanga, U., et al. (2013). The endoplasmic reticulum is the main membrane source for biogenesis of the lytic vacuole in Arabidopsis. *Plant Cell, 25*(9), 3434-3449.

Vivoli, M., Novak, H. R., Littlechild, J. A., Harmer, N. J. (2014). Determination of protein-ligand interactions using differential scanning fluorimetry. *J Vis Exp*(91), 51809.

Wang, J., Tavakoli, J., Tang, Y. (2019). Bacterial cellulose production, properties and applications with different culture methods - A review. *Carbohydr Polym, 219*, 63-76.

Wang, W., Xue, M., Willcox, M., Thakur, A. (2008). Role of nitric oxide in P. aeruginosa keratitis caused by distinct bacterial phenotypes. *Eye Contact Lens, 34*(4), 195-197.

Wang, X., Chung, K. P., Lin, W., Jiang, L. (2017). Protein secretion in plants: conventional and unconventional pathways and new techniques. *J Exp Bot, 69*(1), 21-37.

Wang, X., Xu, M., Gao, C., Zeng, Y., Cui, Y., Shen, W., et al. (2020). The roles of endomembrane trafficking in plant abiotic stress responses. *J Integr Plant Biol, 62*(1), 55-69.

Wang, Z. Y., Seto, H., Fujioka, S., Yoshida, S., Chory, J. (2001). BRI1 is a critical component of a plasma-membrane receptor for plant steroids. *Nature, 410*(6826), 380-383.

Waters, M. G., Serafini, T., Rothman, J. E. (1991). 'Coatomer': a cytosolic protein complex containing subunits of non-clathrin-coated Golgi transport vesicles. *Nature, 349*(6306), 248-251.

Wei, J. H., Seemann, J. (2010). Unraveling the Golgi ribbon. *Traffic, 11*(11), 1391-1400.

Wen, T. J., Hochholdinger, F., Sauer, M., Bruce, W., Schnable, P. S. (2005). The roothairless1 gene of maize encodes a homolog of sec3, which is involved in polar exocytosis. *Plant Physiol, 138*(3), 1637-1643.

White, P. J. (2018). Selenium metabolism in plants. *Biochim Biophys Acta Gen Subj*.

Wisniewska, J., Xu, J., Seifertova, D., Brewer, P. B., Ruzicka, K., Blilou, I., et al. (2006). Polar PIN localization directs auxin flow in plants. *Science, 312*(5775), 883.

Woollard, A. A., Moore, I. (2008). The functions of Rab GTPases in plant membrane traffic. *Curr Opin Plant Biol, 11*(6), 610-619.

Worden, N., Wilkop, T. E., Esteve, V. E., Jeannotte, R., Lathe, R., Vernhettes, S., et al. (2015). CESA TRAFFICKING INHIBITOR inhibits cellulose deposition and interferes with the trafficking of cellulose synthase complexes and their associated proteins KORRIGAN1 and POM2/CELLULOSE SYNTHASE INTERACTIVE PROTEIN1. *Plant Physiol, 167*(2), 381-393.

Xu, T., Dai, N., Chen, J., Nagawa, S., Cao, M., Li, H., et al. (2014). Cell surface ABP1-TMK auxin-sensing complex activates ROP GTPase signaling. *Science, 343*(6174), 1025-1028.

Yoneda, A., Ito, T., Higaki, T., Kutsuna, N., Saito, T., Ishimizu, T., et al. (2010). Cobtorin target analysis reveals that pectin functions in the deposition of cellulose microfibrils in parallel with cortical microtubules. *Plant J, 64*(4), 657-667.

Yorimitsu, T., Sato, K., Takeuchi, M. (2014). Molecular mechanisms of Sar/Arf GTPases in vesicular trafficking in yeast and plants. *Front Plant Sci, 5*, 411.

Zarsky, V., Kulich, I., Fendrych, M., Pecenkova, T. (2013). Exocyst complexes multiple functions in plant cells secretory pathways. *Curr Opin Plant Biol, 16*(6), 726-733.

Zhang, W., Cai, C., Staiger, C. J. (2019). Myosins XI Are Involved in Exocytosis of Cellulose Synthase Complexes. *Plant Physiol, 179*(4), 1537-1555.

Zhang, X., Orlando, K., He, B., Xi, F., Zhang, J., Zajac, A., et al. (2008). Membrane association and functional regulation of Sec3 by phospholipids and Cdc42. *J Cell Biol, 180*(1), 145-158.

Zhang, X., Zajac, A., Zhang, J., Wang, P., Li, M., Murray, J., et al. (2005). The critical role of Exo84p in the organization and polarized localization of the exocyst complex. *J Biol Chem, 280*(21), 20356-20364.

Zhang, Y., Liu, C. M., Emons, A. M., Ketelaar, T. (2010). The plant exocyst. *J Integr Plant Biol, 52*(2), 138-146.

Zhang, Y., Nikolovski, N., Sorieul, M., Vellosillo, T., McFarlane, H. E., Dupree, R., et al. (2016). Golgi-localized STELLO proteins regulate the assembly and trafficking of cellulose synthase complexes in Arabidopsis. *Nat Commun, 7*, 11656.

Zhang, Z., Luo, Z. W., Kishino, H., Kearsey, M. J. (2005). Divergence pattern of duplicate genes in protein-protein interactions follows the power law. *Mol Biol Evol, 22*(3), 501-505.

Zhao, Y., Dai, X., Blackwell, H. E., Schreiber, S. L., Chory, J. (2003). SIR1, an upstream component in auxin signaling identified by chemical genetics. *Science, 301*(5636), 1107-1110.

Zheng, H., Staehelin, L. A. (2011). Protein storage vacuoles are transformed into lytic vacuoles in root meristematic cells of germinating seedlings by multiple, cell type-specific mechanisms. *Plant Physiol, 155*(4), 2023-2035.

Zhu, J., Gong, Z., Zhang, C., Song, C. P., Damsz, B., Inan, G., et al. (2002). OSM1/SYP61: a syntaxin protein in Arabidopsis controls abscisic acid-mediated and non-abscisic acid-mediated responses to abiotic stress. *Plant Cell, 14*(12), 3009-3028.

Zhu, X., Li, S., Pan, S., Xin, X., Gu, Y. (2018). CSI1, PATROL1, and exocyst complex cooperate in delivery of cellulose synthase complexes to the plasma membrane. *Proc Natl Acad Sci U S A, 115*(15), E3578-E3587.

Zouhar, J., Sauer, M. (2014). Helping hands for budding prospects: ENTH/ANTH/VHS accessory proteins in endocytosis, vacuolar transport, and secretion. *Plant Cell, 26*(11), 4232-4244.

CHAPTER 2.   CHARACTERIZATION ON THE SPECIFICITY OF ENDOSIDIN2 ON DIFFERENT PLANT EXO70S

2.1   Abstract

Exocytosis is a conserved cellular process for eukaryotic cells to transport secretory products to the plasma membrane or extracellular environment. The exocyst complex tethers the secretory vesicles to the site of membrane fusion during exocytosis. EXO70 is one subunit of the octameric exocyst complex. There are 23 paralogous EXO70s in Arabidopsis. Endosidin2 (ES2) is an exocytosis inhibitor that targets EXO70A1 in Arabidopsis. It is not known whether ES2 targets only EXO70A1 or other homologous EXO70s in plants. We aimed to analyze the specificity of ES2 on other EXO70 family proteins using Drug Affinity Responsive Target Stability (DARTS) assay and molecular docking approaches. We selected five EXO70 genes of Arabidopsis based on their phylogenetic relationship and obtained the purified proteins through prokaryotic expression and affinity tag purification. Based on DARTS assay, ES2 interacts with EXO70B1, EXO70D2 and EXO70H8 and does not interact with EXO70E2 and EXO70G2. We also performed structure modeling and molecular docking analysis to evaluate the structural basis for the interaction between EXO70s and ES2. Our results show that ES2 targets a subset of EXO70s in plants and provide guidance for using ES2 as an inhibitor of exocytosis process mediated by different EXO70s.

2.2   Introduction

The EXO70 subunit of the exocyst complex is required for the tethering of secretory vesicles to the plasma membrane, which defines its important roles in many cellular processes such as cell adhesion, invasion and migration (Zhu, Wu, & Guo, 2019). In yeast and most mammalian cells, there is usually one single copy of EXO70, but plants have expanded gene families related to EXO70 (Cvrckova et al., 2012). The expression of EXO70 genes primarily takes place in exocytosis-active cells such as tip-growing cells, and no expression was observed in well-developed organs such as the cells of stems and sepals (Li et al., 2010). The diverse expression patterns of plant EXO70s makes their specific functions to be an interesting question.

In Arabidopsis, there are 23 members related to EXO70 gene. These genes are clustered as AtEXO70A-AtEXO70H and each individual member is likely to have its divergent roles in different cell types (Chong et al., 2010). For example, T-DNA inserted *exo70A1* mutants of Arabidopsis exhibit shorter roots and retarded root hairs growth, and subsequently show undeveloped stigmatic papillae leading to lower fertility (Synek et al., 2006). The dwarfness and sterility of AtEXO70A1 mutant plants are well explained by the roles of EXO70A1 in tracheary element (TE) development of xylem tissues. AtEXOA1 mediates exocytic trafficking in TE differentiation and mutated AtEXO70A1 causes aberrant xylem development, which impedes plant growth through interrupting cell expansion and hydraulic transport (Li et al., 2013). Different with EXO70A1, AtEXO70B1 functions in Golgi-independent transport to the vacuole, which is related to plant autophagy (Kulich et al., 2013). Together with AtEXO70B2, AtEXO70B1 plays a critical role in plant immune responses to diverse pathogens (Stegmann et al., 2013;Wang, Liu, Gao, Rui, & Tang, 2019;Wang et al., 2020). AtEXO70C1 and AtEXO70C2 are specially localized in pollen tubes and trichoblast cells. Their mutants exhibit a significant defect in pollen transmission, which defines them as key regulators in pollen optimal tip growth

(Synek et al., 2017). Different from other AtEXO70 paralogs, AtEXO70H4 is a critical up-regulated gene for secondary cell wall maturation in trichomes of Arabidopsis through mediating callose synthase secretion, and thus AtEXO70H4 is involved in silica accumulation which is callose dependent (Kulich et al., 2015;Kulich et al., 2018).

ES2 was screened out from chemical libraries and was identified as a new drug for endomembrane trafficking. Being a useful tool, ES2 probes the association of the exocyst complex and the plasma membrane in plant cells (Zhang et al., 2016). Upon ES2 treatment, Arabidopsis seedlings show shorter roots and less root hairs and are less sensitive to gravity stimulation. PM-localized PIN2 is reduced and transportation of PIN2 to the vacuole is enhanced (Zhang et al., 2016). Through target identification using biochemical analysis such as STD-NMR and DARTS assay, it is proved that ES2 directly targets AtEXO70A1 at C-terminal (Zhang et al., 2016). As a novel exocytosis inhibitor, ES2 shows great potential in revealing biological functions of the exocyst complex and machineries of endomembrane trafficking in plant cells. Because Arabidopsis genome has 23 EXO70 genes, the specificity of ES2 is a crucial question. Whether ES2 targets AtEXO70A1 specifically or it is a board-spectrum exocytosis inhibitor for all AtEXO70 genes is a question.

For target identification, Drug Affinity Responsive Target Stability (DARTS) assay is a quick and inexpensive method. DARTS works well both with the complex protein samples such as whole cell lysates and purified proteins samples. In DARTS assay, aliquots of protein samples are treated with the compound of interest and an inactive analog as the control. After the treatments of drug and control, protein samples are digested using proteases for the same time. Subsequently, the samples are separated by SDS-PAGE and detected. The protected proteins can be identified though the difference of signals of protein bands (Figure 2.1). For analysis, gel-

based approach is the easiest to identify unknown targets with DARTS assay, and gel-free

proteomics methods are used to facilitate the identification of the protected proteins as well. As a

semi-quantitative and unbiased method, DARTS helps the discovery of targets of natural

products, and it is also a way to validate the binding of ligands to protein of interests.

2.3 Materials and Methods

2.3.1 Construction of expression plasmids and *E. coli* transformation

Based on gene cloning methods, external genes are inserted into vectors through DNA

cleavage and ligation using restriction endonucleases and DNA ligase. The expression plasmids

of five EXO70 genes were conducted as shown in Figure 2.1. The pLIC6 plasmids carrying the

EXO70 genes were obtained from Arabidopsis Biological Resource Center (ABRC). The

EXO70 genes were amplified using PCR (Table 2.1) and digested with specific restriction

enzymes (Table 2.2). The plasmid DNA of pRSF-Duet-1 vector was digested with the same

restriction enzymes as each EXO70 gene correspondingly (Table 2.2). After double digestion of

amplified EXO70 genes and pRSF-Duet-1 vector, EXO70 genes were inserted into the vector

through DNA ligation.

pLIC6 plasmid carrying EXO70 genes and pRSF-Duet-1 plasmid was transformed to

DH5α cells. Spectinomycin is the selection marker for pLIC6 and Kanamycin is the selection

marker for pRSF-Duet-1. Plasmids of pLIC6 carrying EXO70 genes and pRSF-Duet-1 were

extracted using Zyppy Plasmid Miniprep Kit (Zymo). Plasmid DNA of pRSF-Duet-1 from

minipreps were digested with restriction enzymes in the following system: 1 μg plasmid DNA, 1

μL restriction enzyme 1, 1 μL restriction enzyme 2, 5 μL 10X NEBuffer, and add ddH$_2$O to 50

μL reaction volume. The whole digestion system was incubated at 37 °C for 1 hour. After PCR,

the desired DNA fragments were purified by gel electrophoresis and recovered using Zyppy Gel

Recovery Kit (Zymo). All enzyme stocks were from NEW ENGLAND Biolab company. Based

on the NEB ligation protocol and NEBioCalculator, the following ligation reaction was set up: 1

μL T4 DNA ligase, 2 μL T4 DNA ligase Buffer (10X), 30 ng Vector DNA, 35 ng Insert DNA,

and add ddH$_2$O to 20 μL reaction volume. Mix the reaction well and incubate in room

temperature for 30 minutes.
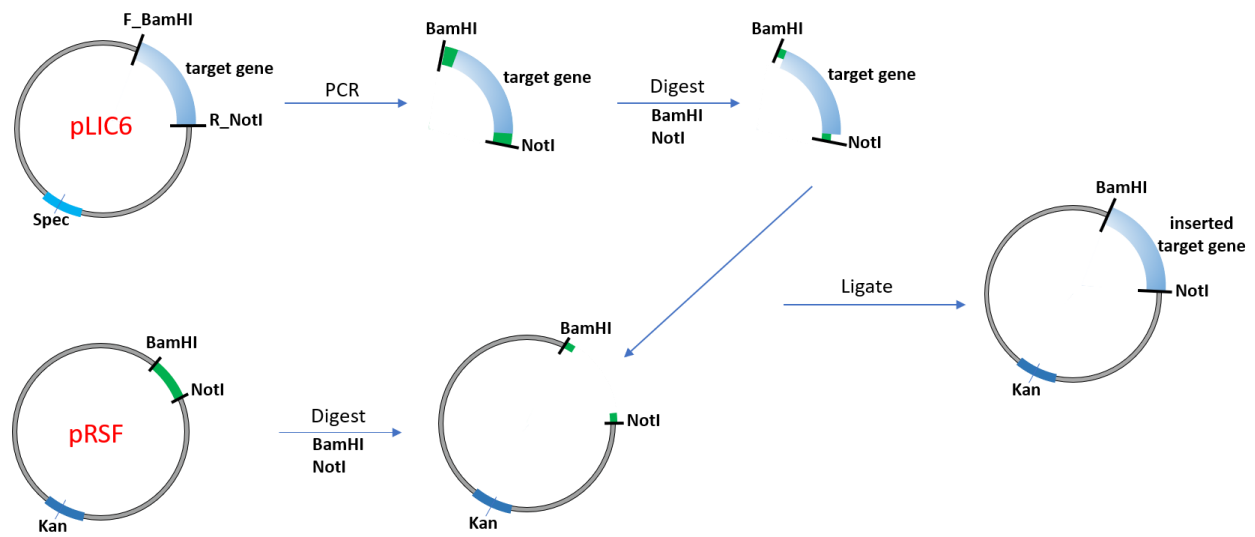
Figure 2.1 Scheme for recombinant plasmids construction (adapted from
https://www.addgene.org/mol-bio-reference/cloning/)

Table 2.1 Primers sequences for amplifying EXO70 genes.

Genes	**Primers**	**DNA sequences**
AtEXO70B1	B1_F_BamHI	5'-CGCggatccATAGACGGTCAGATCTCTCG-3'
	B1_R_NotI	5'-ATTTgcggccgcTCATTTTCTTCCCGTGGTAG-3'
AtEXO70D2	D2_F_EcoRI	5'-CCGgaattcCTCGAGGACGAGCTAAGAAA-3'
	D2_R_NotI	5'-ATTTgcggccgcTCACTGAGACCGTCTCAAAT-3'
AtEXO70E2	E2_F_BamHI	5'-CGCggatccGCTGTGAAGAGAATCCGCAG-3'
	E2_R_NotI	5'-ATTTgcggccgcTCATCTCTTACGAGAGCTGC-3'
AtEXO70H8	H8_F_BamHI	5'-CGCggatccGAACACGTCCACTCTTCTTC-3'
	H8_R_NotI	5'-ATTTgcggccgcTTAAACAGAACCCGAAG-3'

Table 2.2 Restriction cutting sites for EXO70 genes

Genes	**Parent plasmid stock number**	**Restriction sites**
AtEXO70B1	DKLAT5G58430	BamHI/NotI
AtEXO70D2	DKLAT1G54090	EcoRI/NotI
AtEXO70E2	DKLAT5G61010	BamHI/NotI
AtEXO70H8	DKLAT2G28650.1	BamHI/NotI

2.3.2 *E. coli* transformation and recombinant plasmid verification

10 µL of the ligation reaction obtained from above steps were added to the thawed 100 µL DH5α competent cells and keep them on ice for 30 minutes. The competent cell was incubated with the ligation product at 42 °C water bath for 30 seconds and transferred it to ice immediately. After keeping the mixture on ice for 5 minutes, 1 mL SOC outgrowth medium was added to freshly transformed DH5α cells and incubated for 1 hour at 37 °C with shaking. After one-hour incubation, the DH5α cells carrying expression plasmid were plated on LB media with Kanamycin, and plates were kept in 37 °C incubator overnight. The next day, five colonies were selected for colony PCR with the corresponding primers (Table 2.2). The PCR amplification program is: 98 °C for 30s for denaturation, the 30 repeated cycles including 98 °C for 10s, 58 °C for 30s, 72 °C for 90s, and 72 °C for 10 min. Samples were kept at 4 °C after PCR running.

If there was a clear DNA band with correct mass size, the colony of the transformants would be chosen and inoculated into 5 mL liquid LB medium with 50 µg/mL kanamycin to grow at 37 °C for overnight. The plasmids were extracted using Zyppy Plasmid Miniprep Kit (Zymo), and minipreps were digested with corresponding double restriction enzymes for plasmid verification. Plasmids that release DNA fragments with correct size were selected for Sanger sequencing at Purdue Genomic Core Facility.

2.3.3 Protein expression

Transformed verified recombinant plasmid DNA of pRSF-Duet-1 with EXO70 were introduced into BL21 strain for protein expression. A single colony was selected from BL21 transformed with pRSF-Duet-EXO70 and inoculated in 5 mL Luria-Burtani media containing 50 µg/mL kanamycin. After overnight growth at 37°C, 2.5 mL overnight culture was inoculated into 1 L LB media containing 50 µg/mL kanamycin. The culture was grown at 37°C with shaking

until the optical density at 600 nm reached 0.6 ($OD_{600} = 0.6$), and then incubated on ice for 30

minutes. Isopropyl β-D-1-thiogalactopyranoside was added to 0.1 mM to induce protein

expression. The culture was grown at 16°C for 20 hours with shaking at 220 rpm. Bacteria cells

were collected by centrifugation at 4000 rpm for 30 minutes at 4°C. Bacterial pellet was

resuspended in a binding buffer (50mM Tris-HCl, 1M NaCl, pH = 8.0). 1 mM

phenylmethylsulfonyl fluoride (PMSF) was added to resuspended cells to inhibit protease

activity. Bacterial cells were lysed using Fisherbrand Sonic dismembrator and the soluble protein

were separated from cell debris by centrifugation at 20,000 g for 1 hour. The supernatant fraction

was collected after centrifugation and filtered through a 0.22 μm filter to remove large particles.

The filtered supernatant fraction was used for further protein purification.

2.3.4   Protein purification using FPLC system

ÄKTA pure FPLC system from General Electric Company with the 5 mL HisTrap HP

columns was used for the purification of His-tagged proteins. Prior to protein purification,

System Flow program was initiated to wash the whole system with binding buffer (50mM Tris,

1M NaCl, 40mM Imidazole, pH=8.0) until the UV absorbance kept at around zero and

conductivity reached a steady baseline.

Filtered supernatant fraction was loaded to the 50 mL superloop using a syringe. Sample

Application program was initiated to pump the protein solution from sample container to

injection value. As protein solution went through the HisTrap column, protein with His-tag is

trapped by the Ni^{2+} within the column and extra proteins were pumped out with binding buffer.

Wash program was initiated to wash the column for 3-5 column volumes of binding buffer.

Then, Elution program was used to elute the column with elution buffer (50mM Tris, 1M NaCl,

250mM Imidazole, pH=8.0) and purified protein samples were collected into fraction tubes.

High concentration of imidazole has a stronger binder with Ni^{2+}, competing with the His-tagged proteins, so that His-tagged protein is washed out by elution buffer. After collecting the protein, the column was equilibrated with binding buffer and then the whole system was washed with 20% ethanol. Purified protein was collected and dialyzed overnight at 4°C in dialysis buffer (50mM Tris, 1M NaCl, pH=8.0) to remove imidazole that affects the following binding test. A_{280} of the protein sample was measured with the spectrophotometer and its concentration was calculated. Purified proteins were frozen using liquid nitrogen and kept at -80°C for further biochemical assays.

2.3.5   Drug Affinity Responsive Target Stability (DARTS) assay

2.5 µg purified EXO70 protein and 2.5 µg BSA protein were mixed in an Eppendorf tube. The volume of the mixture was adjusted to 800 µL using dialysis buffer (1M NaCl, 50mM Tris-HCl, pH = 8.0). Protein mixture was aliquoted into two 1.5 mL centrifuge tubes, with 396 µL in each tube. 4 µL DMSO was added into one tube and 4 µL 40 mM ES2 was added into the other tube. The mixture was vortexed well and incubated at room temperature for 1 hour with gentle rotation. Each mixture was aliquoted into 7 tubes and 50 µL for each aliquot. One of these tubes was kept as a non-digested control. At exactly 30 second, 1.5 µL 50X diluted pronase solution was added to one aliquot of compounded-treated sample. Exactly 30 seconds later after starting the first digest, at 1 min, 1.5 µL 50X diluted pronase solution was added to one aliquot of the DMSO sample. The digests of rest aliquots were conducted in 30 sec intervals by adding 1.5 µL of the corresponding pronase stock into aliquot of each sample. After 30 mins, reaction of each aliquot was stopped by adding 12.5 µL 5X SDS loading buffer and heated at 100 °C for 10 min.
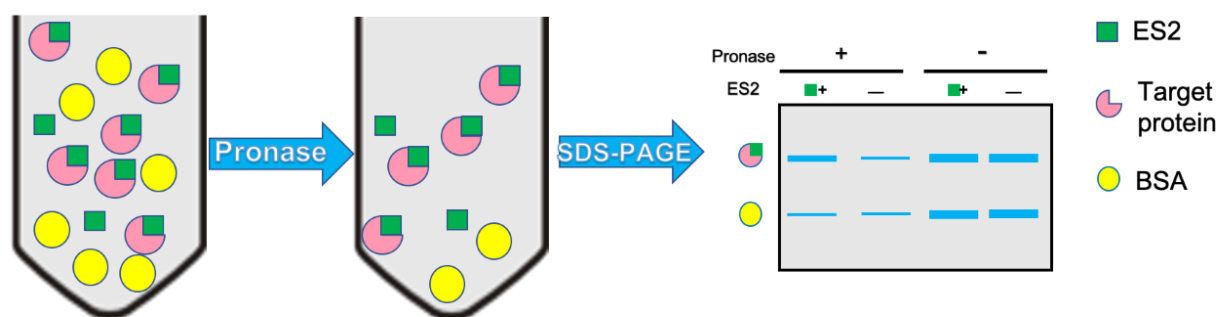
Figure 2.2 Scheme for DARTS assay.

2.3.6 SDS-PAGE

One short plate, one 1.5mm spacer plate, and one 1.5mm comb were cleaned with tap water to remove all dust and small particles and rinse with deionized water. The short plate was placed on the spacer plate. Plates were rocked into the holder. Place the holder on the rack and test the seal. 10 mL 7% separating gel mix was prepared with 4.9 mL ddH$_2$O, 2.3 mL 30% acrylamide/bis stock, 2.6 mL 1.5M Tris-HCl (pH=8.8), 100 µL 10% SDS, 100 µL 10% APS and 10 µL TEMED. The gel mix was loaded between the plates and 2 cm distance between the gel surface and the edge of the short plate were left. Isopropanol was layered on top of the gel solution gently. After 40 minutes, the separating gel has polymerized, the topper isopropanol was removed using paper towel. 5 mL 5% stacking gel mix was prepared with 2.975 mL ddH$_2$O, 670 µL 30% acrylamide/bis stock, 1.25 mL 0.5M Tris-HCl (pH=6.8), 50 µL 10% SDS, 50 µL 10% APS and 5 µL TEMED. The stacking gel solution was loaded between the plates on the top of separating gel to the edge of the short plate. The comb was inserted to the top of the spacers and after 15 minutes, stacking gel polymerized. Both buffer chambers were filled with gel running buffer (25mM Tris, 192mM glycine, 0.1% SDS, pH=8.3). The comb was removed. Samples and molecular mass protein markers were loaded into wells.

65

2.3.7 Silver staining for visualization

After the SDS-PAGE gel electrophoresis, the gel was submerged in fixing solution (50% [v/v] methanol, 5% [v/v] glacial acetic acid), gently shaking for 20 minutes. Next step is to replace the fixing solution with 50% (v/v) methanol solution, the gel was shaking gently for 10 minutes. 50% (v/v) methanol was removed and ddH$_2$O was added for shaking the gel. After 10 minutes, the ddH$_2$O was removed. The gel was submerged in 0.02% (w/v) sodium thiosulfate. After 1 minute, the gel was washed twice with ddH$_2$O for 30 seconds each time. Then, the gel was placed in chilled 0.1% (w/v) silver nitrate solution and incubated at 4 °C for 20 minutes with gentle shaking. Finally, silver nitrate solution was removed. The gel was soaked in developing solution (2% [w/v] sodium carbonate, 0.04% [v/v] formaldehyde) with slight vigorously shaking. When the staining intensity is reached to desired level, the reaction was stopped by replacing developing solution with 5% (v/v) acetic acid. Silver-stained gel was kept in 1% (v/v) acetic acid.

2.3.8 Phylogenetic analysis

The alignment between Saccharomyces cerevisiae EXO70 and Arabidopsis thaliana EXO70 proteins was generated using MUltiple Sequence Comparison (MUSCLE) algorithm. Full length protein sequences from UniProt were analyzed, including 23 amino acid sequences of AtEXO70 and one of ScEXO70. All ambiguous positions were removed for each sequence pair using pairwise deletion option. Evolutionary relationship was inferred using the Neighbor-Joining method. The optimal tree with the sum of branch length = 10.92336306. The bootstrap value is 1000 and the percentage of replicate trees in which the associated taxa clustered together are shown next to the branches. The tree was drawn to scale, with branch lengths in the same units as those of the evolutionary distances used to infer the phylogenetic tree. The evolutionary

distances were computed using the Poisson correction method and are in the units of the number of amino acid substitutions per site. The analysis involved 24 amino acid sequences. There is a total of 886 positions in the final dataset. Evolutionary analyses were conducted in MEGA 7 (Kumar, Stecher, Li, Knyaz, & Tamura, 2018).

2.3.9 Modeling and docking

The structure modeling of 22 homologous Arabidopsis EXO70 proteins was completed using the MPI Bioinformatics Toolkit, based on the AtEXO70A1 three-dimensional structure obtained from Protein Data Bank. All the AtEXO70 modeling structures were established upon full length sequences of the AtEXO70s protein, using protein homology detection by HMM-HMM comparison method (HHpred) and MODELLER (Zimmermann et al., 2018). The modeling structure of 22 AtEXO70s were used for binding pocket prediction using Autodock Vina. The structure of small molecule ES2 was constructed by Maestro software and docking was completed on the open source software, PyRx (Dallakyan & Olson, 2015).

2.4   Results

The large EXO70 family of Arabidopsis has 23 paralogs and can be divided into eight clusters (Figure 2.3). Based on the crystal structure of AtEXO70A1 that is available at Protein Data Bank, the modeling structure of selected homologous AtEXO70s was built up using HHpred and MODELLER which serves for remote protein homology detection and 3D structure establishment. The alignment of EXO70 proteins and the modeling structures of homologous Arabidopsis showed quite conserved C-terminal but variable N-terminal (Figure 2.4).

Because of the tissue-specific expression and the difficulties in obtaining corresponding antibodies, isolating AtEXO70s from total protein complex and visualizing through Western-blot

is not an ideal way to inspect the specificity of ES2 to homologous AtEXO70s. I took advantage

of DARTS assay using purified AtEXO70B1, AtEXO70D2, AtEXO70E2, AtEXO70G2, and

AtEXO70H8, to examine the specificity of ES2. For protein purification, AtEXO70A1 protein

were previously found to be unstable and prone to be degraded when it was expressed in *E. coli*.

To keep its stability and activity, the first 74 amino acids of EXO70A1 was removed for

biochemical analysis and protein crystallization. Based on this evidence, I constructed expression

vectors of homologous AtEXO70s genes without the first 74 amino acids at the N-terminus.

In DARTS assay, BSA was used as the control, which does not interact with ES2. From

the SDS-PAGE gels stained with silver nitrite, protein degradation can be observed clearly, in

both ES2 treated samples and DMSO control samples in the presence of pronase. However,

because of ES2 protection, the targeted proteins is potential to show less sensitivity to pronase

digestion. At each concentration of diluted pronase, same amount of AtEXO70 proteins was

treated with DMSO and ES2 correspondingly for same reaction time. Two groups of proteins are

subsequently digested with equal amount of pronase for the exact same time. After the digestion,

the difference of signal between protein bands in DMSO group and ES2 group were quantified

and the stability of proteins was identified.

For AtEXO70B1 (Figure 2.5), the differences of protein signal between DMSO group

and ES2 group were easily detected at several concentrations of pronase. Especially, at the

concentration of 1:150, 1:200, and 1:250, the signal intensity of ES2 treated samples was 3 to 4

times stronger than DMSO treated samples. Different signal intensity of ES2 groups and DMSO

groups indicated that AtEXO70B1 was protected by ES2. As the control, BSA was not protected

by ES2, and there was no difference in signal intensity between ES2 and DMSO treated samples.

The protein is considered to interact with the ligand if there is difference in protein intensity

between ES2 treated and control samples. Thus, AtEXO70B1 interacts with ES2 in DARTS

assay. We observed similar pattern of ES2 protecting AtEXO70D2 (Figure 2.6) and

AtEXO70H8 (Figure 2.7) from pronase digestion. For AtEXO70D2, 1:100 diluted pronase

protected the protein efficiently. Three independent experiments showed the same binding

pattern, and the ratio of signal intensity was approximately at 2.5 times. For AtEXO70H8, at

1:50 and 1:100 diluted pronase treatments, AtEXO70H8 proteins are protected by ES2, though

no significant differences were detected at other concentrations. However, in DARTS assay,

some EXO70 homologous proteins, such as AtEXO70G2 (Figure 2.8) and AtEXO70E2 (Figure

2.9), did not show any interaction with ES2. For these two proteins, they had a similar

performance to the BSA control. The signal difference at each concentration did not show any

changes, and the average ratio were around 1.0, no more than 1.5 times. From the DARTS assay

with these five purified AtEXO70 proteins, some AtEXO70 proteins showed a very good

binding pattern, such as AtEXO70B1, AtEXO70D2, and AtEXO70H8, but AtEXO70E2 and

AtEXO70G2 did not show binding patterns.

For the potential targeted proteins, AtEXO70B1, AtEXO70D2, and AtEXO70H8, the

binding pockets of ES2 were predicted through Autodock. The conformation of ES2 can fit well

in the C-terminal pocket of AtEXO70B1 (Figure 2.5) with lowest free energy, and the binding

cavity was principally composed of the hydrophobic amino acids GLY395 and HIS399. For

AtEXO70D2 (Figure 2.6), the binding pocket was consisted of GLU118, LEU140, and ASP142.

The residues THB479 and GLU481 of AtEXO70H8 (Figure 2.7) were likely to interact with ES2

and formed the hydrogen binds.
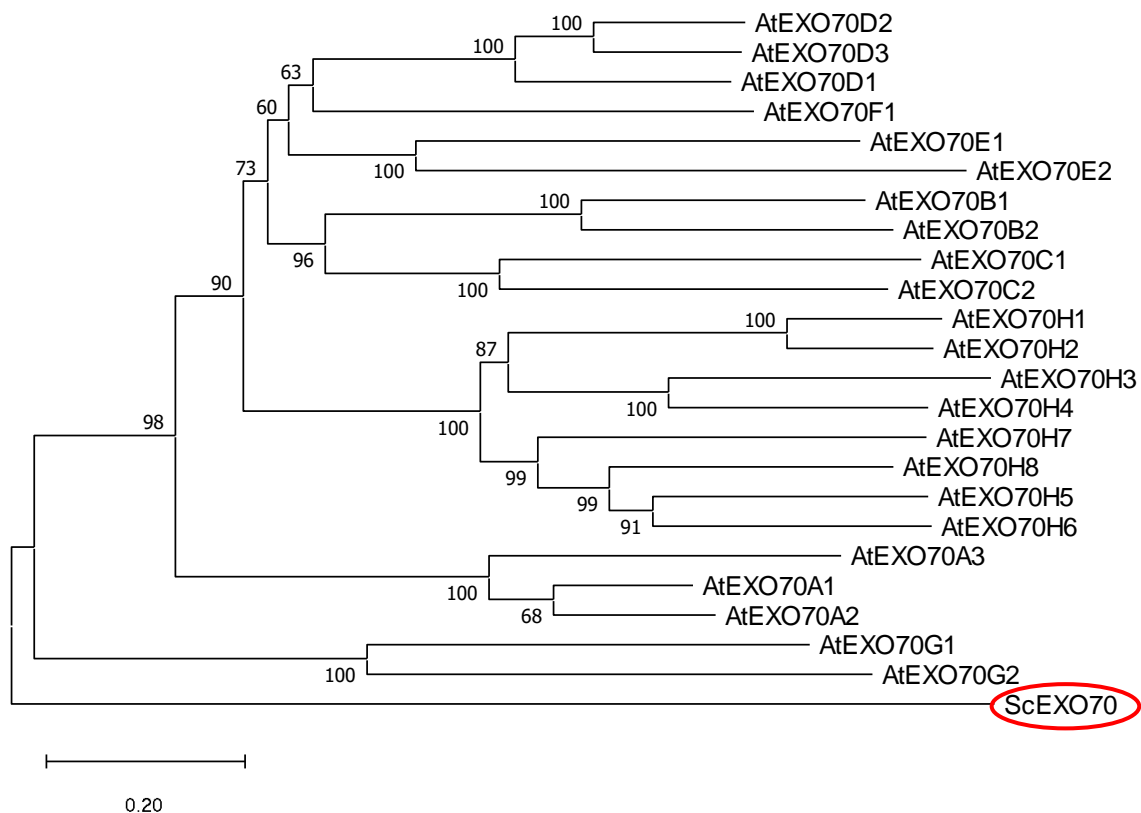
Figure 2.3 Phylogenetic relations between Saccharomyces cerevisiae EXO70 and Arabidopsis thaliana EXO70 proteins. Phylogenetic tree of ScEXO70 and AtEXO70s was established on full length protein sequences obtained from UniProt. The tree was constructed by the neighboring-joining algorithm in the MEGA-7 program using p-Distance. Boostrap values supporting the branch points are expressed as the percentage of 1000 replicates. EXO70 from yeast (ScEXO70) are highlighted with red circle.

Figure 2.4 Modeling structures of AtEXO70 proteins based on the crystal structure of AtEXO70A1, visualized by PyMOL. (A) the crystal structure of AtEXO70A1, which was obtained from PBD, ID:4RL5. (B) modeled structure of AtEXO70B1. (C) modeled structure of AtEXO70D2. (D) modeled structure of AtEXO70E2. (E) modeled structure of AtEXO70G2. (F) modeled structure of AtEXO70H8
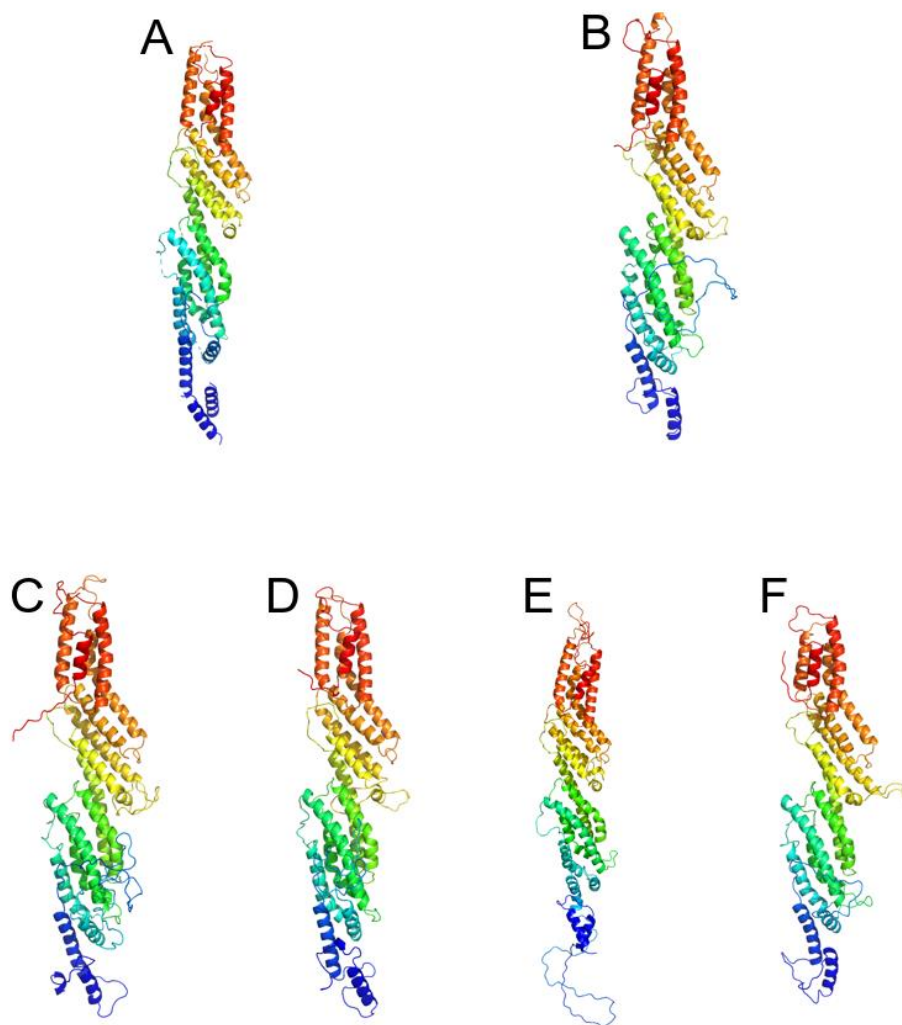
Figure 2.5 DARTS assay for the interaction between ES2 and AtEXO70B1 with a series of pronase concentration gradients. (A) Silver staining of proteins from DARTS assay. (B) Quantification of ratios of AtEXO70B1 and BSA intensities in samples treated with ES2 and DMSO, as shown in A. Samples treated with different concentrations of pronase, ranging from 50X dilution to 300X dilution. The signal intensity ratio between ES2 and DMSO against AtEXO70B1 and BSA under different dilutions of pronase was measured using ImageJ. The error bars represent SDs of three independent experiments. (C) Predicted binding pocket for AtEXO70B1, visualized by PyMOL.

Figure 2.6 DARTS assay for the interaction between ES2 and AtEXO70D2 with a series of pronase concentration gradients. (A) Silver staining of proteins from DARTS assay. (B) Quantification of ratios of AtEXO70D2 and BSA intensities in samples treated with ES2 and DMSO, as shown in A. Samples treated with different concentrations of pronase, ranging from 1X dilution to 10000X dilution. The signal intensity ratio between ES2 and DMSO against AtEXO70D2 and BSA under different dilutions of pronase was measured using ImageJ. The error bars represent SDs of three independent experiments. (C) Predicted binding pocket for AtEXO70D2, visualized by PyMOL.
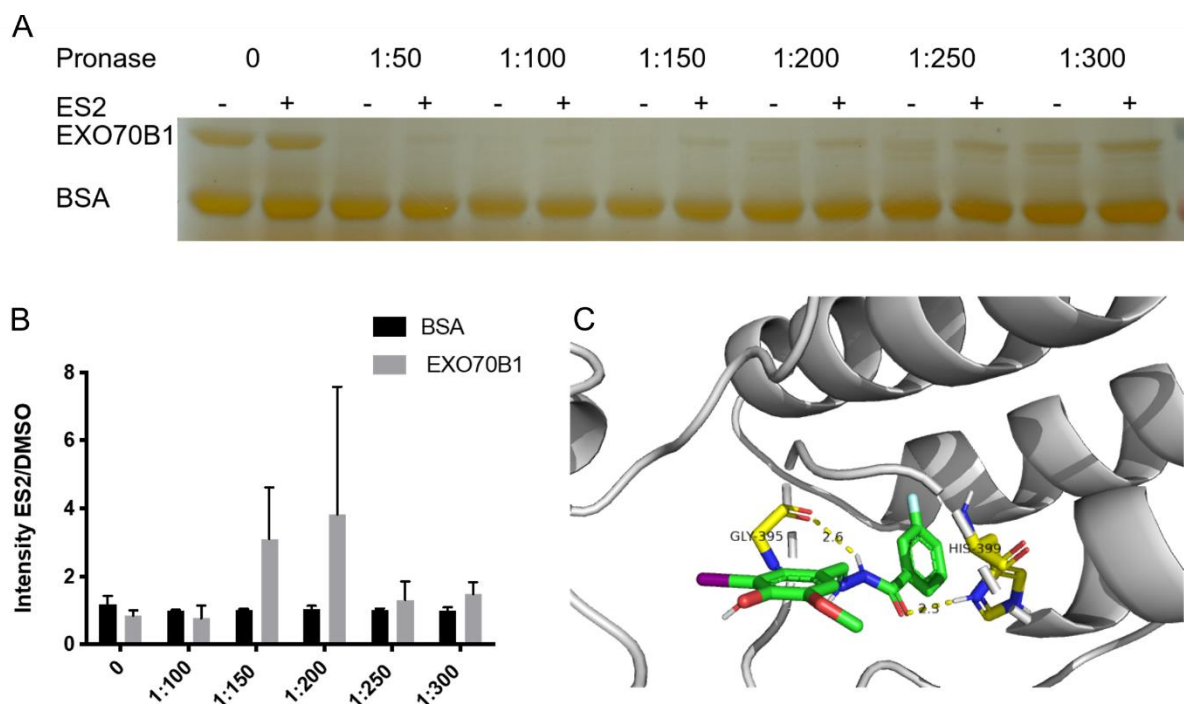
Figure 2.7 DARTS assay for the interaction between ES2 and AtEXO70H8 with a series of pronase concentration gradients. (A) Silver staining of proteins from DARTS assay. (B) Quantification of ratios of AtEXO70H8 and BSA intensities in samples treated with ES2 and DMSO, as shown in A. Samples treated with different concentrations of pronase, ranging from 50X dilution to 300X dilution. The signal intensity ratio between ES2 and DMSO against AtEXO70H8 and BSA under different dilutions of pronase was measured using ImageJ. The error bars represent SDs of three independent experiments. (C) Predicted binding pocket for AtEXO70H8, visualized by PyMOL.
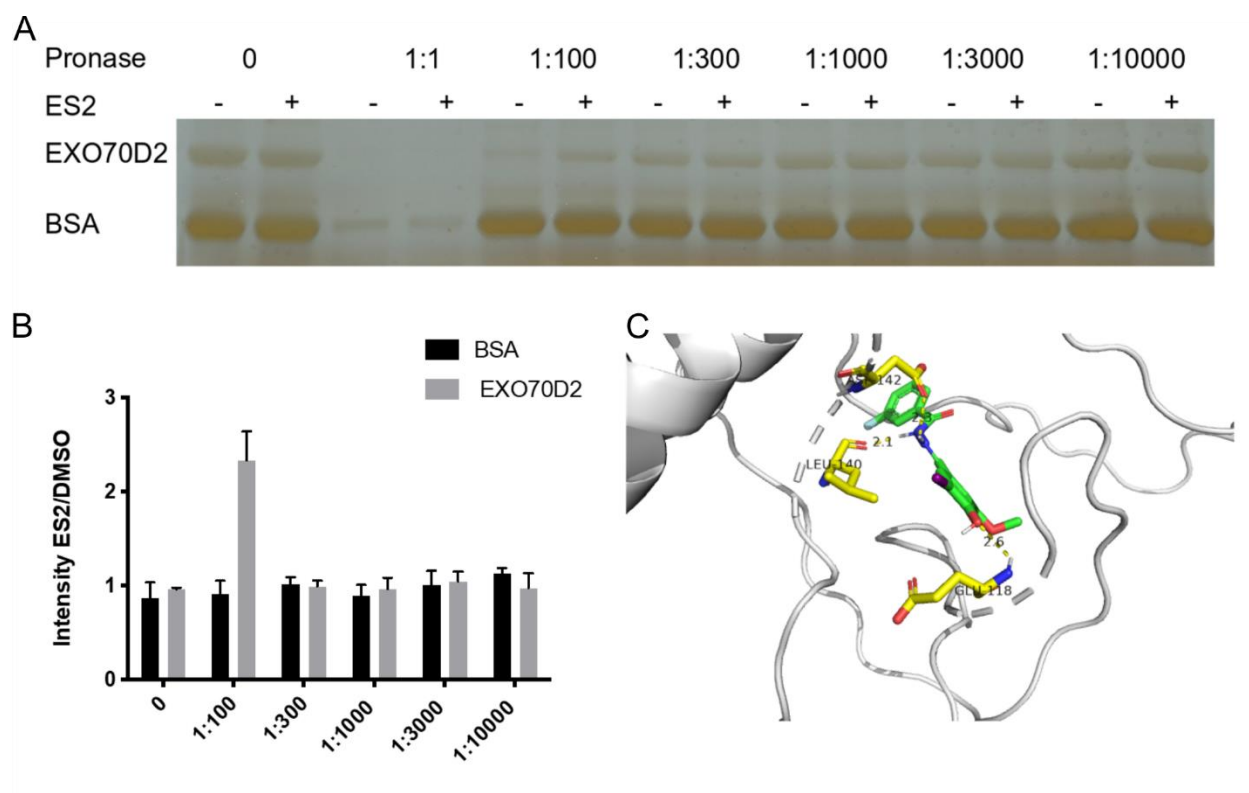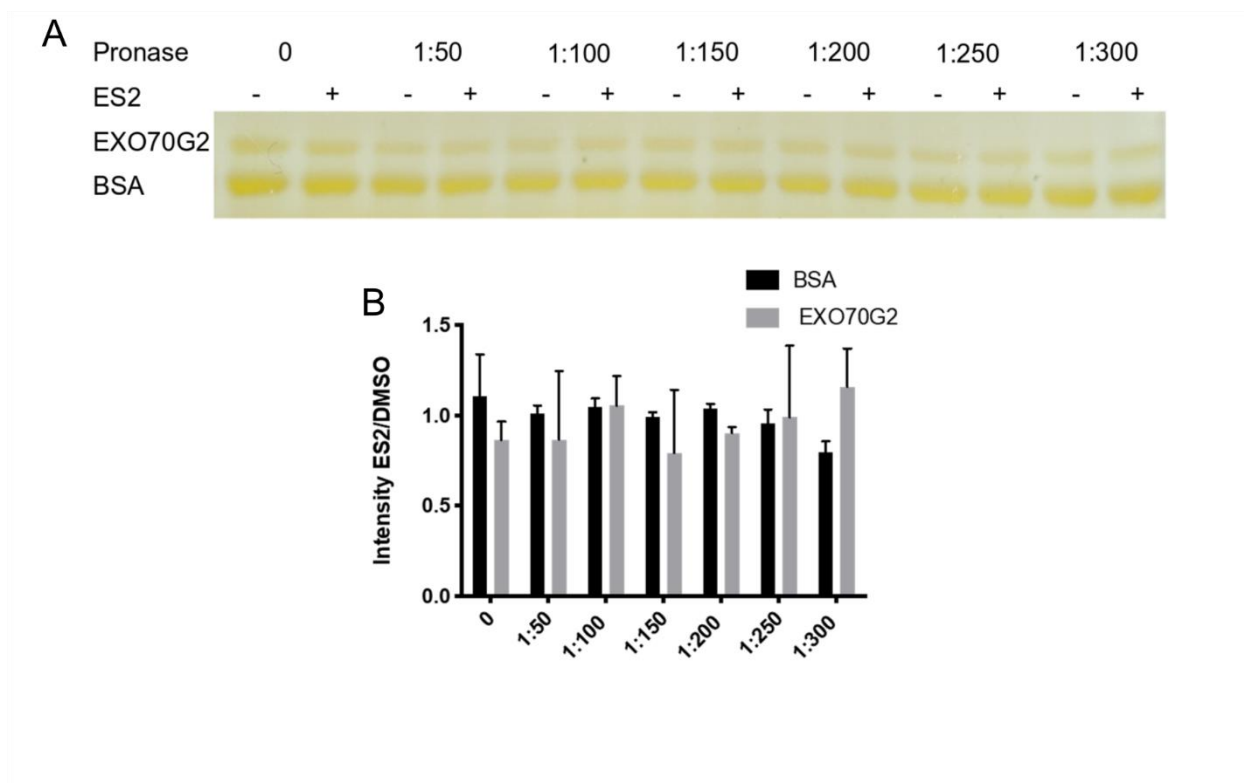
Figure 2.8 DARTS assay for the interaction between ES2 and AtEXO70G2 with a series of pronase concentration gradients. (A) Silver staining of proteins from DARTS assay. (B) Quantification of ratios of AtEXO7G2 and BSA intensities in samples treated with ES2 and DMSO, as shown in A. Samples treated with different concentrations of pronase, ranging from 1X dilution to 10000X dilution. The signal intensity ratio between ES2 and DMSO against AtEXO70G2 and BSA under different dilutions of pronase was measured using ImageJ. The error bars represent SDs of three independent experiments.
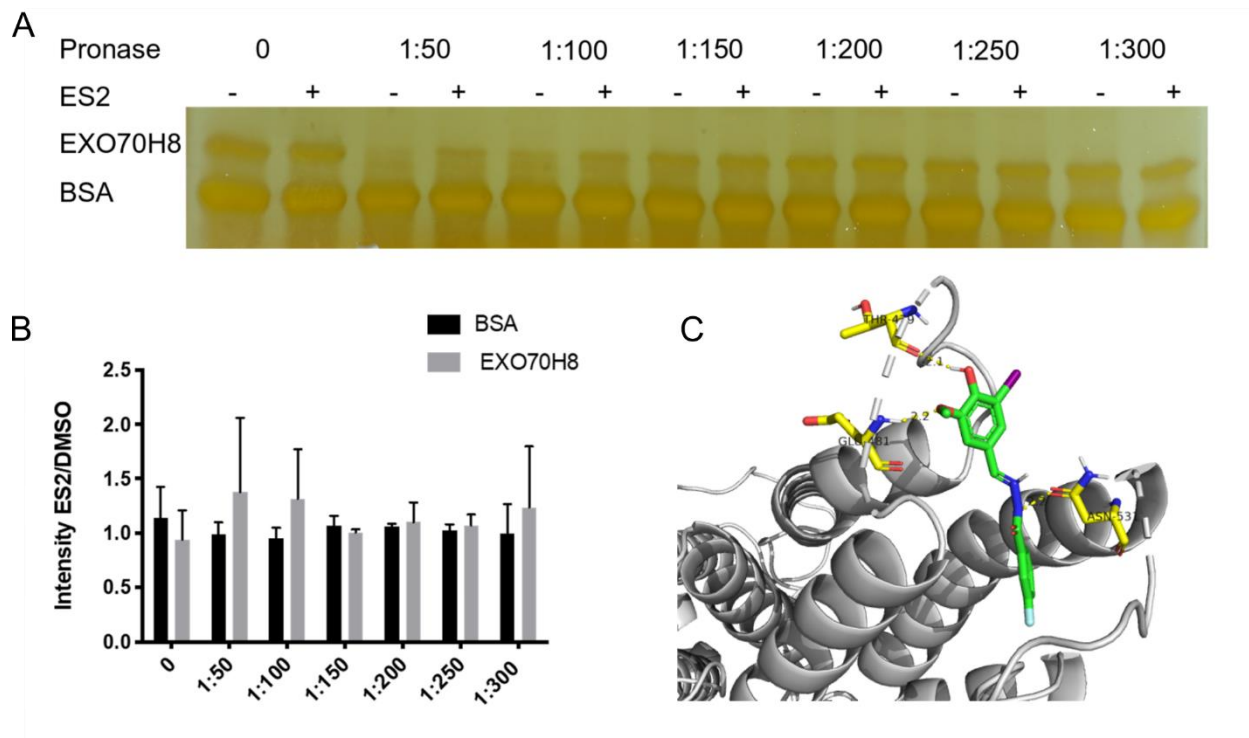
Figure 2.9 DARTS assay for the interaction between ES2 and AtEXO70E2 with a series of pronase concentration gradients. (A) Silver staining of proteins from DARTS assay. (B) Quantification of ratios of AtEXO70E2 and BSA intensities in samples treated with ES2 and DMSO, as shown in A. Samples treated with different concentrations of pronase, ranging from 50X dilution to 300X dilution. The signal intensity between ES2 and DMSO group of AtEXO70E2 and BSA under different dilutions of pronase was measured using ImageJ. The error bars represent SDs of three independent experiments.
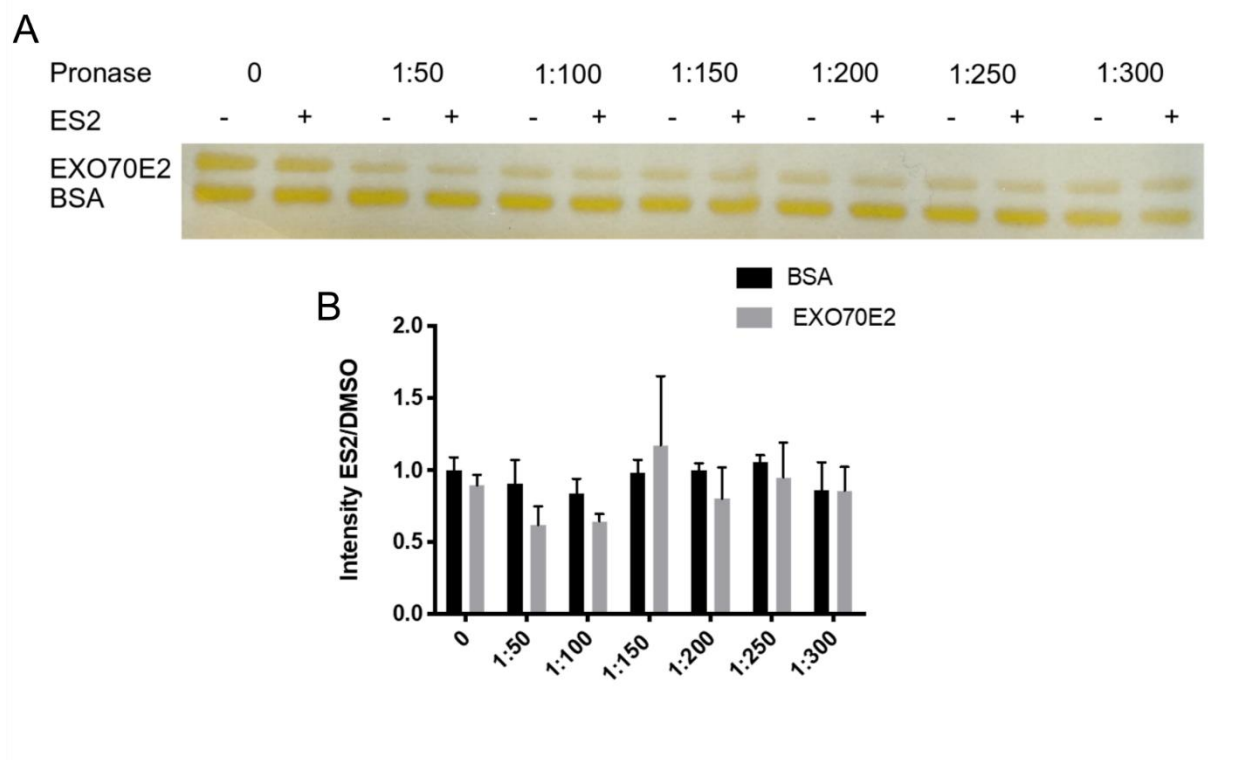
2.5   Discussion

Because of the high instability of isolated AtEXO70 proteins, the binding buffer of FPLC system for purifying proteins contains high salted ions and the concentration of NaCl was kept at 1M. Once the concentration of NaCl decreased to standard 150 mM, the AtEXO70 proteins would be precipitated. However, the high concentration of salted ions can cause the small molecules to interact with non-targeted proteins, resulting the false positive for binding pattern. Therefore, for ensuring the target proteins of ES2, the consistence from three and more independent experiments are necessary, and two and more consistent conclusions from other target identification methods are needed.

Exocytosis is conserved in eukaryotic cells, and the exocyst complex is evolutionarily conserved from yeasts to mammals. In mammalian cell, insulin assists in the targeting of glucose transporter Glut4 to the plasma membrane, which requires the support of the exocytosis complex and EXO70 interacts with G protein TC10 in response to insulin (Inoue, Chang, Hwang, Chiang, & Saltiel, 2003). In *Drosophila*, glutamatergic neurons and octopaminergic neurons contains EXO70, and in presynaptic cells, EXO70 mediates the outgrowth of synapses (Liebl, Chen, Karr, Sheng, & Featherstone, 2005;Gerges, Backos, Rupasinghe, Spaller, & Esteban, 2006). Drosophila EXO70 mutants exhibits temperature-sensitive defects in neurite outgrowth and adult lethality, which suggests the role of EXO70 in thermal stress survival (Koon et al., 2018). However, the molecular mechanism of exocytosis and precise roles of EXO70 in different species remain distinct and unclear. Chemicals suppress exocytosis through targeting EXO70, such as ES2, has the potential to contribute the drug designs for cancer treatment (Zhang et al., 2016).

ES2 significantly contributes to the understanding of plant exocytosis mechanisms, and analogs of ES2 that have similar chemical structures have the potential to reveal more information. ES2-14 is analog of ES2, which has an iodine taking place of methoxy group at the same position. With a structural minor change, ES2-14 exhibits stronger inhibition of exocytosis than ES2 in Arabidopsis and even in fungal pathogens (Huang et al., 2019). ES2-14 not only targets AtEXO70A1, but also targets MoEXO70 and BcEXO70 that come from fungus *M. oryzae* and *B. cinereal*. ES2 and its derivatives potentially provide a useful tool for studying fungus-plant interactions.

2.6   References

Chong, Y. T., Gidda, S. K., Sanford, C., Parkinson, J., Mullen, R. T., Goring, D. R. (2010). Characterization of the Arabidopsis thaliana exocyst complex gene families by phylogenetic, expression profiling, and subcellular localization studies. *New Phytol, 185*(2), 401-419.

Cvrckova, F., Grunt, M., Bezvoda, R., Hala, M., Kulich, I., Rawat, A., et al. (2012). Evolution of the land plant exocyst complexes. *Front Plant Sci, 3*, 159.

Dallakyan, S., Olson, A. J. (2015). Small-molecule library screening by docking with PyRx. *Methods Mol Biol, 1263*, 243-250.

Gerges, N. Z., Backos, D. S., Rupasinghe, C. N., Spaller, M. R., Esteban, J. A. (2006). Dual role of the exocyst in AMPA receptor targeting and insertion into the postsynaptic membrane. *EMBO J, 25*(8), 1623-1634.

Huang, L., Li, X., Li, Y., Yin, X., Li, Y., Wu, B., et al. (2019). Endosidin2-14 Targets the Exocyst Complex in Plants and Fungal Pathogens to Inhibit Exocytosis. *Plant Physiol, 180*(3), 1756-1770.

Inoue, M., Chang, L., Hwang, J., Chiang, S. H., Saltiel, A. R. (2003). The exocyst complex is required for targeting of Glut4 to the plasma membrane by insulin. *Nature, 422*(6932), 629-633.

Koon, A. C., Chen, Z. S., Peng, S., Fung, J., Zhang, X., Lembke, K. M., et al. (2018). Drosophila Exo70 Is Essential for Neurite Extension and Survival under Thermal Stress. *J Neurosci, 38*(37), 8071-8086.

Kulich, I., Pecenkova, T., Sekeres, J., Smetana, O., Fendrych, M., Foissner, I., et al. (2013). Arabidopsis exocyst subcomplex containing subunit EXO70B1 is involved in autophagy-related transport to the vacuole. *Traffic, 14*(11), 1155-1165.

Kulich, I., Vojtikova, Z., Glanc, M., Ortmannova, J., Rasmann, S., Zarsky, V. (2015). Cell wall maturation of Arabidopsis trichomes is dependent on exocyst subunit EXO70H4 and involves callose deposition. *Plant Physiol, 168*(1), 120-131.

Kulich, I., Vojtikova, Z., Sabol, P., Ortmannova, J., Nedela, V., Tihlarikova, E., et al. (2018). Exocyst Subunit EXO70H4 Has a Specific Role in Callose Synthase Secretion and Silica Accumulation. *Plant Physiol, 176*(3), 2040-2051.

Kumar, S., Stecher, G., Li, M., Knyaz, C., Tamura, K. (2018). MEGA X: Molecular Evolutionary Genetics Analysis across Computing Platforms. *Mol Biol Evol, 35*(6), 1547-1549.

Li, S., Chen, M., Yu, D., Ren, S., Sun, S., Liu, L., et al. (2013). EXO70A1-mediated vesicle trafficking is critical for tracheary element development in Arabidopsis. *Plant Cell, 25*(5), 1774-1786.

Li, S., van Os, G. M., Ren, S., Yu, D., Ketelaar, T., Emons, A. M., et al. (2010). Expression and functional analyses of EXO70 genes in Arabidopsis implicate their roles in regulating cell type-specific exocytosis. *Plant Physiol, 154*(4), 1819-1830.

Liebl, F. L., Chen, K., Karr, J., Sheng, Q., Featherstone, D. E. (2005). Increased synaptic microtubules and altered synapse development in Drosophila sec8 mutants. *BMC Biol, 3*, 27.

Stegmann, M., Anderson, R. G., Westphal, L., Rosahl, S., McDowell, J. M., Trujillo, M. (2013). The exocyst subunit Exo70B1 is involved in the immune response of Arabidopsis thaliana to different pathogens and cell death. *Plant Signal Behav, 8*(12), e27421.

Synek, L., Schlager, N., Elias, M., Quentin, M., Hauser, M. T., Zarsky, V. (2006). AtEXO70A1, a member of a family of putative exocyst subunits specifically expanded in land plants, is important for polar growth and plant development. *Plant J, 48*(1), 54-72.

Synek, L., Vukasinovic, N., Kulich, I., Hala, M., Aldorfova, K., Fendrych, M., et al. (2017). EXO70C2 Is a Key Regulatory Factor for Optimal Tip Growth of Pollen. *Plant Physiol, 174*(1), 223-240.

Wang, W., Liu, N., Gao, C., Cai, H., Romeis, T., Tang, D. (2020). The Arabidopsis exocyst subunits EXO70B1 and EXO70B2 regulate FLS2 homeostasis at the plasma membrane. *New Phytol, 227*(2), 529-544.

Wang, W., Liu, N., Gao, C., Rui, L., Tang, D. (2019). The Pseudomonas Syringae Effector AvrPtoB Associates With and Ubiquitinates Arabidopsis Exocyst Subunit EXO70B1. *Front Plant Sci, 10*, 1027.

Zhang, C., Brown, M. Q., van de Ven, W., Zhang, Z. M., Wu, B., Young, M. C., et al. (2016). Endosidin2 targets conserved exocyst complex subunit EXO70 to inhibit exocytosis. *Proc Natl Acad Sci U S A, 113*(1), E41-E50.

Zhu, Y., Wu, B., Guo, W. (2019). The role of Exo70 in exocytosis and beyond. *Small GTPases, 10*(5), 331-335.

Zimmermann, L., Stephens, A., Nam, S. Z., Rau, D., Kubler, J., Lozajic, M., et al. (2018). A Completely Reimplemented MPI Bioinformatics Toolkit with a New HHpred Server at its Core. *J Mol Biol, 430*(15), 2237-2243.

CHAPTER 3.   IDENTIFY GENES RELATED TO CELLULOSE SYNTHASE COMPLEX TRAFFICKING

3.1   Abstract

A major component of the plant cell wall is cellulose, which is the most widely distributed and most abundant polysaccharide on earth and benefits human life in diverse aspects. Cellulose in plant cells is synthesized by Cellulose Synthase Complex (CSC), catalyzing the cell wall formation at the plasma membrane. CSC is delivered from the ER to the plasma membrane as a protein cargo in endomembrane trafficking. Some proteins, such as CSI1 and PATROL1, are known to be involved in CSC trafficking. However, other proteins related to CSC trafficking remain undiscovered. Chemical genetics is an efficient method which uses small molecules to probe the entire molecular signaling pathway and identify new genes participating in the process. Endosidin20 (ES20) is a small molecule that targets CESA6 and screening for mutants that are hypersensitive to ES20 was conducted to find out new genes involved in CSC trafficking. Ethyl methanesulfonate (EMS) mutagenized PIN2::PIN2:GFP and CESA6::CESA:YFP populations were screened for plants with increased sensitivity to ES20 inhibition. We identified nine mutants from PIN2::PIN2: GFP population and ten mutants from CESA6::CESA:YFP population that are hypersensitive to ES20. The mutated CESA6 gene showing resistance to ES20 have potential agricultural value, and ES20 is a good candidate to be developed into herbicide.

3.2   Introduction

Small molecules exhibit great potential in dissecting intricate molecular mechanisms of plant biology, such as endomembrane trafficking, plant immune response and hormone signaling (Hicks & Raikhel, 2012). As an early discovered small molecule, Brefeldin A (BFA) targets Sec7 domain of ARF GEF and inhibits the ER-Golgi trafficking route (Renault, Guibert, & Cherfils, 2003;Mossessova, Corpina, & Goldberg, 2003). Taking advantage of BFA, several components involved in endomembrane trafficking are screened out using fluorescent imaging, such as BIG2 and ARFA1C (Tanaka, Kitakura, De Rycke, De Groodt, & Friml, 2009;Tanaka et al., 2014;Kitakura et al., 2017). Through hypersensitive screening with synthetic small molecule Sortin1, *s1h2-50* and *mtv6* mutants are identified to have defects in flavonoid biosynthesis and vacuolar trafficking (Rosado et al., 2011). These successful gene identification highlights unparalleled advantages of small molecules in discovering of new regulators in endomembrane trafficking. Small molecules generate transient manipulation on specific trafficking components acutely and reversibly, which can be directly visualized by live-cell imaging (Huang, Li, & Zhang, 2019).

Recently characterized clusters of small molecules contribute to endomembrane network significantly. Through primary screening on aberrant germination and morphology of tobacco pollen and secondary screening using membrane markers, 123 molecules are selected, which makes up a pool of chemicals and representative molecules are named endosidins (Drakakaki et al., 2011). Similar with BFA, Endosidin4 targets Sec7 domain of ARF GEFs and interferes the membrane fusion activated by ARF1 GTPases (Kania et al., 2018). Endosidin9 binds with N-terminal domain (nTD) of clathrin heavy chain and inhibits clathrin-mediated endocytosis (Dejonghe et al., 2016;Dejonghe et al., 2019). Endosidin16 perturbs nonbasal protein trafficking through interacting with RabA GTPases (Li et al., 2017). These novel molecules cause unique

features in endomembrane pathways, which assists in revealing complicated machineries of membrane trafficking network.

Endosidin20 (ES20) has been recently identified as the cellulose synthase inhibitor that targets CESA6 at the catalytic site directly (Huang et al., 2020). When exposed to ES20, the roots of Arabidopsis are shorter and swollen. The phenotypes induced by ES20 are similar with cellulose synthase mutants. For plant cells, when the formation of cell wall is interrupted, the plant cell will lose shape and the root becomes shorter and swollen (Gillmor, Poindexter, Lorieau, Palcic, & Somerville, 2002). ES20 targets CESA6, resulting in misfunction of CESA6 in cellulose synthesis and interruption of cell wall formation. There are many cellulose synthesis inhibitors such as isoxaben and indaziflam that are helpful to inspect the functions and dynamics of CSCs, but it is not known that what their targets are and how they interact with CESAs. It is the limitation preventing their utilization in the chemical genetic analysis of CSC (Huang & Zhang, 2020). Through chemical genetic screening, mutants that are hypersensitive to ES20 are likely to have altered regulation in CSC trafficking pathway, which facilitates the identification of new components in this pathway.

The inhibition of cellulose synthesis caused by ES20 is broad-spectrum. ES20 significantly inhibits the root growth of dicotyledon plants, such as tomato and soybean, and monocotyledon plants, such as rice and maize. Besides these agricultural crops, ES20 have inhibitory effects on the common weeds as well, such as dandelion and Kentucky Bluegrass (Huang & Zhang, 2020). The mutated CESA6 gene allows Arabidopsis to tolerate ES20 inhibition, and ES20 spraying on seedlings in soil kills the plants. ES20 has the potential to be developed into an herbicide, through generation of transgenic crops. Carrying mutated CESA6 gene, transgenic crops exhibit high ES20 tolerance (Huang & Zhang, 2020).

3.3   Materials and Methods

3.3.1   Plant seeds sterilization and growth media

Arabidopsis seeds were used for the growth assay, and they were sequentially sterilized with 50% (v/v) bleach (5.25% [w/v] sodium hypochlorite) and 75% (v/v) ethanol. After that, seeds were washed with sterilized water for several times to get rid of the bleach and ethanol. Sterilized seeds were kept in water and darkness at 4°C for 3 days for vernalization, and then sowed on one-half strength MS growth medium (2.2g/L Murashige and Skoog, 1%[w/v] Sucrose, 0.8%[w/v] agar, pH = 5.8) or 0.7 μM drug medium (2.2g/L Murashige and Skoog, 1%[w/v] Sucrose, 0.8%[w/v] agar, pH = 5.8, 0.7 μM Endosidin20).

3.3.2   Chemical screening

The seeds of PIN2::PIN2:GFP and CESA6::CESA:YFP were treated with Ethyl methanesulfonate (EMS) to generate random mutations in genome. After EMS treatment, the mutagenized seeds were sowed into soil and seeds were harvested from these plants, which was the second generation (M2). Compared with the untreated seedlings on growth medium, the seedlings that had shorter and swollen roots on 0.7 μM ES20 medium were selected. The selected seedlings were transferred to growth medium for recovery. We then select for seedlings whose roots recovered to normal growth without ES20, and harvest their seeds, which is M3 generation. With M3 generation seeds, the confirmation test was conducted through sowing them on ½ MS and low dosage ES20 plates (0.7 μM) respectively to observe the difference of root growth to verify their hypersensitivity. After the confirmation test, the candidate hypersensitive mutants were selected. The confirmed mutant plants were crossed to *Ler* ecotype to generate the

84

mapping population. The mutants in the F2 population resulting from this cross were selected for high-throughput sequencing to clone the mutant gene.

3.3.3   Agrobacterium-mediated transformation

For one transformation experiment, 100-150 seeds of Micro-Tom were sterilized in 1% (v/v) sodium hypochloride solution for 2 minutes and were sequentially rinsed with sterile water for three times. The seeds were kept in sterile water overnight for imbibition and sowed on germination medium (4.4g/L MS, 15g/L Sucrose, 4g/L agar, pH=5.8) in sterile magenta boxes. Seeds required 7-10 days at 25°C with light for germination. When the cotyledons were fully expanded and the true leaves are slightly visible, the seedlings were ready for *Agrobacterium* infection. For inoculation, the Agrobacterium culture were collected by centrifugation and the pelleted cells were resuspended in infection medium (4.4g/L MS, 30g/L Sucrose, 100μM acetosyringone, 10 μM mercaptoethanol, pH=5.8). The distal end of cotyledons from 7- to 10-day-old seedlings were cut off and the explants were soaked in the bacterial suspension for 30 minutes with rotation. The explants were taken out and dried on sterilized paper towel. 30-40 explants were placed on one co-cultivation medium (4.4g/L MS, 30g/L Sucrose, 100μM acetosyringone, 1.5mg/L zeatin, 4g/L agar, pH=5.8) with abaxial side of the leaf upwards. The plates with infected cotyledons were placed in darkness at 25°C for 2-3 days. The rigid green explants were transferred to callus induction medium (4.4g/L MS, 30g/L Sucrose, 1.5mg/L zeatin, 7.5mg/L Hygromycin, 375mg/L Augmentin, 4g/L agar, pH=5.8) with the abaxial side down and the plates were kept at 25°C with light for callus induction and for all the following transformation steps. The transformation was repeated every 10 days. After two weeks, the explants were transferred with shoot buds to shoot induction medium (4.4g/L MS, 30g/L Sucrose, 1mg/L zeatin, 7.5mg/L Hygromycin, 375mg/L Augmentin, 4g/L agar, pH=5.8) for

shoot development. Once the elongated shoot reached to 1-2 cm, they were transferred to root medium (2.2g/L MS, 15g/L Sucrose, 1.5mg/L zeatin, 3.75mg/L Hygromycin, 375mg/L Augmentin, 4g/L agar, pH=5.8) for root generation. When roots grew to 5 cm, they were transferred to soil and took to greenhouse until they became into individual plants. After two-month growth in greenhouse, the seeds were collected from each transformant line and dried overnight in hood. Seeds were kept in plastic bags and stored at 4°C in darkness.

3.4 Results

Before screening, the wild type seeds of Arabidopsis Col-0 on ES20 media was tested with a series of concentration gradients from 0.6μM to 1μM (Figure 3.1). ES20 inhibits the cellulose synthesis for the cell wall so that the plants have shorter and swollen roots. The inhibition caused by ES20 was visualized using inhibition ratio which was the major selection criteria for hypersensitive screening. Inhibition ratio is calculated according to the following equation.

$$\text{Inhibition ratio} = \frac{\Delta root\ length}{root\ length\ on\ growth\ media}$$

From the test, at 0.6 μM, the inhibition ratio is around 5%, and it reaches to 35% when it comes to 0.8μM. The range of inhibition ratio allows us to detect the genetic changes through phenotypes, so the low dosage concentration of ES20 was defined as 0.7 μM. At this concentration of ES20, the roots start to show shorter and swollen phenotypes. The effects of ES20 at 0.7 μM are mild enough on wild type plants such that the hypersensitive mutants can be distinguished from them. For the screening, the inhibition ratio of wild type seedlings is between 5% and 35%.

In screening, some proteins whose locations and trafficking pathways are already known are used for markers. For my hypersensitive screening, I conducted hypersensitive screening with two transgenic lines carrying PIN2::PIN2:GFP and CESA6::CESA: YFP (Figure 3.2). Same with PIN1, PIN2 is an auxin efflux carrier trafficking from the ER to the plasma membrane where it works for translocating the auxin. PIN2 proteins fused with GFP is used as a marker to show the trafficking processes of ER-PM. In addition, we took the CESA6 protein fused with GFP as a marker protein to visualize the CESA6 trafficking route in Arabidopsis cells. CESA6::CESA: YFP is a better background to visualize the changes of CESA trafficking caused by the ES20, which facilitates the identification of novel genes involved in endomembrane trafficking. For hypersensitive mutants screening, we expected to find new proteins assisting CSC trafficking.

The phenotypic screening for hypersensitive mutants with Arabidopsis seeds was started in PIN2::PIN2:GFP background. Seeds of the Arabidopsis plant carrying a PIN2::PIN2:GFP transgene were treated with EMS and produced M1 seeds. Their progenies were self-fertilized and randomly divided into 47 pools. For the M2 seeds, seeds from 33 pools were tested on 0.7 µM ES20 media and 1/2 MS growth media as the control. Nearly 2000 seeds were sowed on 1/2 MS growth media as the control and another 2000 seeds from the same pool on 0.7 µM ES20. The seedlings with short and swollen roots on ES20 media were selected and transferred them on half MS growth media to confirm their growth without ES20. Some seedlings recovered back to normal growth and roots started to grow longer, but some seedlings remained short and swollen. However, the exogenous application of ES20 causes the temporal interruption of molecular pathways, indicating that plants recover without drug. Those seedlings whose roots kept shorter and swollen are likely caused by mutations rather than ES20. Therefore, only the M2 seedlings

showing responses to ES20 and recovering to normal growth without ES20 were selected for M3 generation, and there were 417 lines in total selected for M3. All the M3 lines were screened and their ability to recover was confirmed in the same way as the M2 seedlings. The seedlings that had shorter and swollen roots were able to recover were selected. Finally, nine candidates for ES20 hypersensitivity were obtained.

For the screening with CESA6::CESA:YFP, the strategy for hypersensitivity was not the same that for PIN2::PIN2:GFP (Figure 3.2). 432 seedlings from M1 seeds have been selected based on the shorter root length, which was transferred in soil and produced M2 seeds by self-fertilization. Each individual plant formed a family, and there are 48 families of M2 seeds. After growing test on M2 seeds, the seedlings of M2 seeds showed segregation on drug media, and each family had seedlings with normal growth and seedlings with shorter and swollen roots. Because the phenotype of short roots is dominant, the M2 generation of EMS seeds showed phenotypic segregation. According to the approximate segregation ratio and shorter swollen roots, 48 seedlings were selected and 23 of them recover without ES20. I transferred these 23 lines into soil and outcrossed them to Arabidopsis *Ler* ecotype. The progenies of plants from these 23 lines which were selected to outcross were double tested on drug media to confirm the hypersensitivity. From the confirmation test, ten candidate lines were selected, and 5 of them were likely to be homozygous because all the seedings keep the same to be short and swollen. The progenies of outcrossed seeds were sowed in soil and produced the next generation by selfing. The offspring tested on ES20 media that exhibits homozygous phenotype with short and swollen roots and high inhibition ratio, will be selected for whole genomic sequencing.

The selection criteria for hypersensitive mutants is the higher inhibition ratio. The seedlings were considered as the hypersensitive candidates if they showed swollen roots and had

a higher inhibition ratio than PIN2:GFP or CESA:YFP that was the negative control. All candidates are ranked according to the inhibition ratios in Table 3.1. In PIN2:GFP lines, 34-4 family has the highest inhibition ratio that is 40.22%, and the inhibition ratio for the control, PIN2:GFP, is 20.72%. (Figure 3.3). For transgenic lines with CESA6:YFP, 412-2 is one of the ten hypersensitive potential lines and it has the highest inhibition ratio 48.53%, compared with the CESA:YFP whose is 14.37% (Figure 3.4). Besides the higher inhibition ratios, the seedlings of 34-4 line and 412-2 line showed swollen roots, which is the specific phenotype caused by ES20. Swollen roots are the major selection criteria as well. Some lines that showed this specific phenotype strongly but did not have a high inhibition ratio were still considered as good hypersensitive mutant, such as 39-40 with PIN2::PIN2: GFP and 240-1 with CESA6::CESA: YFP. For 39-40 (Figure 3.5). Low dosage ES20 caused no statistical difference on PIN2 control, as well as no significant difference on 39-40, but the mutant 39-40 has enhanced swollen roots. The segregation of the 39-40 on drug medium suggests it is likely to have a heterozygous allele. In addition, 240-1 with CESA6::CESA: YFP is another example for swollen phenotype (Figure 3.6). There is no statistical difference on CESA6 wild type and the inhibition ratio is 15.77%, but the inhibition of 240-1 is 34.23% which is significantly different. Interestingly, a majority of 240-1 seedlings showed tiny and swollen roots and the swollen phenotype on drug media was enhanced, which is the specific phenotype caused by ES20. The defects in cellulose synthesis can cause abnormal growth of roots, and the application of exogenous ES2 enhanced the defective phenotypes.

The Arabidopsis CESA6 carrying a mis-sense mutation at the catalytic site was transformed into Micro-Tom tomato using Agrobacterium-mediated transformation (Figure 3.7). The mis-sense mutation changes Glutamic acid at 929 position to Lysine. The mutated CESA6

gene with its native promoter was obtained from Arabidopsis and inserted into binary vector

EH105 with YFP tag at the N-terminal. Using agrobacterium, the recombinant plasmid was

transformed into tomatoes. Hygromycin is the selection marker, and three independent lines at T_0

generation were isolated. When it comes to T_1, the insertion was confirmed through PCR-based

genotyping with YFP primers. The confirmed seedlings are growing up to T3 generation.

Table 3.1 Hypersensitive candidates with their inhibition ratios at 0.7 μM ES20

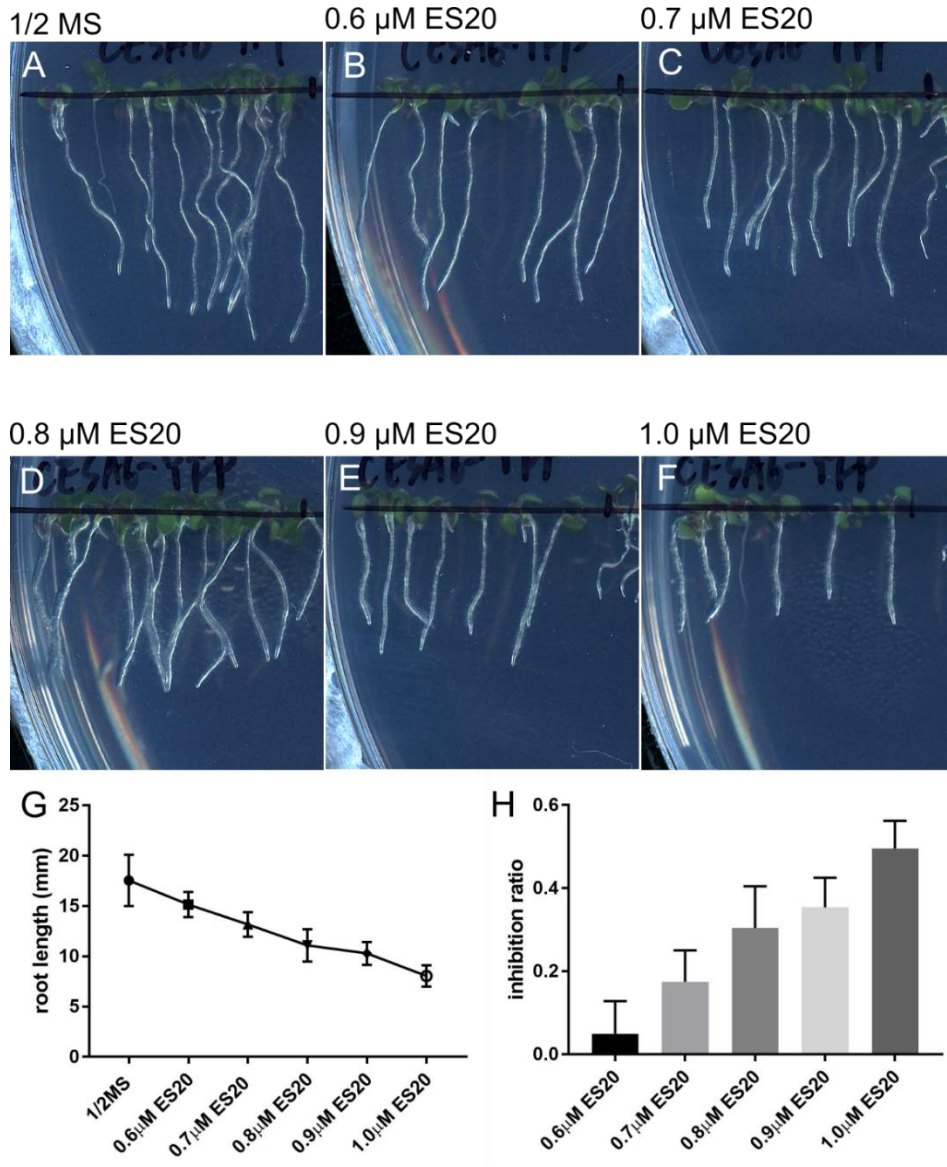| Candidates with PIN2::PIN2:GFP	Inhibition ratios	Candidates with CESA6::CESA:YFP	inhibition ratios
34-4	40.22%	412-2	48.53%
31-10	35.48%	317-1	46.10%
27-9	34.16%	84-1	44.96%
38-18	27.65%	412-1	42.93%
30-15	27.08%	412-3	40.51%
32-22	27.00%	402-2	39.28%
31-12	25.78%	240-1	34.23%
37-9	25.00%	155-1	34.17%
39-40	23.84%	198-3	30.84%
		193-1	27.57%

Figure 3.1 6-day-old Col-0 seedlings with CESA6::CESA:YFP grown in the presence of a series of concentrations of ES20. The seeds of Col-0 with CESA6::CESA:YFP were sowed on ½ MS medium (A), 0.6μM ES20 medium (B), 0.7 μM ES20 medium (C), 0.8 μM ES20 medium (D), 0.9 μM ES20 medium (E) and 1.0 μM ES20 medium (F) respectively for 6 days. The root lengths were measured using ImageJ and showed in (G). The error bars represent SDs. The inhibition ratio at each concentration was calculated and showed (H).

EMS

M1 seeds
(PIN2-GFP)

M1 pools

M2 seedlings

M3 lines

M3 seedlings

EMS

M1 sees
(CesA6-YFP)

M1 seedlings

M2 lines

OutCrossed F1

X

Ler
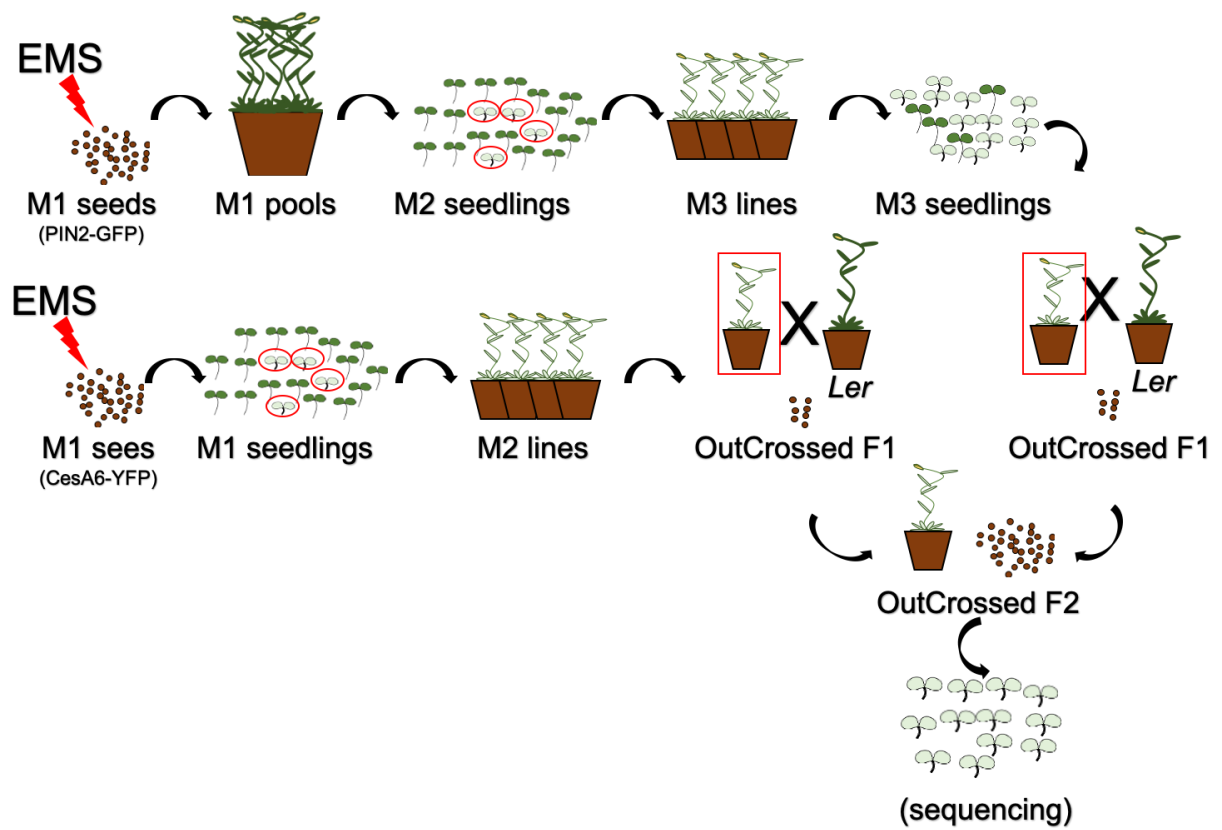
OutCrossed F1

X

Ler

OutCrossed F2

(sequencing)

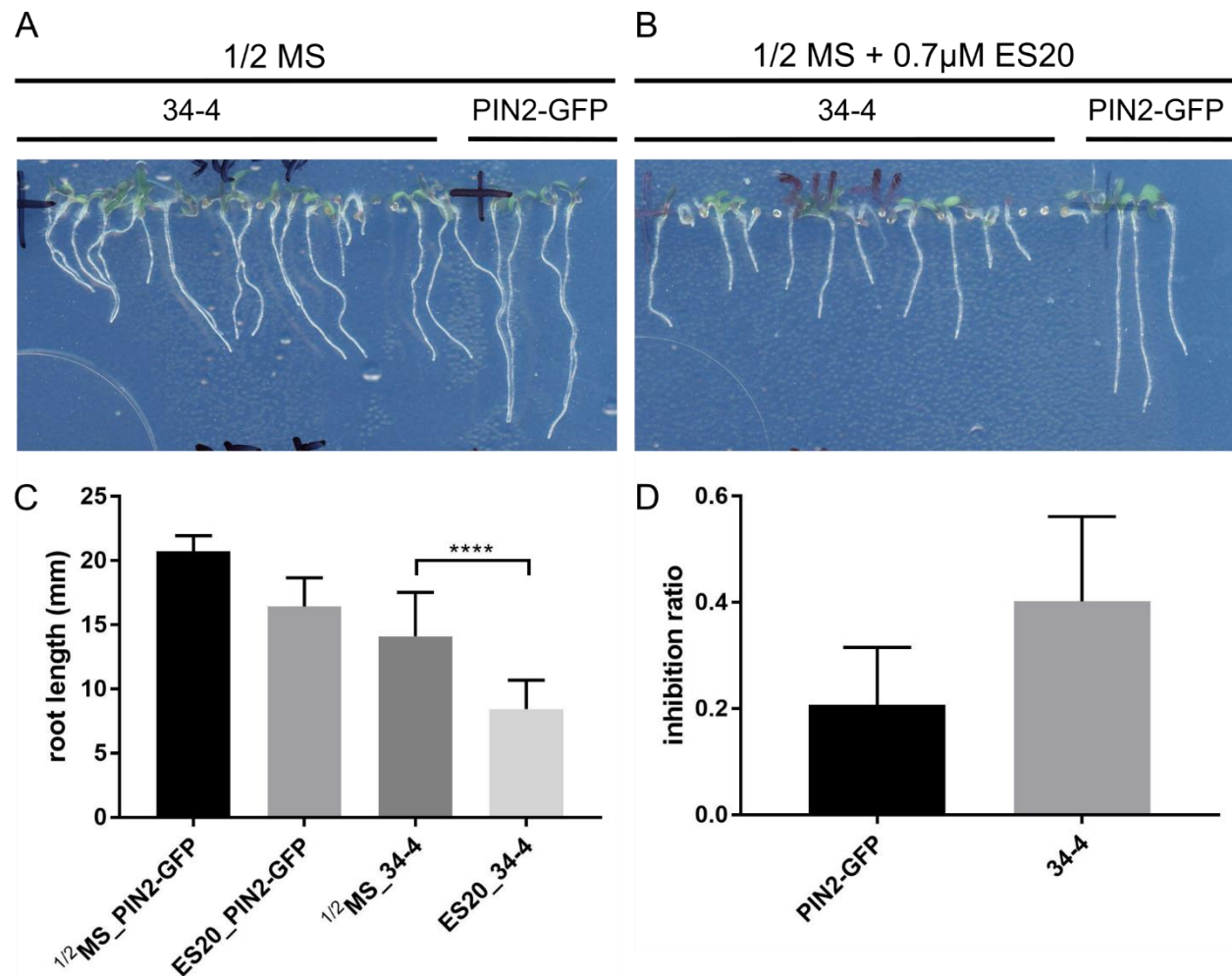Figure 3.2 Schematic diagram of the hypersensitive mutants screening.

Figure 3.3 Hypersensitive mutant candidate 34-4 in PIN2::PIN:GFP background. The selected
M3 seeds of 34-4 line were sowed on ½ MS medium (A) and 0.7 μM ES20 medium (B)
respectively for 6 days. The root lengths were measured using ImageJ and t-test was conducted
(C). **** refers to the significant difference in statistics (P<0.0001). The error bars represent
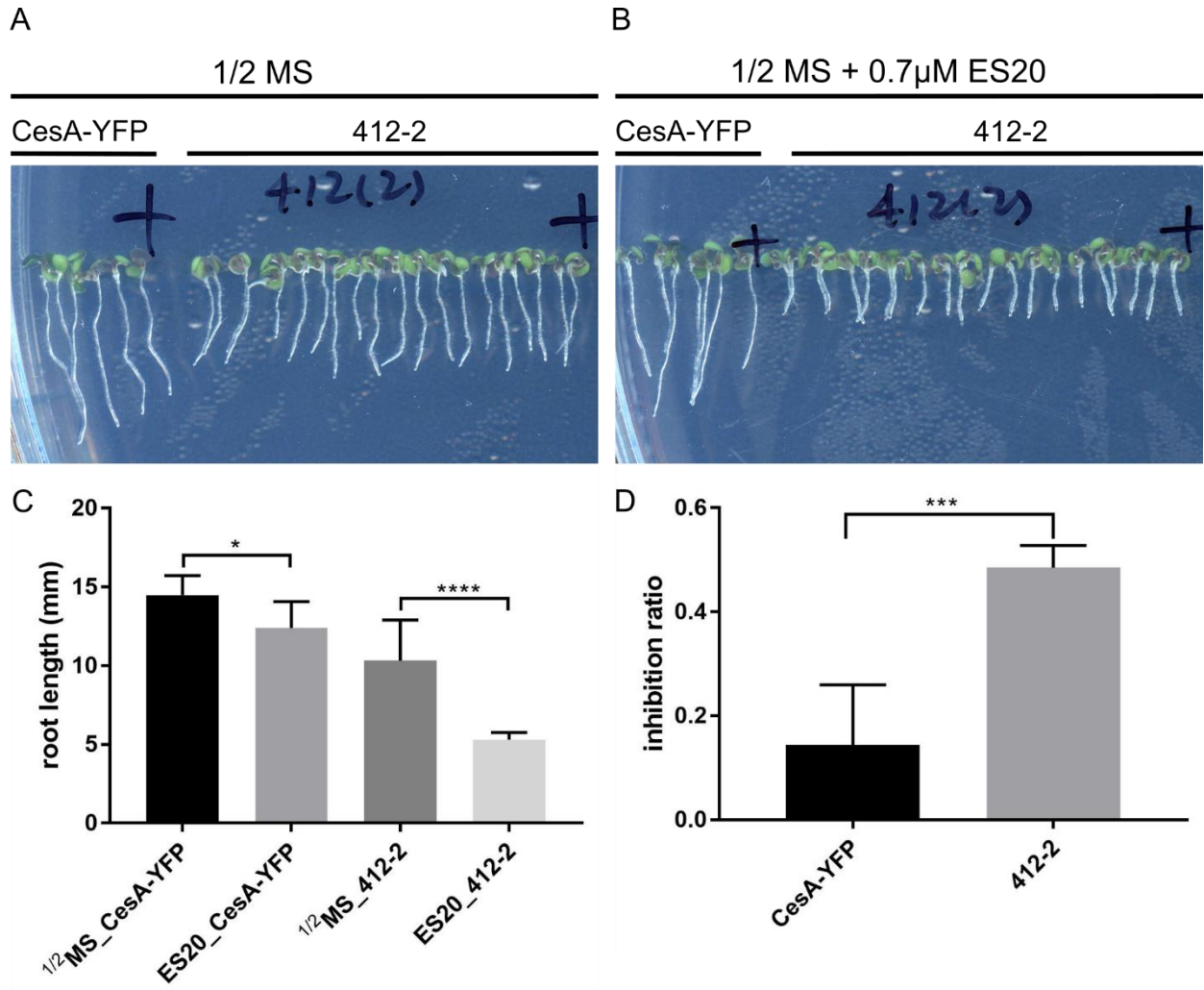SDs. The inhibition ratio was calculated and showed in (D).

Figure 3.4 Hypersensitive mutant candidate 412-2 in CESA6::CESA:YFP background. The selected M2 seeds of 412-2 line were sowed on ½ MS medium (A) and 0.7 μM ES20 medium (B) respectively for 6 days. The root lengths were measured using ImageJ and t-test was conducted (C). * refers to the significant difference in statistics ($P<0.05$), *** refers to significant difference in statistics ($P<0.001$), **** refers to significant difference in statistics ($P<0.0001$). The error bars represent SDs. The inhibition ratio was calculated and showed in (D).
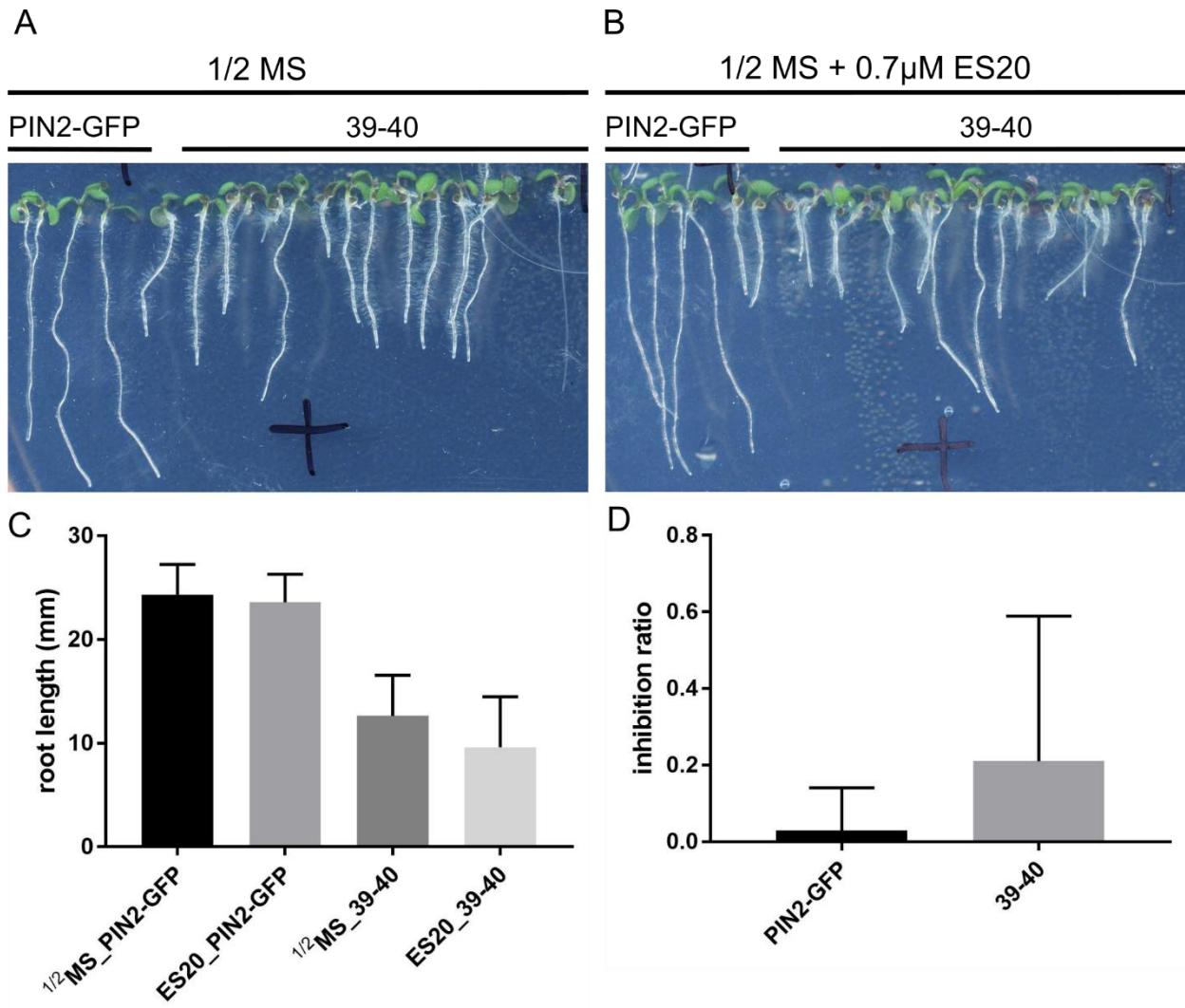
Figure 3.5 Hypersensitive mutant candidate 39-40 in PIN2::PIN:GFP background. The selected M3 seeds of 39-40 line were sowed on ½ MS medium (A) and 0.7 µM ES20 medium (B) respectively for 6 days. The root lengths were measured using ImageJ and t-test was conducted (C). The error bars represent SDs. The inhibition ratio was calculated and showed in (D).
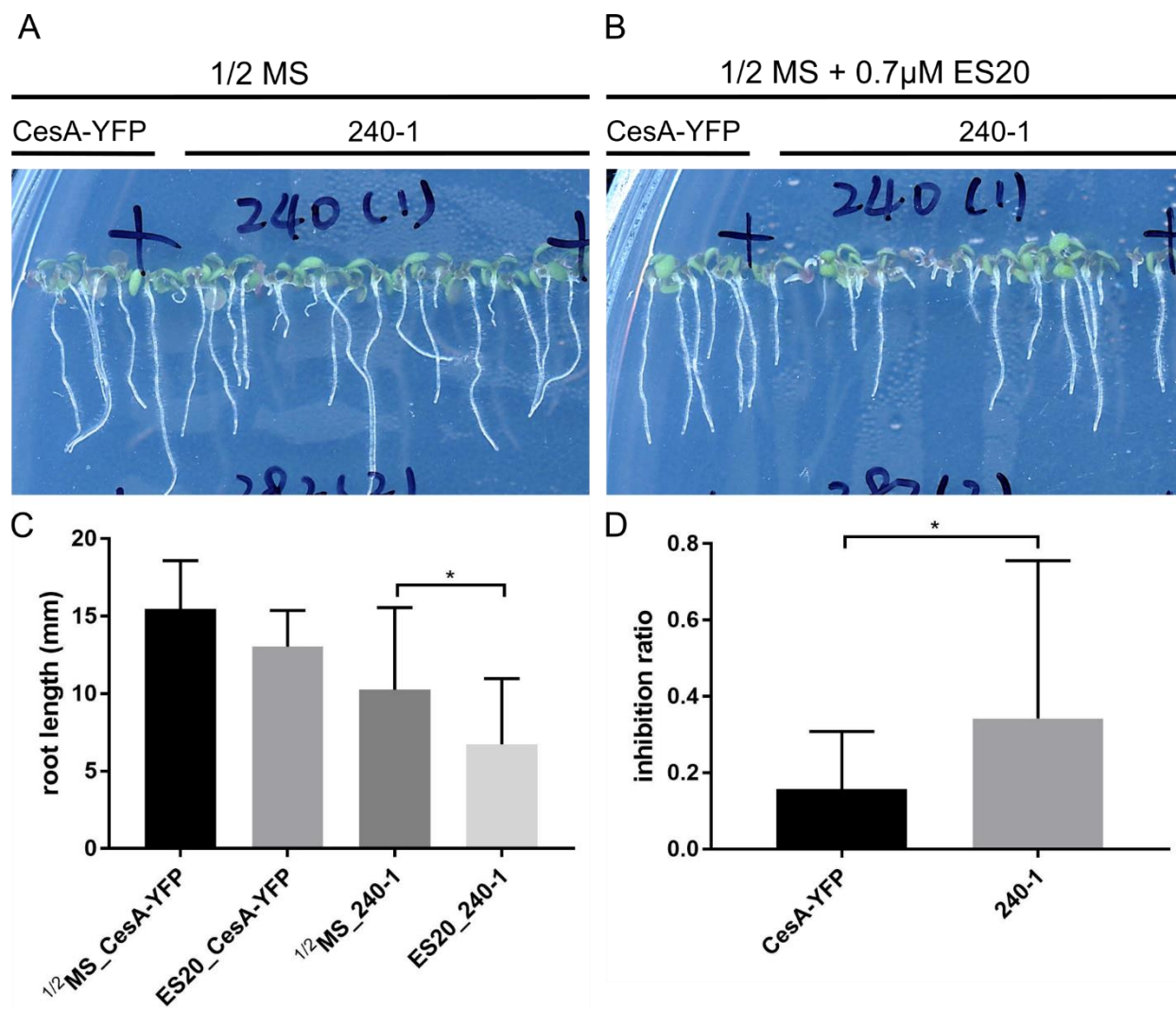
Figure 3.6 Hypersensitive mutant candidate 240-1 in CESA6::CESA:YFP background. The selected M2 seeds of 240-1 line were sowed on ½ MS medium (A) and 0.7 μM ES20 medium (B) respectively for 6 days. The root lengths were measured using ImageJ and t-test was conducted (C). * refers to the significant difference in statistics ($P<0.05$). The error bars represent SDs. The inhibition ratio was calculated and showed in (D).
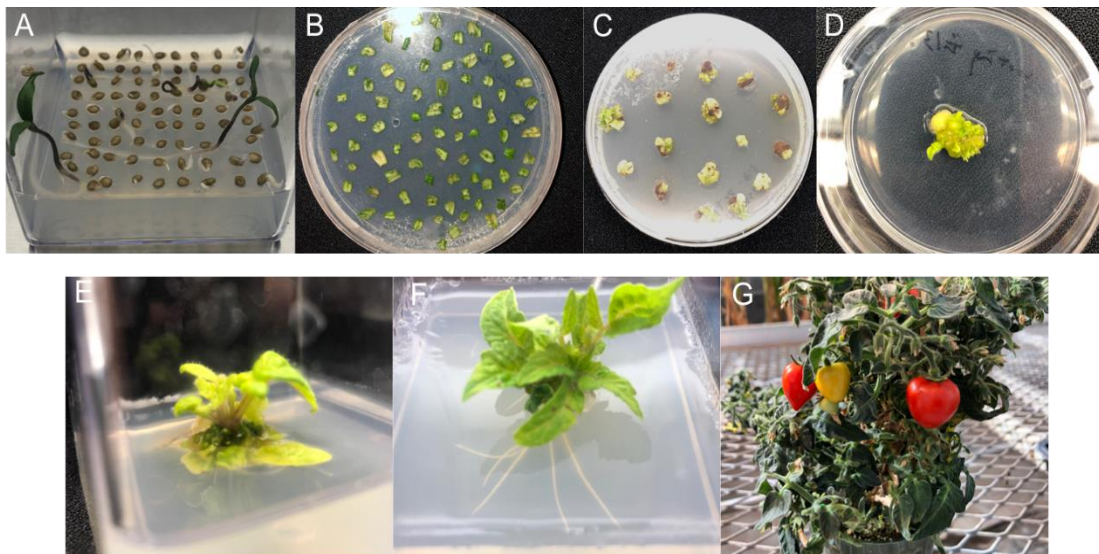
Figure 3.7 Different stages of transformation of tomato. (A) Germinated seeds and seedlings in vitro. (B) Explants in co-cultivation medium after the infection of Agrobacterium carrying the EHA105 binary vector. (C) Cotyledonary explants on callus induction with the antibiotic Hygromycin as the selection marker. (D) Regenerated callus from explant. (E) callus with regenerating shoot buds growing on shoot development medium. (F) Young plantlet with well-developed roots on root medium. (G) Individual transformed T_0 plants

3.5   Discussion

All of the hypersensitive lines, nine lines of PIN2::PIN2:GFP and ten lines of

CESA6::CESA:YFP are supposed to be outcrossed with *Ler*. The F2 progenies of the

outcrossing lines are harvested and tested on ES20 medium. The homozygous lines showing the

shorter and swollen roots without segregation will be used to do whole genome sequencing. Next

generation sequencing generates millions of short DNA sequencing reads and the mutations of

interest can be identified by differences on single nucleotide polymorphisms (SNPs) distribution.

Phenotypes usually result from mutations in single genes. Next-generation sequencing allows

linking a phenotype to its underlying genes. Co-segregating with causal mutation, genetic

markers and mutation are detected as over-representation. In recombinants populations, the

analysis of allele frequencies are used to link the phenotype to a genomic region (Schneeberger,

2014).

There are many cellulose synthesis inhibitors such as isoxaben and indaziflam that are

helpful to inspect the functions and dynamics of CSCs, but it is not known what their targets are

and how they interact with CESAs, which is the limitation preventing their utilization in the

chemical genetic analysis of CSC (Huang & Zhang, 2020). As a novel cellulose inhibitor, ES20

targets CESA6 at its catalytic domain directly and deletes CSC from the plasma membrane. In

the mutant screening with ES20, all resistant mutations localized within CESA6 rather than other

CESAs, which highlights the tight interaction between ES20 and CESA6 (Huang & Zhang,

2020).

From developing cotton fibers, CESA, as the homologous gene of bacterial cellulose

synthase, was first isolated (Pear, Kawagoe, Schreckengost, Delmer, & Stalker, 1996).

Consequently, other higher land plants such as maize and rice exhibit diverse CESA family (Yin,

Huang, & Xu, 2009). Because of sequence similarity, a group of cellulose synthase-like (CSL) genes are identified. In Arabidopsis, there are totally 30 CSL genes, and together with CESAs, they make up a CESA/CSL superfamily (Richmond & Somerville, 2000). This superfamily significantly contributes to the cell wall formation in crops such as rice, whose mechanism and precise functions are under exploration (Wang et al., 2010).

3.6   References

Dejonghe, W., Kuenen, S., Mylle, E., Vasileva, M., Keech, O., Viotti, C., et al. (2016). Mitochondrial uncouplers inhibit clathrin-mediated endocytosis largely through cytoplasmic acidification. *Nat Commun, 7*, 11710.

Dejonghe, W., Sharma, I., Denoo, B., De Munck, S., Lu, Q., Mishev, K., et al. (2019). Disruption of endocytosis through chemical inhibition of clathrin heavy chain function. *Nat Chem Biol, 15*(6), 641-649.

Drakakaki, G., Robert, S., Szatmari, A. M., Brown, M. Q., Nagawa, S., Van Damme, D., et al. (2011). Clusters of bioactive compounds target dynamic endomembrane networks in vivo. *Proc Natl Acad Sci U S A, 108*(43), 17850-17855.

Gillmor, C. S., Poindexter, P., Lorieau, J., Palcic, M. M., Somerville, C. (2002). Alpha-glucosidase I is required for cellulose biosynthesis and morphogenesis in Arabidopsis. *J Cell Biol, 156*(6), 1003-1013.

Hicks, G. R., Raikhel, N. V. (2012). Small molecules present large opportunities in plant biology. *Annu Rev Plant Biol, 63*, 261-282.

Huang, L., Li, X., Zhang, C. (2019). Progress in using chemical biology as a tool to uncover novel regulators of plant endomembrane trafficking. *Curr Opin Plant Biol, 52*, 106-113.

Huang, L., Li, X., Zhang, W., Ung, N., Liu, N., Yin, X., et al. (2020). Endosidin20 Targets the Cellulose Synthase Catalytic Domain to Inhibit Cellulose Biosynthesis. *Plant Cell*.

Kania, U., Nodzynski, T., Lu, Q., Hicks, G. R., Nerinckx, W., Mishev, K., et al. (2018). The Inhibitor Endosidin 4 Targets SEC7 Domain-Type ARF GTPase Exchange Factors and Interferes with Subcellular Trafficking in Eukaryotes. *Plant Cell, 30*(10), 2553-2572.

Kitakura, S., Adamowski, M., Matsuura, Y., Santuari, L., Kouno, H., Arima, K., et al. (2017). BEN3/BIG2 ARF GEF is Involved in Brefeldin A-Sensitive Trafficking at the trans-Golgi Network/Early Endosome in Arabidopsis thaliana. *Plant Cell Physiol, 58*(10), 1801-1811.

Huang, L., Zhang, C. (2020). Endosidin20 is a broad-spectrum cellulose synthesis inhibitor with an herbicidal function. *Biorxiv.*

Li, R., Rodriguez-Furlan, C., Wang, J., van de Ven, W., Gao, T., Raikhel, N. V., et al. (2017). Different Endomembrane Trafficking Pathways Establish Apical and Basal Polarities. *Plant Cell, 29*(1), 90-108.

Mossessova, E., Corpina, R. A., Goldberg, J. (2003). Crystal structure of ARF1*Sec7 complexed with Brefeldin A and its implications for the guanine nucleotide exchange mechanism. *Mol Cell, 12*(6), 1403-1411.

Pear, J. R., Kawagoe, Y., Schreckengost, W. E., Delmer, D. P., Stalker, D. M. (1996). Higher plants contain homologs of the bacterial celA genes encoding the catalytic subunit of cellulose synthase. *Proc Natl Acad Sci U S A, 93*(22), 12637-12642.

Renault, L., Guibert, B., Cherfils, J. (2003). Structural snapshots of the mechanism and inhibition of a guanine nucleotide exchange factor. *Nature, 426*(6966), 525-530.

Richmond, T. A., Somerville, C. R. (2000). The cellulose synthase superfamily. *Plant Physiol, 124*(2), 495-498.

Rosado, A., Hicks, G. R., Norambuena, L., Rogachev, I., Meir, S., Pourcel, L., et al. (2011). Sortin1-hypersensitive mutants link vacuolar-trafficking defects and flavonoid metabolism in Arabidopsis vegetative tissues. *Chem Biol, 18*(2), 187-197.

Schneeberger, K. (2014). Using next-generation sequencing to isolate mutant genes from forward genetic screens. *Nat Rev Genet, 15*(10), 662-676.

Tanaka, H., Kitakura, S., De Rycke, R., De Groodt, R., Friml, J. (2009). Fluorescence imaging-based screen identifies ARF GEF component of early endosomal trafficking. *Curr Biol, 19*(5), 391-397.

Tanaka, H., Nodzylski, T., Kitakura, S., Feraru, M. I., Sasabe, M., Ishikawa, T., et al. (2014). BEX1/ARF1A1C is required for BFA-sensitive recycling of PIN auxin transporters and auxin-mediated development in Arabidopsis. *Plant Cell Physiol, 55*(4), 737-749.

Wang, L., Guo, K., Li, Y., Tu, Y., Hu, H., Wang, B., et al. (2010). Expression profiling and integrative analysis of the CESA/CSL superfamily in rice. *BMC Plant Biol, 10*, 282.

Yin, Y., Huang, J., Xu, Y. (2009). The cellulose synthase superfamily in fully sequenced plants and algae. *BMC Plant Biol, 9*, 99.